ANALYSIS OF STRUCTURE AND FUNCTION OF THE SEROTONIN TYPE-3 RECEPTOR USING SITE-DIRECTED MUTAGENESIS, STRUCTURE-ACTIVITY RELATIONSHIP AND CHIMERIC CONSTRUCTS

By

Asha Suryanarayanan

RECOMMENDED:

Advisory Committee Chair

Department Head

APPROVED:

Dean, College of Natural Science & Mathematics

Dean of the Graduate School

April 8, 2005

Date

ANALYSIS OF STRUCTURE AND FUNCTION OF THE SEROTONIN TYPE-3 RECEPTOR USING SITE DIRECTED MUTAGENESIS, STRUCTURE ACTIVITY RELATIONSHIP AND CHIMERIC CONSTRUCTS

A

THESIS

Presented to the Faculty

of the University of Alaska Fairbanks

in Partial Fulfillment of the Requirements

for the Degree of

DOCTOR OF PHILOSOPHY

By

Asha Suryanarayanan, B.Pharm.

Fairbanks, Alaska

May 2005

Abstract

The serotonin type-3 receptor (5-HT_3R) is a cation conducting ligand gated ion channel that mediates fast synaptic transmission. The 5-HT_3R belongs to the Cys loop superfamily of ligand gated ion channels that also includes the nicotinic acetylcholine, glycine and $GABA_A$ receptors. The 5-HT_3R has been implicated in several processes such as emesis, gastrointestinal motility, drug abuse, alcoholism and nociception. Studies involving the ligand-binding domain will thus aid in development of new drugs that modulate these physiological and pathophysiological processes. The ligand-binding site of this receptor is comprised of six putative loops, viz. loop A-F. The focus of this thesis was to study the interactions of both agonists and antagonists with the 5-HT_3R. Interactions of two agonists, 5-HT and *m*CPBG, with the loop C region of the receptor were studied employing biochemical and receptor modeling studies. These studies identify novel determinants of 5-HT and *m*CPBG interactions with the 5-HT_3 receptor. Similar studies involving granisetron, a competitive 5-HT_3R antagonist also reveal novel amino acids that interact with this antagonist. In order to further understand antagonist interactions with this receptor, the approach of structure activity relationship (SAR) studies was also employed to study the functional group interactions of lerisetron, a novel 5-HT_3R antagonist. Taken together with data from loops A, B, D and E, these data reveal an emerging picture of ligand interactions with the 5-HT_3R.

Table of Contents

Page

Page

Page

Page

Page

Page

Page

List of Figures

Page

List of Tables

Acknowledgements

First and foremost, I thank my major advisor, Dr. Marvin Schulte for providing me an opportunity to pursue my graduate career in his laboratory. He not only provided me financial and academic support, but also created a friendly atmosphere in his laboratory, which quickly became a 'home away from home' for me. I would like to thank my parents, Dr. Suryanarayanan and Jayalakshmi for their love and support. I also thank my parents-in-law, Ramesh and Shailaja Joshi, and my sister-in-law, Pradnya Joshi for their continual support and for motivating me to travel across the world to pursue my Ph.D. This work would have been impossible without my husband and lab colleague, Prasad Joshi, who was always there to make this journey so enjoyable.

I would like to thank all my committee members for their help in editing this dissertation. I also thank all my past colleagues from the University of Louisiana at Monroe. I am also grateful to the Department of Chemistry and Biochemistry and the Graduate School at the University of Alaska Fairbanks for accepting me in their program. It has been a privilege to study and live in the beautiful State of Alaska. I would also like to thank Mary Van Muelken for editing my research proposals and this dissertation. I finally thank the funding agencies, American Heart Association, National Science Foundation and Alaska INBRE for supporting this work.

Chapter 1: Introduction

1.1 Ion channels:

Ion channels are critical for maintaining the physiological milieu of every cell in the body. These integral membrane proteins form a pore that spans the membrane lipid bilayer. Their function is diverse, from being responsible for cellular excitation (brain and muscle) to being responsible to salt homeostasis. More than 100 genes coding for subunits of ion channels have been identified so far. The role of ion channels in membrane excitation is as crucial as the role of enzymes in cellular metabolism. The opening and closing of specific channels cause changes in membrane potential and lead to characteristic electrical messages such as inhibitory/excitatory signals and graded potentials.

Structure determination for ion channels is a critical component in the elucidation of drug–receptor interactions and also, in understanding the pathophysiology of diseases. (Barrantes, 1997; Celesia, 2001; Celesia, 2003). Structure elucidation is also critical for advances in lead development and rational drug design.

1.2 Classification of ion channels:

An illustration of different ion channels and their topologies is provided in Figure 1.1. Ion channels can be broadly classified into four major classes:

1.2.1 Voltage-gated ion channels:

Voltage-gated channels sense the transmembrane potential, open or close in response to change in voltage (depolarization or hyperpolarization) and shape the action

potential. Types of voltage-gated ion channels are potassium, calcium, sodium and chloride channels. Potassium channels are comprised of a pore-forming tetramer of α subunits, which associate with accessory β subunits that are regulatory in nature (Hanlon and Wallace, 2002). Each α subunit contains six transmembrane segments, S1-S6, along with intracellularly located N and C termini (Kamb et al., 1987). The 'P' region, which appears to be involved in conferring the K^+ selectivity is located between transmembrane segments S5 and S6 (Kamb et al., 1987). The K^+ channel is the only ion-selective channel for which an α subunit structure has been crystallographically solved (Doyle et al., 1998). In case of calcium channels, as many as five subunits may form the channel: α1, β, α2δ, and γ. Similar to K^+ channels, the α1 subunit is the pore-forming component and contains the gate and voltage sensor. The β subunit is cytoplasmic and plays a regulatory role. The α2δ subunit of calcium channels consists of a cytoplasmic α2 fragment linked to the membrane via a disulfide bond to a transmembrane δ fragment. Similar to the K^+ channel, the pore-forming component of the Ca^{2+} channel is comprised of four domains. In a Ca^{2+} channel, however, instead of four separate subunits, these segments are derived from a single polypeptide chain, i.e, the α1 subunit, and are designated domains I-IV (Figure 1.1). Each highly homologous, but non identical, domain consists of six transmembrane segments and is linked to the next domain by an intracellular loop region. As with the K_v channel, the pore is comprised of a total of eight transmembrane segments, two (S5 and S6) contributed by each domain. The α subunit of Na^+ channels has the same topological arrangement as Ca^{2+} channels. Ten different genes, SCN1A to SCN10A, are known to encode four-domain alpha subunits of voltage-

gated sodium channels. Multiple types of alpha subunits have been cloned (Malo et al., 1994). One or two modulatory β subunits are present in most Na^+ channels (Catterall, 1986). Similar to Ca^{2+} channels, the Na^+ channel is comprised of four homologous domains (I-IV), each consisting of six transmembrane segments (S1-S6), all domains coming from the same polypeptide chain. Similar to Ca^{2+} channels, the pore is formed from four different P regions located between S5 and S6 in each domain (Yellen et al., 1991). Although a low resolution cryo-electron microscopy map is available (Sato et al., 2001), to date, no molecular structure of a Na^+ channel has been crystallographically solved. Nine different human genes encoding voltage-gated chloride channels have been identified (CLCN1 to CLCN7; CLCNA/B). These genes encode channels CLC1 to CLC7, CLCKA, and CLCKB, which do not structurally resemble any other ion channel family. They do not contain any charged segments such as S4 segments of voltage-gated Na^+, Ca^{+2} and K^+ channels. A combination of glycosylation and electrophysiological experiments on mutant proteins has revealed that both NH_2 and COOH terminals are located intracellularly and that the S8-S9 interlinker is extracellular because of a glycosylation site.

1.2.2 Inward rectifier K^+ (IRK) channels:

IRK channels possess a basic channel-forming structure with only a P domain, as shown for other voltage-gated ion channel members. The P domains of IRK channels exhibit limited sequence similarity to those of other voltage-gated ion channels. They are also comprised of two flanking transmembrane spanners and can form homo- or heterooligomers. IRK channels are designed to allow more K^+ flow into the cell than out.

Their voltage-dependence may be regulated by external K^+, internal Mg^{2+}, internal ATP and/or G-proteins (Lu, 2004). Inward rectifiers play a role in setting cellular membrane potentials. The closing of these channels upon depolarization allows long duration action potentials with a plateau phase. Inward rectifiers do not contain the intrinsic voltage sensing helices that are found in voltage-gated ion channels (Figure 1.1).

1.2.3 Gap junction channels:

Gap junctions are special intercellular channels that connect the cytoplasm of one cell with the neighboring cell. These channels allow the intercellular transport of ions and small molecules without leakage into extracellular space. Many gap junctions cluster together to form 'plaques' and bridge the gap between two close neighboring cells. Purves et al. (2001) reported that six connexin subunits from each cell join to make an aqueous pore connecting such neighboring cells, leading to formation of a 12 subunit tube. Gap junction channels do not resemble any other known ion channels. Each connexin subunit has 4 transmembrane domains with extracellular loops that determine which connexin subtypes it joins from the next cell.

1.2.4 Intracellular ligand-gated ion channels:

Intracellular ion channels are located on cell organelles and akin to extracellular ligand-gated ion channels; they perform functions *inside* the cell. These channels are difficult to characterize electrophysiologically, since they are intracellularly located. Therefore, relatively less is known about intracellular ion channels. Various intracellular ligand-gated ion channels include the CFTR (cystic fibrosis transmembrane conductance regulator), ATP-sensitive K^+ channels as well as ion channels involved in sense

perception. These are often activated indirectly by G-protein coupled receptors. Other common intracellular ligands which activate intracellular channels include calcium ions, ATP, cyclic AMP and GMP as well as phosphatidyl inositol (PI).

1.2.5 Extracellular LGICs (ligand-gated ion channels):

This family is comprised of the nicotinic acetylcholine (nAch), serotonin type-3 ($5\text{-}HT_3$), glycine (Gly) and γ-aminobutyric acid ($GABA_A$) receptors. This family is also called as the 'Cys' loop ligand-gated ion channel superfamily due to the presence of a characteristic disulfide bond located in the extracellular domains of these receptors (Figure 1.1.5). All members of this family are pentameric and can form either homo- or heteromeric receptors (A detailed description of characteristics of this family is provided below).

Two other gene families; cation selective glutamate receptors (GluR) and the ATP/purinergic nucleotide receptors (P2XR) are also ligand-gated receptors, but are not evolutionally related to the Cys-loop family of ligand-gated ion channels. These receptors differ from the nAChRs in the folds of their peptide chains and in the number of subunits that form the channel. The GluRs are tetrameric and the exact number of subunits in P2XRs has not been determined so far.

1.3 The Cys-loop LGIC (ligand-gated ion channel) family:

1.3.1 Physiological role:

The Cys-loop family of ligand-gated ion channels (LGICs) plays a critical role in mediating fast synaptic transmission in the body. These channels are less selective and

allow two or more types of ions to pass through the channel pore, in contrast to voltage-gated ion channels which shape the action potential by typically allowing only one type of ion. After the propagation of an action potential to the presynaptic terminal, neurotransmitters such as acetylcholine are released via synaptic vesicles into the synaptic cleft. Binding of the neurotransmitter (ligand) to the corresponding LGICs causes channel opening and a fast postsynaptic response that typically last only a few tens of milliseconds or less. The postsynaptic response can be either inhibitory or excitatory depending upon the ion permeability of the LGIC. GABA and glycine receptors are inhibitory because their channels are permeable to Cl^-; whereas 5-HT_3 and nAChRs are excitatory due to their cation permeability.

1.3.2 Multiple subunit types:

All members of this family form homo- or heteropentameric receptors. Multiple subunits (more than 2) have been cloned for all members of this family. For example, ten α subunits (α1–α10) and four β subunits (β1–β4) have been cloned for the nAChR. Of these, α2–α10 and β2–β4 are neuronal subunits, while α1 and β1 are muscle subunits (Arneric and Brioni, 1999). The assembly of different subunits in different stoichiometries forms receptors with different pharmacological and biophysical properties. Depending on age or their location in the body, nAChRs vary in their subunit compositions (Gu and Hall, 1988a; Gu and Hall, 1988b). Muscle nAChRs are either $\alpha_2\beta\gamma\delta$ (fetal) or $\alpha_2\beta\varepsilon\delta$ (adult) while neuronal nAChRs are composed of α and β subunits (Mishina et al., 1986). Similarly, various subunits (α, β, δ,γ, ρ) of the $GABA_AR$ have been cloned and their biophysical characterization has shown that multiple subunits can

combine to give multiple receptor subtypes. Only heteropentameric $GABA_A$Rs are found in the body (Enna and Bowery, 1997). The glycine receptor consists mainly of α and β subunits and at least 2 α and β subunits have been cloned so far. These subunits assemble as homo or heteropentameric glycine receptors in the body (Zafra et al., 1997).

1.3.3 Membrane topology and architecture:

The membrane topology of the Cys-loop family of LGICs is shown in Figure 1.1.5. Based on hydrophobicity plots and sequence homology, all members of this family are purported to contain a large N-terminal domain, a transmembrane region which spans the membrane four times (forming M1-M4 domains, 2 intracellular and 1 extracellular loop) and a short C-terminal region. A characteristic Cys-Cys disulfide bond is present in the N-terminal region of all members of this family. Five such subunits coassemble to form a pentameric ion channel, wherein the M2 region from each subunit contributes to the channel pore (as shown in Figure 1.1.6).

1.3.4 Examples of ligand-gated channelopathies:

ACh receptor channelopathies include autosomal dominant frontal nocturnal epilepsy, congenital myasthenia gravis syndromes, familial infantile myasthenia gravis, myasthenia gravis, neonatal transient and endplate acetylcholinesterase deficiency (Celesia, 2001). Defects in nAChRs or their loss can also contribute to Alzheimer's and Parkinson's diseases and schizophrenia. Glycine receptor channelopathies include hyperekplexia (familial startle disease) and spastic paraparesis (Celesia, 2001). Mutations of the γ_2 $GABA_A$ subunit are found in families affected by febrile epileptic seizures

(Celesia, 2003). No naturally occurring mutations or channelopathies have been reported so far for 5-HT_3Rs.

1.4 5-Hydroxytryptamine (Serotonin) type 3 receptor [5-HT_3R]:

This thesis focuses on the 5-HT_3R. The murine 5-HT_{3A}R was cloned in 1991 from N1E-115 neuroblastoma cells by Maricq et al. (Maricq et al., 1991). Five 5-HT_{3A}R subunits coassemble to yield homomeric LGIC receptors. The membrane topology of the 5-HT_{3A}R subunit is shown in Figure 1.1.5. The mouse 5-HT_{3A}R is comprised of 487 amino acids and weighs ~50 Kda (~65 Kda when glycosylated) (Hovius et al., 1998; McKernan et al., 1990). ~243 amino acids are thought to contribute to the large N-terminal domain. The transmembrane domain consists of 4 regions; M1-M4. Three loops are thought to connect the M1-M4 regions; the M1-M2, M2-M3 and M3-M4 loops. Of these loops, the M2-M3 loop is extracellularly located. A short C-terminal domain is also extracellularly located. The N-terminal domain has as many as six possible glycosylation sites. The M3-M4 loop has three putative phosphorylation sites, of which (S414) appears to be phosphorylated *in vivo* (Lankiewicz et al., 2000). Receptor phosphorylation has been implicated to play a role in 5-HT_3 receptor conductance levels (Van Hooft and Vijverberg, 1995) and desensitization rates (Hubbard et al., 2000). The M2 region lines the channel pore, and contributes to cation selectivity, channel gating and desensitization (Panicker et al., 2002).

1.4.1 Historical background about the discovery of 5-HT_3Rs :

It is now known that serotonin (5-HT) can activate both the fast ligand-gated ion channel (5-HT_3R) and the slow G-protein coupled metabotropic 5-HT receptors which

include the 5-HT_{1-2} and 5-HT_{4-7} receptors. However, the action of 5-HT and the elucidation of putative 5-HT receptors was confusing until it was determined that 5-HT_3Rs are ligand-gated ion channels.

In 1953, Rocha E et al. reported that the contractile actions of 5-HT in the guinea pig ileum are due to a discharge of post-ganglionic cholinergic fibers (Rocha et al., 1953). Gaddum e and Picarelli later reported that effects of 5-HT and tryptamine are via 'tyrptamine receptors'. They also proposed that 5-HT causes contraction of the guinea pig ileum by acting on two types of receptors viz., D (blocked by dibenzyline) and M (blocked by morphine) (Gaddum and Picarelli, 1957). The next 5-HT receptor classification was reported by Peroutka and Snyder. This group used radioligand binding assays and classified 5-HT receptors as 5-HT_1 (with low affinity for 5-HT) and 5-HT_2 (high affinity for 5-HT) receptors (Peroutka and Snyder, 1979). The 5-HT_1 receptors appeared similar to the D type of receptor proposed earlier, but neither receptor was similar to the M type 5-HT receptor. Studies by Fozard and Mobarok later showed that application of 5-HT induced tachycardia in a rabbit heart preparation and could be blocked by metoclopramide and (-) cocaine. This receptor was similar to the M type receptor (Fozard and Mobarok, 1978). This observation led to the synthesis of MDL 72222, a very potent M receptor antagonist, which was more specific than metoclopramide and (-) cocaine (Fozard, 1984). More selective M-receptor antagonists such as tropisetron, ondansetron, granisetron and zacopride were subsequently synthesized (Kilpatrick et al., 1990; King, 1994; Richardson, 1995).

Bradley et al. reclassified the M type receptor as the 5-HT_3 receptor in 1986. Using localization studies and measurement of 5-HT_3 antagonist activity, it was determined that in the periphery, 5-HT_3Rs are located on pre- and postganglionic autonomic neurons, enteric nervous system, neurons of the sensory nervous system, somatic and vagal afferent fibers and on peripheral terminals of vagal afferents. In the central nervous system, 5-HT_3Rs are located on central terminals of vagal afferents, brain and spinal cord (Leslie et al., 1994; Sanger and Jones, 1994).

1.4.2 Cloning of 5-HT_3Rs:

The first 5-HT_3R cDNA (now designated as the 5-HT_{3A}R) was cloned from the murine N1E-115 neuroblastoma cell line by Maricq et al. in 1991 (Maricq et al., 1991). Two splice variants, short and long, were also cloned from neuroblastoma-glioma cell lines (NCB-20 and NG108-15). A second subunit, 5-HT_{3B} was cloned by Davies et al. in 1999 (Davies et al., 1999). Genes encoding 5-HT_{3C}, 5-HT_{3D} and 5-HT_{3E} subunits have also been reported (Niesler et al., 2003).

1.4.3 Properties of 5-HT_3R splice variants and subunits:

Two splice variants of the 5-HT_{3A}; 5-HT_{3AS} (short) and 5-HT_{3AL} (long) are known (Werner et al., 1994). Differences between splice variants in agonist pharmacology are small (Downie et al., 1994; Hope et al., 1993), with changes seen in efficacy of *m*CPBG and 2-methyl 5-HT compared to 5-HT. Intracellular kinases may functionally discriminate between the short and long variants (Hubbard et al., 2000). In addition to the A subunit, the 5-HT_{3B} subunit has also been cloned from human, (Davies et al., 1999; Dubin et al., 1999) mouse and rat species (Hanna et al., 2000). The 5-HT_{3B} subunits share

~45% sequence identity with their 5-HT_{3A} homologues, but cannot form functional homopentameric receptors (Davies et al., 1999). However, the 5-HT_{3B} subunit forms functional 5-HT_{3AB} heteromers when coexpressed with the 5-HT_{3A} subunit. 5-HT_{3B} receptor subunits have putative extracellular N-glycosylation and intracellular phosphorylation consensus sites comparable with the 5-HT_{3A} subunit. The 5-HT_{3AB} heteromeric receptors are pharmacologically and functionally distinct from 5-HT_{3A}Rs. For example, the 5-HT_{3AB}Rs display 30 times higher conductance as compared to 5-HT_{3A}Rs. Three arginine residues at positions 432, 436 and 440 in the second intracellular loop (a region called HA stretch) have been shown to play a major role in determining channel conductance. These three positively charged residues are thought to hinder cation conduction in the homomeric receptors. This stretch is absent in the B receptors and may explain why the heteromeric 5-HT_{3AB} receptors have higher conductance (Kelley et al., 2003b). These different properties of 5-HT_{3AB}Rs help explain the functional differences observed between native and recombinant 5-HT_3 receptors, that could not be explained by existence of splice variants of the 5-HT_{3A}R.

1.4.4 5-HT_3Rs are centrally and peripherally distributed:

In rat, 5-HT_3Rs are located in cortical and limbic areas. It has been shown that 5HT_3R-immunoreactive neurons are present in the forebrain, brainstem, dorsal and ventral horns of the spinal cord (Bloom and Morales, 1998). In rat neocortex and hippocampus, the majority of 5-HT_3Rs are expressed on GABAergic neurons, suggesting a modulatory role of 5-HT_3R in release of GABA and it's mediation of inhibitory neurotransmission (Bloom and Morales, 1998; Morales and Bloom, 1997).

In the rat, 5-HT_{3A} and 5-HT_{3AB} receptors are peripherally located; whereas only homomeric 5-HT_{3A}Rs are centrally located (Morales and Wang, 2002). In the periphery, 5-HT_3R is expressed in dorsal root and nodose ganglia, vagus nerve and intestinal submucosal plexus. In the rat gastrointestinal system, 5-HT_3Rs are localized to neurons of the myenteric and submucosal plexus, fibers in the circular and longitudinal muscles, submucosa, and mucosa (Glatzle et al., 2002).

In humans, 5-HT_3Rs are located in brainstem, spinal cord, amygdala, area postrema (chemoreceptor trigger zone, CTZ) and hippocampus (Waeber et al., 1989). Both 5-HT_3 A and B subunits have been detected in the human amygdala, caudate and hippocampus (Davies et al., 1999). Expression of 5-HT_3 D and 5-HT_3 E subunits is restricted to only three and two tissues, respectively (D- adult: kidney, colon, liver; fetal: colon and kidney; E- adult: colon, intestine). On the other hand 5-HT_3C is more widely expressed (adult: brain, colon, intestine, lung, muscle, stomach; fetal: colon and kidney) (Niesler et al., 2003). Therefore, the expression pattern of 5-HT_3C resembles more closely that of 5-HT_3A and 5-HT_3 B subunits.

1.4.5 Physiological role and clinical relevance of 5-HT_3R:

1.4.5.1 Emesis:

5-HT_3Rs located on the area postrema and nucleus solitarius are involved in mediating the vomiting reflex. 5-HT_3R antagonists such as granisetron, ondansetron and palanosetron are clinically used in the treatment of chemotherapy induced nausea and emesis (Aapro, 2004). These antagonists antagonize emesis produced by cisplatin, other

emetogenic chemotherapeutic agents and by radiation therapy. These 5-HT_3R antagonists are thought to act by blockade of 1) 5-HT_3Rs in the area postrema and nucleus solitarius and 2) 5-HT_3Rs present on vagal afferents in the gut (Andrews, 1994).

1.4.5.2 Female and male behavior:

It has been shown by studies in mice that knock out of the 5-HT_3 receptor differentially affects behavior of males and females in the Porsolt forced swim and defensive withdrawal tests. The Porsolt forced swim test is used to detect anti-depressant efficacy, while the defensive withdrawal test is used to measure anxiety. Results from these studies suggest that the 5-HT_3 receptor regulates behavior related to depression and anxiety differently in males and females.

1.4.5.3 Nociception:

5-HT_3 receptors are important in nociceptive processing (Alhaider et al., 1991; Eide and Hole, 1993; Zeitz et al., 2002), consistent with expression on primary sensory afferents in the dorsal root ganglion (DRG), on neurons in the dorsal horn of the spinal cord and sensory nerve endings in the periphery (Hamon et al., 1989; Kidd et al., 1993, Tecott et al., 1993; Kia et al., 1995; Morales and Wang, 2002; Zeitz et al., 2002). Using the antisense approach, the effect of knocking out 5-HT_3Rs on analgesia produced by 5-HT_3R agonists such as 5-HT and 2-methyl-5-HT were studied. In mice tested with intrathecal 5-HT and 2-methyl 5-HT, tail-flick analgesia attenuated in mice treated with the 5-HT_3R antisense oligos, suggesting a role for 5-HT_3Rs in spinal antinociception.

1.4.5.4 Anxiety:

5-HT_3 receptors have been implicated in CNS functions such as cognition and anxiety as well as sympathetic, parasympathetic, and sensory functions in the peripheral nervous system (PNS) (Jackson and Yakel, 1995; Johnson and Heinemann, 1995; Morales and Wang, 2002). Targeted gene deletion of the 5-HT_{3A} receptor subunit produces an anxiolytic-like behavioral phenotype in mice (Kelley et al., 2003a). These anxiolytic-like effects were similar to pharmacological blockade of 5-HT_3 receptors produced by 5-HT_3R antagonists such as ondansetron. This observation supports a role for 5-HT_3R in modulation of anxiety and is also consistent with studies concluding the effectiveness of 5-HT_3R antagonists in animal models of anxiety.

1.4.5.5 Gastrointestinal motility:

5-HT_3 receptors on vagal sensory afferents modulate visceral afferent and efferent information in the gastrointestinal tract (Leslie et al., 1990; Merahi et al., 1992; Veelken et al., 1993; Sevoz-Couche et al., 2003). In the enteric nervous system, 5-HT_3 receptors also regulate gut motility and peristalsis (Galligan, 2002).

1.4.5.6 Urinary function:

Within the lower urinary tract, presynaptic 5-HT_3 receptors have been implicated in parasympathetic transmission to the urinary bladder through neuronal acetylcholine (ACh) release and smooth muscle contraction (Chen, 1990; Barras et al., 1996). Recently, 5-HT_{3A} mutant mice with a channel mutation (V13'S mutation in M2 region) were shown to exhibit urinary dysfunction. This channel mutation has been shown to render the 5-HT_3 receptor ~70-fold more sensitive to serotonin and produced constitutive active receptors

when coexpressed with the 5-HT_{3B} subunit (Dang et al., 2000). These data in combination with the data from mutant mice suggest that persistent activation of the hypersensitive and constitutively active 5-HT_{3A} receptor *in vivo* leads to excitotoxic neuronal cell death and functional changes in the urinary bladder, resulting in bladder hyperdistension, urinary retention, and overflow incontinence.

1.4.5.7 Reflex bradycardia:

The 5-HT_3R is believed to play a role in the hypotension following 5-HT infusion. This type of hypotension or bradycardia is known as the von Bezold Jarisch reflex and is thought to be mediated by the 5HT_3Rs on the vagus (Richardson et al., 1985).

1.4.6 Clinical uses of 5-HT_3R antagonists and agonists:

The traditional use of 5-HT_3R antagonists such as ondansetron has been in treatment of chemotherapy induced emesis (by targeting the 5-HT3Rs in the CTZ). However, recent studies have also demonstrated the usefulness of 5-HT_3R antagonists in the treatment of irritable bowel syndrome (IBS), anxiety, early onset alcoholism and drug abuse. In a clinical trial with diagnosed alcoholics, it was concluded that ondansetron is an effective treatment for early-onset alcoholism, where patients generally respond poorly to psychosocial treatment alone. The use of antagonists in alcoholism and drug abuse is believed to be associated with 5-HT_3Rs found in reward centers in the brain. Tropisetron and ondansetron reduce morphine self-administration in both naïve and morphine-dependent rats (Hui et al., 1993). Injection of ondansetron into the rat nucleus accumbens attenuates the action of cocaine (Herges and Taylor, 2000). 5-HT_3Rs in areas such as the nucleus accumbens are thought to be involved in pre-synaptic modulation of

dopaminergic neurotransmission. Ondansetron has also been shown to reduce cognitive impairment caused by the muscarinic antagonist, scopolamine and the NMDA receptor antagonist, MK-801 (Costall and Naylor, 2004).

In addition to the aforesaid uses of antagonists, 5-HT_3R agonists also show promise in the treatment of various types of constipation, and certain other gastrointestinal motility disorders including gastroesophageal reflux disease (GERD) (Coleman et al., 2003; Imanishi et al., 2003; Revel et al., 1999)

1.4.7 Chemical classification of 5-HT_3R ligands:

The chemical structures of various 5-HT_3 agonists, partial agonists and antagonists are shown in Figures 1.2, 1.3 and 1.4.

1.4.7.1 5-HT_3R agonists:

The major classes of 5-HT_3R agonists (see Figure 1.2) include the following:

1. 5-HT and other 5-HT analogs such as 5-HTQ, and 2-methyl 5-HT. 2-methyl-5-HT is a partial agonist with ~12% relative efficacy compared to 5-HT on the murine short form of the 5-HT_{3A}R. This compound is also potent on 5-HT_6Rs and is therefore less specific.

2. Phenylbiguanides (*m*CPBG) and phenylguanides (*m*CPG): *m*CPBG is a partial agonist of the 5-HT_3Rs. In case of the short form of murine 5-HT_{3A}R, it has ~93% relative efficacy compared to 5-HT.

3. Piperazinylquinolines such as quipazine and its analogs,

4. Miscellaneous compounds including certain tetrahydrothiazolopyridines (Imanishi et al., 2003), aminoalkyl- and imidazoloalkyl-indenothiazoles (YM-31636)

reported recently (Imanishi et al., 2003), and dihydrofurano[2,3-b]pyridine 5-HT_3R/nAChα$_7$R agonist PSAB-OFP (Broad et al., 2002).

1.4.7.2 5-HT_3R partial agonists:

In addition to 2-methyl 5-HT and *m*CPBG discussed above, certain benzylidene-anabeseines and quipazine analogs (see Figure 1.2) are also partial agonists of the 5-HT_3R. Partial agonists are valuable tools in studying receptor gating mechanisms. Changes in efficacy value of a partial agonist relative to the full agonist can provide valuable information about the gating mechanism (or signal transduction to open state) of an ion channel. More detailed information about employing partial agonists to decipher gating effects is discussed in chapter 3.

1.4.7.3 5-HT_3R antagonists:

Compared to 5-HT_3R agonists, extensive numbers of antagonists have been synthesized because of their clinical application for the treatment of chemotherapy induced emesis. Many 5-HT_3 antagonists were also synthesized as pharmacological tools for the characterization of the M type 5-HT receptor, which we now know as the 5-HT_3R.

The original 5-HT_3 antagonist pharmacophore developed by Hibert et al. consisted of an aromatic group, a carbonyl group and basic nitrogen, which is 1.7Å above the plane of the aromatic ring (Hibert et al., 1990). This pharmacophore has been further modified by contributions from various studies (Hibert et al., 1990; Rizzi et al., 1993; Rizzi et al., 1990; Swain et al., 1991). This revised pharmacophore is shown in Figure 1.4. Most 5-HT_3R antagonists fit this pharmacophore. 5-HT_3R antagonists can be classified as indoles (tropisteron), benzoates (MDL 72222), indazoles (granisetron),

carbazoles (ondansetron) and benzamides (zacopride). Structures of these compounds are shown in Figure 1.4. Orjales et al. reported a novel benzimidazole ring containing 5-HT_3R antagonist, lerisetron (Piperazinyl N-benzyl benzimidazole). As shown in Figure 1.5, the structure of lerisetron fits the Hibert pharmacophore, but also contains an additional N1 substituent, which appears to confer increased affinity. In addition to these antagonists, (+)-tubocurarine (dTC), a potent nAChR antagonist, is also a very potent 5-HT_3R antagonist. This large compound differs markedly from all other 5-HT_3R antagonists.

1.4.8 Ligand-binding site of the 5-HT_3R:

A cryo-electron micrograph has been determined at a 4.6Å resolution for the nAChR (Miyazawa et al., 1999). In addition to extensive site-directed mutagenesis, several approaches including photoaffinity labeling, detailed single channel analysis, NMR studies of peptide fragments have been utilized to study the nAChR. Unlike the nAChR, most of the information about the structure and function of 5-HT_3R has been derived from mutagenesis studies.

The discovery of the Acetylcholine Binding Protein (AChBP) has led to rapid developments in the understanding of the ligand-binding site of LGICs. This soluble binding protein bears a significant degree of sequence and structural homology to the N-terminal domain of all ligand-gated ion channel receptors. This protein shares about 25% sequence homology with the N-terminal extracellular regions of Cys-loop LGIC receptors. The crystal structure of the AChBP has been solved (Brejc et al., 2001).Based on the structure of AChBP, much of the previous biochemical data for LGIC receptors

can now be placed in a 3-D perspective. Thus, AChBP-based homology models of all LGIC receptors have been developed. These models represent static pictures of the extracellular domain and do not provide direct information about the activation mechanism and conformational changes that occur on ligand binding. Based on a combination of previous experimental data and AChBP-based homology models, the ligand-binding site of 5-HT_3R (and other LGICs) is thought to be comprised of a principal (+) face and a complementary (-) face. Each face of the binding site includes three loops that contribute to ligand interactions. The + face contains Loops A-C and the – face contains loops D-F (See Figure 1.1.5).

1.4.8.1. Loop A residues:

E129 of Loop A region has been proposed to interact with the NH_2 group of the agonist 5-HT via an ionic or hydrogen bond interaction (This residue is designated as E106 according to the author's numbering). In AChBP-based 5-HT_3R homology models, this residue is farther than 4Å of docked ligands. Therefore, it is unclear if this residue actually forms a part of the ligand-binding site. Mutation of F130 selectively alters electrophysiological responses to 5-HT, but not *m*CPBG. (This residue is designated as F107 according to the author's numbering). Mutation of this residue to Asparagine (F130N) produces receptors that can be activated by acetylcholine, suggesting that this residue may play a role in ligand recognition. Homology and docking studies of 5-HT_3R predict that this residue is over 4Å from docked ligands, indicating that this residue may not form a part of the ligand-binding site. It is possible that F130 is important for ligand recognition or ligand 'processing' before the ligand actually enters the binding site.

1.4.8.2. Loop B residues:

Site directed mutagenesis of all tryptophan residues in the 5-HT_3R N-terminal identified W183 of the Loop B region as a critical component of the binding site (Spier and Lummis, 2000). Mutation of this residue to either alanine or tyrosine ablated radioligand binding. Concomitantly, large changes in affinities of both 5-HT and *m*CPBG were seen. Using unnatural amino acid substitutions, it has been postulated that this tryptophan residue forms a cation-pi interaction with the NH_2 (amino) group of 5-HT, i.e., the positively charged amino group of the ligand (5-HT) interacts with the pi cloud of the aromatic ring of tryptophan. The homologous residue in the nAChR was shown to participate in a cation- pi interaction with acetylcholine (Beene et al., 2002; Zhong et al., 1998). The homologous residue in GABA receptors has also been shown to be involved in ligand binding. Thus this residue is a critical aromatic residue for ligand binding in all members of the LGIC family. The importance of this residue is also supported by homology and docking studies of LGICs. The roles of other residues in the putative Loop B region have not been studied.

1.4.8.3. Loop C residues:

Residues E225, Y234 and E236 from the loop C region of the mouse 5-HT_3R have been postulated to play a role in the ligand binding and/or gating (Price and Lummis, 2004; Schreiter et al., 2003). However, the assignment of a role in gating for these residues is speculative since it is based only on changes in EC_{50} and/or K_i values (Colquhoun, 1998). A comparison of unliganded and liganded crystal structures of AChBP suggests that the loop C region undergoes the largest movement after agonist

binding (Celie et al., 2004). A substituted cysteine accessibility method (SCAM) study of the loop C region of the β_2 $GABA_AR$ also implicates this region in conformational changes after agonist binding (Wagner and Czajkowski, 2001). However, a detailed evaluation of the role of each loop C residue of the 5-HT_3R in ligand binding and gating was unavailable prior to the presentation of this thesis.

1.4.8.4. Loop D residues

Using alanine scanning mutagenesis of the putative Loop D region, Yan et al. showed that residues in this region differentially interact with ligands. The affinity for d-TC was reduced by mutations at W89, and the affinity for serotonin was reduced by substitution at R91 (Yan et al., 1999). On the other hand, affinity for granisetron was reduced by mutations at W89, R91, and Y93. Based on the 'every-other-residue' periodicity of the effects of Loop D mutations on affinity for granisetron, Yan et al. concluded that this region of the binding site adopts a β conformation. This structure for the Loop D region has now been verified by AChBP-based homology models of the 5-HT_3R. These models also suggest that the tertiary ammonium ions of antagonists interact with W90 via a cation-pi interaction (Maksay et al., 2003).

1.4.8.5. Loop E residues:

Using alanine scanning mutagenesis, Venkataraman et al. showed that three tyrosine residues (Y141, Y143 and Y153) from the Loop E region interact with both agonists (5-HT, *m*CPBG and antagonists (d-TC and lerisetron) (Venkataraman et al., 2002b). Mutation of Y153 to alanine caused significant changes in 5-HT induced response kinetics. It was also shown that 5-HT and *m*CPBG interact with Y143, d-TC

interacts with Y141 and lerisetron interacts with both Y143 and Y153. Based on the overall data, it was suggested that this region of the 5-HT_3R adopts a loop conformation. This prediction has also been verified by AChBP-based homology models of the 5-HT_3R.

1.5 Activation of LGIC receptors:

The nAChR is the most characterized member of the LGIC family. Quantitative studies of the muscle nAChR have been possible due to the rich abundance of these receptors in the electric organ of the *Torpedo* ray. The structure of the muscle nAChR has been elegantly studied using electron microscopy. These studies have led to development of three dimensional map of the closed form of the receptor at 9Å and 4.6Å levels (Miyazawa et al., 1999; Unwin, 1993). The structural transition from the closed to the open-channel conformation of the receptor has been analysed at 9Å resolution by comparing three-dimensional maps of the closed and open conformations (Unwin, 1995). A detailed comparison of the two structures indicated that the binding of ACh initiates two interconnected events in the extracellular domain. The first is a local disturbance, involving all five subunits, in the region of the binding sites, and the second is an extended conformational change, involving predominantly the two α subunits, which communicates to the transmembrane portion. In the open form, the M2 transmembrane helices rotate and switch to a new configuration in which they point outwards instead of pointing towards the axis of the pore, as in the closed form. These experiments give a picture of the receptor in closed and open-channel conformations, but do not provide any information about the events that lead to this transition.

A more precise description of the extended conformational change has recently been obtained by a comparing the 4.6Å structure of the nAChR extracellular domain with the crystal structure of the AChBP. It was found that there are two alternative extended conformations of the receptor subunits - one characteristic of either α subunit before activation (α form), and the other characteristic of the three non-α subunits (non-α form). Binding of ACh converts the structures of the two α subunits to the non-α form (Unwin et al., 2002). In the closed state, the α subunits are initially distorted (rigid) due to their interactions with neighboring subunits, and the free energy of binding overcomes these distortions, making the whole assembly more symmetrical and similar to the ligand-bound AChBP. This transition to the activated conformation of the receptor is believed to involve relative movements of the inner and outer parts of the β-sandwich in the binding site, which compose the core of the α subunit around the Cys-loop disulfide bond (see Figure 1.6). It has been suggested that these movements are translated to the transmembrane region via the interaction of the Cys-loop and/or the β_1–β_2 loop with the proximal M2-M3 extracellular loop. In $GABA_A$ and glycine receptors, it has been shown that such electrostatic interactions exist between residues in Cys-loop and the M2-M3 loop and may form the trigger to channel opening. Similar interactions have not yet been shown in either the nACh or 5-HT_3Rs. In case of 5-HT_3Rs, R222 a pre-M1 residue has been shown to be important for gating. Although the mechanism of channel opening may be similar across all LGICs, there may be differences in the types of interactions formed and the residues involved. In the 5-HT_3R, it is unclear if there is a Cys-loop to M2-M3

connection, involvement of M1 region or some other part of the protein in the signal transduction pathway.

1.6 Role of 5-HT_3 B subunit in the ligand-binding site:

Although the role of residues of the HA stretch in the M3-M4 region of the B subunit in contributing to the higher conductance of heteromeric AB receptors has been elucidated, the contribution (if any) of the B subunit to the binding site of AB receptors is not known. The stoichiometry of AB receptors is also unknown. An ER retention signal (CRAR sequence) in the transmembrane region of the 5-HT_3B subunit has been shown to play a role in intracellular retention of the 5-HT_3B subunit. However, replacement of this ER retention signal in 5-HT_3B to the corresponding sequence in the A subunit (SGER) does not lead to cell surface expression, suggesting the presence of other signals or mechanisms that control the surface expression of 5-HT_{3B}Rs.

1.7 Overview of approaches used to study structure of ligand-gated ion channels:

1.7.1 Electron Microscopy of 5-HT_3 receptors

Electron microscopy studies have described the 5-HT_3R as a doughnut-shaped toroidal ring with a stain-filled center and a diameter of 70Å (Boess et al., 1992; Green et al., 1995). This structure is similar to the purified Torpedo ray nAChR. These results support a quaternary structure of 5-HT_3 receptors similar to that of nACh and $GABA_A$ receptors. The eventual aim of the electron microscopy studies was to obtain purified 5-HT_3R receptor in amounts sufficient to perform X-ray crystallography and structure determination. However, such studies have not been reported with this purified receptor.

The inability to obtain high concentrations of pure receptor is a major hindrance in carrying out such detailed structural studies.

1.7.2 X-ray crystallography:

X-ray crystallography requires pure crystalline protein for structure determination. Structure depictions by X-ray crystallography are static and typically do not explain function/movements in the crystallized protein. In addition, highly flexible/mobile structural parts such as surface loops are often not resolved via X-ray crystallography. Combining high resolution structures of proteins (obtained by X-ray crystallography/NMR) with electron micrographs by superposition of the two distinct structures provides more insights into the protein structure.

Membrane proteins such as LGICs are difficult to crystallize since they tend to precipitate out of solution due to unfavorable protein-protein and protein-solute interactions. To be kept soluble in aqueous solution, membrane proteins need the addition of detergents. Detergents, however, often interfere with regular arrangements of the protein complexes in the crystal, resulting in a diffuse diffraction pattern. Several groups have attempted to truncate extracellular domains of large membrane-bound ion channels in order to obtain fragments that may be relatively easy to crystallize (as compared to the entire receptor). This approach has been used for the glutamate receptor, GluR2. In GluR2, the ligand binding domain is composed of S1 and S2 segments, which are separated by transmembrane segments M1, M2 and M3 in the full length receptor. Several recombinant 'HS1S2' constructs were designed wherein an N-terminal Histidine (His) tag was added. These constructs were engineered to produce different deletions at

the S1 and S2 termini and S1-S2 linkers (Chen et al., 1998). One of the constructs, 'HS1S2I' was found to yield large amounts of biologically active GluR2 ligand binding domains in *E coli* cells. This construct was readily amenable to structure determination by X-ray crystallography in the absence and presence of glutamate, alpha-amino-3-hydroxy-5-methyl-4-isoxazole-propionic acid (AMPA) and kainate. This study also facilitated the crystallization of the ligand binding core of another novel S1S2 construct in the apo state (absence of ligand) and in the presence of the antagonist 6,7-dinitroquinoxaline-2,3-dione (DNQX), partial agonist kainate, and full agonists glutamate, and AMPA. These ligand-bound crystal structures provided the first views of the ligand binding core of a ligand-gated ion channel in distinct conformations that may be associated with different functional states of the channel, thus lending insight into receptor activation, antagonism, and the molecular basis for ligand specificity.

Obtaining a soluble version of an extracellular domain (ECD) for a Cys-loop ligand-gated ion channel has been a challenging task since these receptors are multimeric. The truncated S1S2 construct of GluR2, described above, is a monomer. Similar truncated multimeric constructs for the Cys-loop family would be harder to crystallize since the binding site is located at intersubunit interfaces and it would be necessary to preserve all important intersubunit contacts. Attempts to obtain a truncated, crystallizable version of the nicotinic acetylcholine receptor have not proven to be successful so far (Wells et al., 1998). Although the muscle nAChR is found in large amounts in the electric organ of Torpedo ray, no X-ray crystallography data is yet available for this receptor. An electron microscopy map of 4.6Å is available for the nAChR (Miyazawa et al., 1999).

1.7.3. Use of NMR spectroscopy in structure elucidation

For structure elucidation by NMR, high concentrations of pure, solubilized proteins are typically required. As discussed in the X-ray crystallography section, the extracellular ligand-binding (S1S2) core of the GluR2 has been expressed in bacteria as a soluble, monomeric protein. Based on the ligand bound crystal structure of this construct, a S1-S2 domain closure upon ligand binding was postulated, but details of intradomain motions could not be investigated. Using NMR relaxation measurements on the fully deuterated S1S2 protein, motions of the ligand-binding core of GluR2 bound to glutamate were studied. ^{15}N longitudinal (T1) and transverse (T2) relaxation measurements as well as [^{1}H]-^{15}N nuclear Overhauser effects at 500 and 600MHz were measured. It was found that residues in the agonist-binding pocket exhibited two main classes of motion. Those contacting the α-substituents of the ligand glutamate exhibited minimal internal motion, whereas those contacting the γ-substituents exhibited exchange dynamics, indicating two dynamically distinct portions of the binding pocket. Also, two residues in transdomain linkers between lobes 1 and 2 show exchange, providing new insight into the previously proposed domain closure hypothesis. In addition, the concerted motion of helix F suggests a pathway for ligand dissociation (ligand exit from the binding site) without the necessity of domain reopening. Such details about intradomain motions were not obtained from the X-ray structures of the S1S2 domain crystallized with ligands.

1.7.4 Photoaffinity labeling:

Photocovalent modification of a protein can provide valuable information about the location and architecture of the ligand-binding site. In photoaffinity experiments, use

of a purified protein preparation is very helpful, since it decreases nonspecific background labeling. After a labeled protein has been detected, competitors are co-incubated with the photoaffinity label and the target protein to establish if the labeling is selective. Specifically labeled proteins are those that are competitively displaced by a 100 to 1000-fold excess of the unlabelled probe. Specifically labeled proteins are isolated and subjected to limited proteolytic digestion or chemically induced cleavage at specific residues. The most radioactive fragments are localized by electrophoretic or HPLC separation, and the size and composition can be analysed by matrix-assisted laser-desorption and ionization, coupled with time-of-flight (MALDI–TOF) mass spectroscopy or by Edman degradation.

Photoaffinity labeling has been used to identify several important residues in the Torpedo ray nAChR. For example, a choline analog, [^{3}H]4-Benzoylbenzoylcholine (Bz(2)choline) was synthesized as a photoaffinity probe for the Torpedo ray nicotinic acetylcholine receptor (nAChR). Photoaffinity labeling and N-terminal sequence analysis identified the residues γ L109 and δ L111 as the primary, specific sites of Bz(2)choline photoincorporation (Wang et al., 2000). Using the photoaffinity reagent, DDF [p(Dimethylamino)benzenediazonium fluoroborate], residues W149, Y190, C192, C193 were labeled in an agonist-protective manner (Dennis et al., 1988).

1.7.5 Chemical modification studies:

This method is based on the use of group-specific modifying agents. Chemicals that selective modify specific amino acids are employed in this technique. By doing protection experiments, one can also determine if the residue being modified resides is

near the substrate-binding regions. In some instances, one can use irreversible, group-specific, chemical modifiers to react with the protein, followed by protease digestion and peptide sequencing to identify the location of the residue(s) being targeted (similar to the method described for photoaffinity labeling studies).

Miquel et al. employed chemical modification techniques in a study involving purified 5-HT_3Rs from NG108-15 cell membranes (Miquel et al., 1991). Among others, these reagents included NBS (N-Bromosuccinimide): selective for Tryptophan; DTT (dithioethreitol): selective for Cysteine and EEDQ (N-ethoxycarbonyl-2-ethoxy-1,2-dihydroquinolone): selective for Aspartate. The effects of these protein modifying reagents on specific binding of [^{3}H] zacopride binding to 5-HT_3Rs were evaluated. Agents such as EEDQ, which alkylate carboxyl groups did not affect specific binding to zacopride, suggesting that carboxyl group containing residues such as aspartate and glutamate do not participate in recognition of zacopride by 5-HT_3R. On the other hand, NBS significantly inhibited the specific binding of zacopride, suggesting that tryptophan residues participate in an interaction with this antagonist.

1.8: The approach of mutagenesis for protein structure elucidation:

Many of the techniques described above are not suitable for structure elucidation of 5-HT_3R since they require high levels of purified protein. Approaches such as chemical modification studies have been used to study 5-HT_3R binding site, however, these data require confirmation using other methods such as site-directed mutagenesis. Mutagenesis studies also require extensive binding and functional assays for data interpretation. Mutagenesis has proven to be a valuable tool for structure/function studies

in proteins. A systematic, scanning approach is also employed in some instances, where an area of interest in a protein is selected and is sequentially mutated to an amino acid such as alanine or cysteine. This approach is also called "scanning mutagenesis". Different types of scanning mutagenesis are discussed below.

1.8.1. ASM: Alanine Scanning Mutagenesis.

This technique was first reported by Cunningham et al. who performed ASM on the human growth hormone (hGh) receptor to map receptor interactions (Cunningham and Wells, 1989). Subsequently, ASM has been utilized to study a myriad of proteins including human prolactin (Goffin et al., 1992), insulin-like growth factor-1 (IGF-I) receptor (Whittaker et al., 2001), interleukin 4 (IL-4) receptor (Morrison and Leder, 1992), Na,K-ATPase (Arguello et al., 1999), ATP-Gated $P2X_2$ receptor (Koshimizu et al., 1998; Li et al., 2004), calcium channels (Kraus et al., 1998; Peterson et al., 1997; Tedford et al., 2004), Potassium channels (Collins et al., 1997; Harris et al., 2003; Perry et al., 2004; Swartz and MacKinnon, 1997), sodium channels (Maejima et al., 2002; McPhee et al., 1994; McPhee et al., 1995; Yarov-Yarovoy et al., 2002), muscarinic acetylcholine receptors (Lee et al., 1996; Lu and Hulme, 1999; Lu et al., 2001; Ward et al., 1999).

Relatively few ASM studies have been reported so far in the field of ligand-gated ion channels. An ASM study of extracellular loop between the second and third transmembrane domains (TM2–TM3) of the $GABA_A$ receptor has been reported (O'Shea and Harrison, 2000). Two ASM studies have been reported for the glycine receptor, one involving the signature Cys-loop (Schofield et al., 2004) and the other involving residues

in the M1-M2 loop and the M2-M3 loop (Lynch et al., 1997). In case of the nAChR, ASM has been employed to explore the contribution of α TM4 amino acid residues of mouse AChR to channel gating (Bouzat et al., 1998). In 5-HT_3R, ASM has been employed to study D and E binding loops (Yan et al., 1999, Venkataraman et al., 2002). A major aim of this thesis involved the characterization of binding loop C of the murine 5-HT_3R by ASM.

1.8.1.1 Principle of ASM:

In ASM, each amino acid of a chosen region of the protein is sequentially mutated to alanine. Each alanine mutant is characterized and the results are compared with those obtained for WT (wild-type) receptor. Alanine is a good candidate for amino acid replacement for the following reasons:

(a) It does not have any side chain beyond the β-carbon,

(b) It does not alter the main chain conformation, like a glycine and proline substitution,

(c) It does not impose strong steric and electrostatic effects, and

(d) Alanine is the most abundant amino acid in nature and can be found in buried or exposed positions, and in all secondary structures.

1.8.1.2 Data interpretation using ASM:

The effects of individual alanine mutations can be used as a basis for postulating the role of side chain of the mutated amino acid in receptor function, assuming no changes in backbone structure or global conformation have occurred because of the alanine substitution. Since alanine residues are naturally found in both buried and

exposed parts of proteins, alanine substitutions are very well accommodated by a protein. An alanine substitution of a residue that is critical to ligand interactions, receptor structure and/or mechanism will lead to significant changes in expression, binding and/or function.

ASM provides an initial map of a potentially important region, especially for a protein about which very little structural information is available. For the 5-HT_3 receptor, very few residues in the ligand-binding site were known before ASM studies were carried out on B, D, C and E loop regions of the binding site. After identification of potentially key residues from the initial alanine scan, these residues can be further studied using other mutations. Approaches such as use of partial agonists to decipher role of mutated residue in gating, molecular modeling based on the homologous AChBP and immunofluorescence assays to study cellular localization of the mutant receptor can also be employed to clarify the importance of a specific amino acid. ASM can also sometimes be used to map secondary structure. After the entire region of interest has been evaluated by ASM, if every second residue shows a large change compared to WT, then the secondary structure is interpreted as β-sheet. If every third of fourth residue shows a large change, the data would better support an α-helix.

1.8.2 SCAM: Substituted cysteine accessibility method:

The substituted cysteine accessibility method (SCAM) was initially used to study the secondary structure of pore-lining domains of ion channels (Akabas, 1998; Akabas et al., 1992). In this method, cysteine residues are sequentially introduced into the protein domain of interest. Cysteine reactivity is then assayed by exposure to highly soluble,

sulfhydryl-specific reagents, such as methanethiosulfonate (MTS) derivatives (Karlin and Akabas, 1998). If a functional property of the channel is irreversibly modified upon exposure to such a reagent, it is assumed that that the cysteine is exposed to the water-accessible protein surface. If every second residue is reactive, then the secondary structure is interpreted as β-sheet(Akabas et al., 1992). If every third or fourth residue is exposed, the structure is interpreted as α-helical (Akabas et al., 1994). Later studies have also employed SCAM to study the structure of extracellular domains of ion channels (Lynch et al., 2001; Wagner and Czajkowski, 2001). However, a disadvantage of applying this approach outside the pore regions is that a lack of functional modification of a residue does not necessarily indicate that the residue has not reacted, i.e., negative results cannot be interpreted. However, this limitation is less likely to affect SCAM studies looking at channel pore regions, wherein the environment is spatially restricted and the attachment of a large side chain usually alters channel kinetics. Thus SCAM studies of pore regions tend to more accurately reflect cysteine reactivity. The other limitation of SCAM is that the Cysteine substitution can itself alter function significantly in comparison to the WT receptor.

Two separate SCAM studies on the murine 5-HT_{3A}R have concluded that the M2 region of the channel is α-helical in structure, although conclusions about the exact location of the gate in the M2 region were different in each study (Panicker et al., 2002; Reeves et al., 2001). Various extensions to this technique have also been employed. For example, by determining changes in cysteine reactivity in various functional states (such

as closed, open, and desensitized), it may be possible to draw conclusions about state-dependent structural changes (Pascual and Karlin, 1998).

1.8.3 WSM: Tryptophan scanning mutagenesis:

This approach involves sequentially introducing tryptophan residues one at a time into the domain of interest. Because tryptophan side chains are bulky, it is assumed that if they protrude into the relatively fluid lipid bilayer they should be less likely to disrupt receptor structure and function than if they protrude towards the protein interior (Choe et al., 1995). Functional parameters such as agonist EC_{50} are measured for each mutant receptor, and then a correlation is drawn between the position of the introduced tryptophan and the severity of the functional change seen as compared to WT receptor. As with SCAM, any resulting periodicity is interpreted as β-sheet or α-helix.

1.1.1 Sodium channel

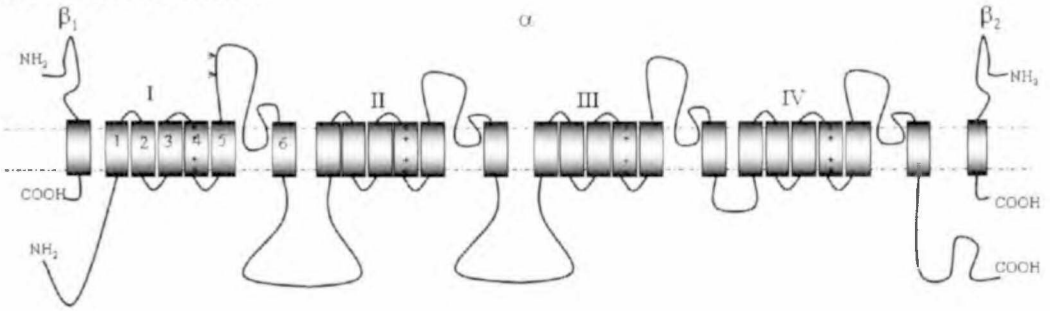

1.1.2 Calcium channel

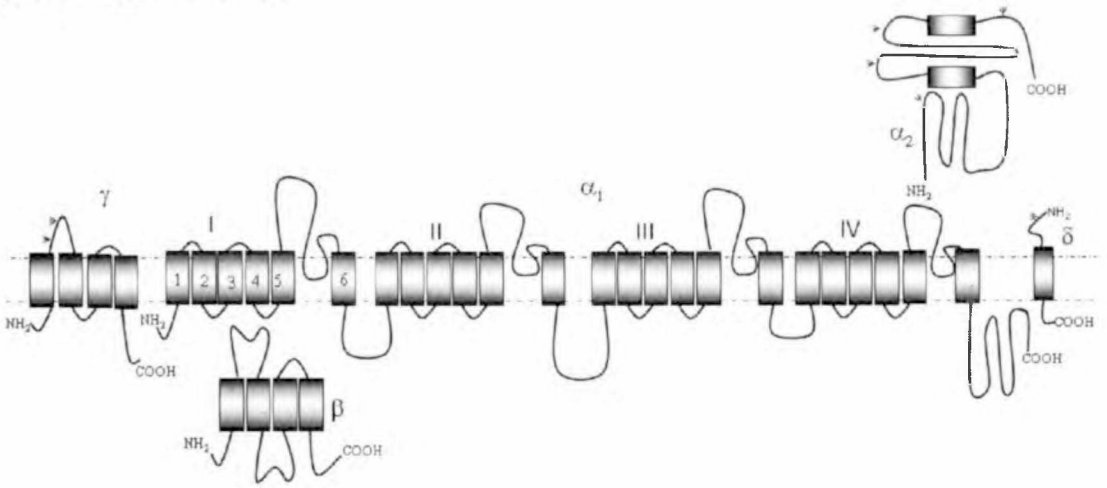

1.1.3 Potassium channel

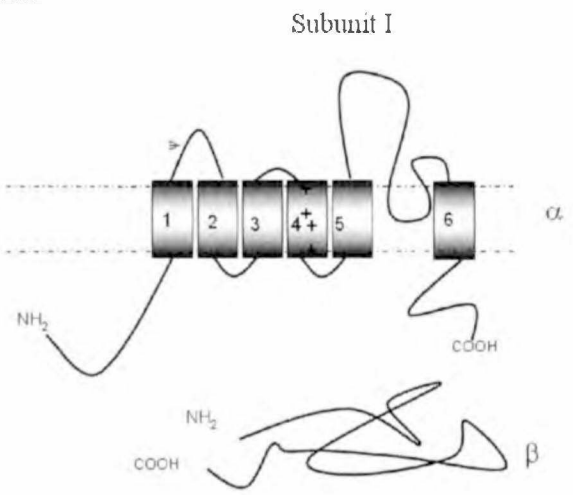

1.1.4 Inward rectifier potassium channel

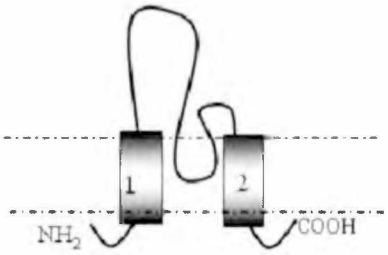

1.1.5 5-HT_3 receptor: Member of the extracellular ligand -gated ion channel family

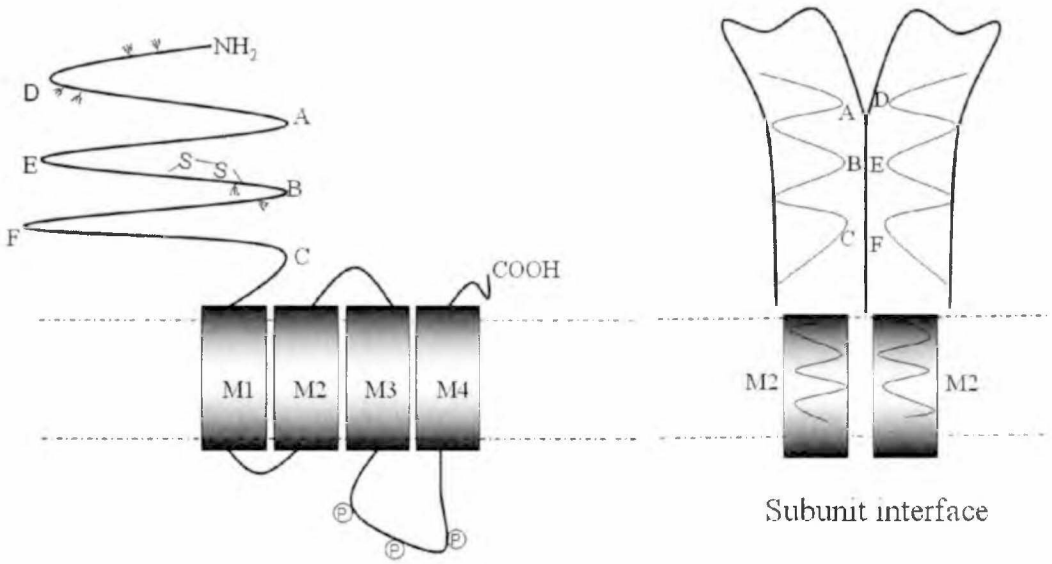

1.1.6 Pore formation and symmetry in ion channels

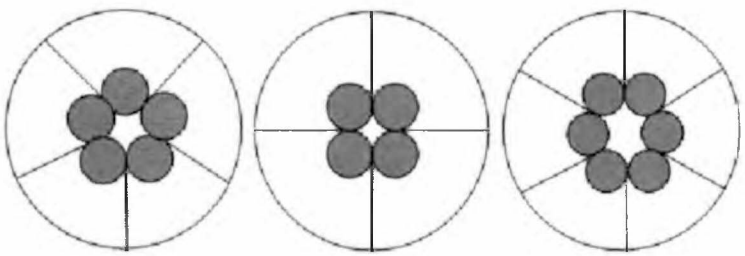

Voltage-gated **Ligand-gated** **Gap junction**

Figure 1.1 Ion channels: This figure illustrates the membrane topology and arrangement of different classes of ion channels.
Figure 1.1.1 Sodium channel : This figure shows the topology of a sodium channel
Figure 1.1.2 Calcium channel: This figure shows the topology of a calcium channel.

Figure 1.1.3 Potassium channel: This figure illustrates a single subunit of a potassium channel;

Figure 1.1.4 Inward rectifier potassium channel: This figure illustrates an inward rectifier potassium channel.

Figure 1.1.5 5-HT_3 receptor: Member of the extracellular ligand -gated ion channel family: This figure shows the topology of a single subunit of a 5-HT_3R, which belongs to the Cys-loop ligand gated ion channel family.

Figure 1.1.6 Pore formation and symmetry in ion channels: This figure compares the pore formation and symmetry in voltage-gated, ligand-gated and gap junction ion channels.

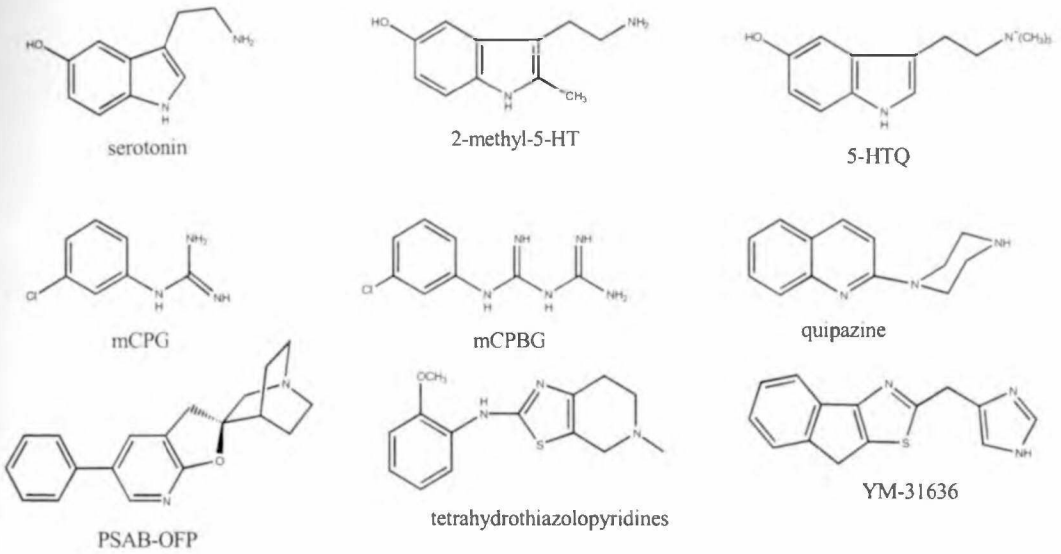

Figure 1.2 Chemical structures of 5-HT_3R agonists
This figure shows the chemical structures of different classes of 5-HT_3R agonists.

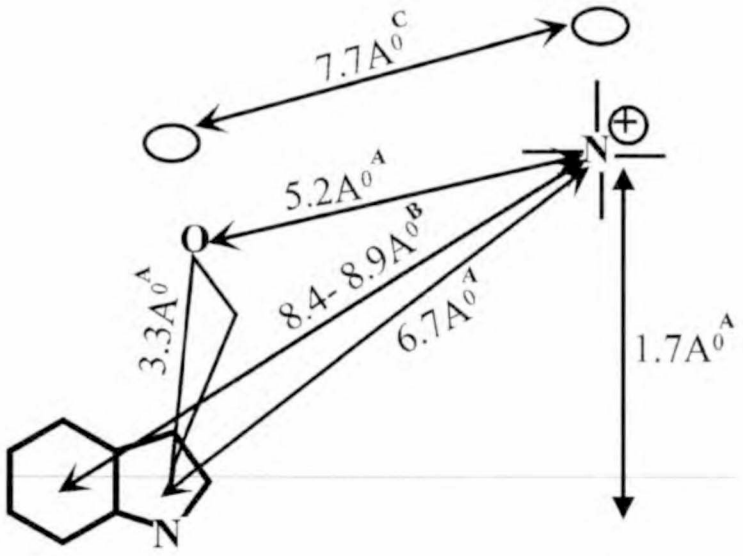

Figure 1.3 Summary of the revised 5-HT_3R antagonist pharmacophore originally developed by Hibert et al..

Summary of 5-HT_3R antagonist pharmacophore model put forth by various research groups. [a] Results put forth by Hibert et al. [b] Results put forth by Swain et al [c] Results put forth by Rizzi et al.

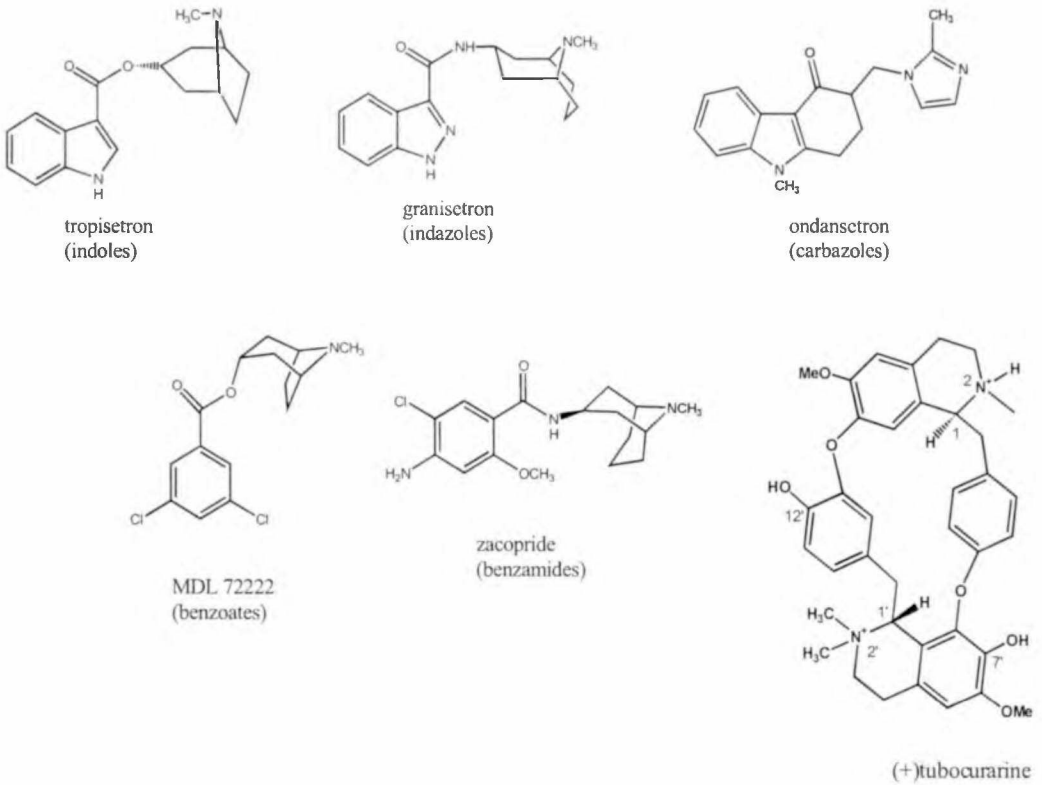

Figure 1.4 Chemical structures of some 5-HT_3R antagonists:
This figure shows the chemical structures of different classes of 5-HT_3R antagonists.

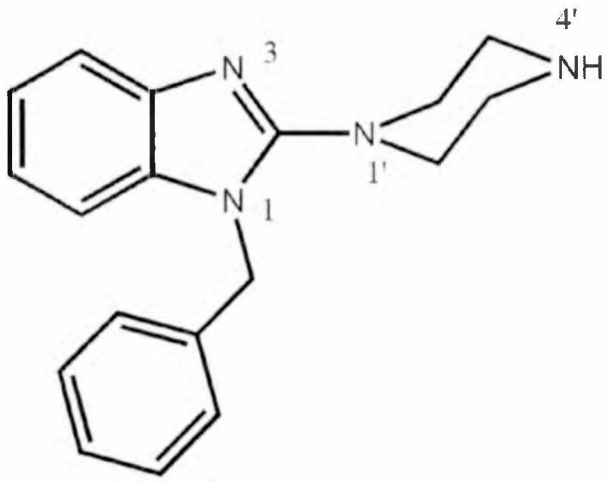

lerisetron

Figure 1.5 Chemical structure of lerisetron
This figure shows the chemical structure of lerisetron, a novel benzimidazole ring-containing 5-HT_3R antagonist.

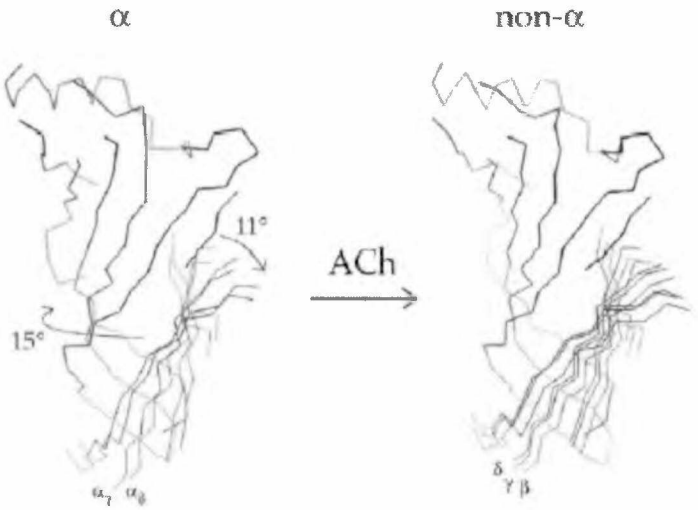

Figure 1.6 Suggested mechanism of activation of muscle nAChR
The mechanism of activation of muscle nAChR proposed by Unwin et al (2002), based on comparison of open and closed state structures of the receptor at 4.6Å.

References

Aapro M (2004) Granisetron: an update on its clinical use in the management of nausea and vomiting. *Oncologist* **9**(6):673-686.

Akabas MH (1998) Channel-lining residues in the M3 membrane-spanning segment of the cystic fibrosis transmembrane conductance regulator. *Biochemistry* **37**(35):12233-12240.

Akabas MH, Kaufmann C, Archdeacon P and Karlin A (1994) Identification of acetylcholine receptor channel-lining residues in the entire M2 segment of the alpha subunit. *Neuron* **13**(4):919-927.

Akabas MH, Stauffer DA, Xu M and Karlin A (1992) Acetylcholine receptor channel structure probed in cysteine-substitution mutants. *Science* **258**(5080):307-310.

Andrews P (1994) 5-HT3 receptor antagonists and antiemesis. 5-Hydroxytryptamine-3 receptor antagonists. (BJJaGJS and King FD eds) pp 255-317, CRC press, Boca Raton.

Arguello JM, Whitis J and Lingrel JB (1999) Alanine scanning mutagenesis of oxygen-containing amino acids in the transmembrane region of the Na,K-ATPase. *Arch Biochem Biophys* **367**(2):341-347.

Arneric SP and Brioni JP (1999) in *Neuronal Nicotinic Receptors Pharmacology and Therapeutic Oppurtunities* pp 43-64, Wiley-Liss (A John Wiley & Sons, Inc.), New York, NY.

Barrantes FJ (1997) The acetylcholine receptor ligand-gated channel as a molecular target of disease and therapeutic agents. *Neurochem Res* **22**(4):391-400.

Beene DL, Brandt GS, Zhong W, Zacharias NM, Lester HA and Dougherty DA (2002) Cation-pi interactions in ligand recognition by serotonergic (5-HT3A) and nicotinic acetylcholine receptors: the anomalous binding properties of nicotine. *Biochemistry* **41**(32):10262-10269.

Bloom FE and Morales M (1998) The central 5-HT3 receptor in CNS disorders. *Neurochem Res* **23**(5):653-659.

Boess FG, Lummis SC and Martin IL (1992) Molecular properties of 5-hydroxytryptamine3 receptor-type binding sites purified from NG108-15 cells. *J Neurochem* **59**(5):1692-1701.

Bouzat C, Roccamo AM, Garbus I and Barrantes FJ (1998) Mutations at lipid-exposed residues of the acetylcholine receptor affect its gating kinetics. *Mol Pharmacol* **54**(1):146-153.

Brejc K, van Dijk WJ, Klaassen RV, Schuurmans M, van Der Oost J, Smit AB and Sixma TK (2001) Crystal structure of an ACh-binding protein reveals the ligand-binding domain of nicotinic receptors. *Nature* **411**(6835):269-276.

Broad LM, Felthouse C, Zwart R, McPhie GI, Pearson KH, Craig PJ, Wallace L, Broadmore RJ, Boot JR, Keenan M, Baker SR and Sher E (2002) PSAB-OFP, a selective alpha 7 nicotinic receptor agonist, is also a potent agonist of the 5-HT3 receptor. *Eur J Pharmacol* **452**(2):137-144.

Catterall WA (1986) Molecular properties of voltage-sensitive sodium channels. *Annu Rev Biochem* **55**:953-985.

Celesia GG (2001) Disorders of membrane channels or channelopathies. *Clin Neurophysiol* **112**(1):2-18.

Celesia GG (2003) Are the epilepsies disorders of ion channels? *Lancet* **361**(9365):1238-1239.

Chen GQ, Sun Y, Jin R and Gouaux E (1998) Probing the ligand binding domain of the GluR2 receptor by proteolysis and deletion mutagenesis defines domain boundaries and yields a crystallizable construct. *Protein Sci* **7**(12):2623-2630.

Choe S, Stevens CF and Sullivan JM (1995) Three distinct structural environments of a transmembrane domain in the inwardly rectifying potassium channel ROMK1 defined by perturbation. *Proc Natl Acad Sci U S A* **92**(26):12046-12049.

Coleman NS, Marciani L, Blackshaw E, Wright J, Parker M, Yano T, Yamazaki S, Chan PQ, Wilde K, Gowland PA, Perkins AC and Spiller RC (2003) Effect of a novel 5-HT3 receptor agonist MKC-733 on upper gastrointestinal motility in humans. *Aliment Pharmacol Ther* **18**(10):1039-1048.

Collins A, Chuang H, Jan YN and Jan LY (1997) Scanning mutagenesis of the putative transmembrane segments of Kir2.1, an inward rectifier potassium channel. *Proc Natl Acad Sci U S A* **94**(10):5456-5460.

Costall B and Naylor RJ (2004) 5-HT3 receptors. *Curr Drug Targets CNS Neurol Disord* **3**(1):27-37.

Cunningham BC and Wells JA (1989) High-resolution epitope mapping of hGH-receptor interactions by alanine-scanning mutagenesis. *Science* **244**(4908):1081-1085.

Dang H, England PM, Farivar SS, Dougherty DA and Lester HA (2000) Probing the role of a conserved M1 proline residue in 5-hydroxytryptamine(3) receptor gating. *Mol Pharmacol* **57**(6):1114-1122.

Davies PA, Pistis M, Hanna MC, Peters JA, Lambert JJ, Hales TG and Kirkness EF (1999) The 5-HT3B subunit is a major determinant of serotonin-receptor function. *Nature* **397**(6717):359-363.

Dennis M, Giraudat J, Kotzyba-Hibert F, Goeldner M, Hirth C, Chang JY, Lazure C, Chretien M and Changeux JP (1988) Amino acids of the Torpedo marmorata acetylcholine receptor alpha subunit labeled by a photoaffinity ligand for the acetylcholine binding site. *Biochemistry* **27**(7):2346-2357.

Downie DL, Hope AG, Lambert JJ, Peters JA, Blackburn TP and Jones BJ (1994) Pharmacological characterization of the apparent splice variants of the murine 5-HT3 R-A subunit expressed in *Xenopus laevis* oocytes. *Neuropharmacology* **33**(3-4):473-482.

Doyle DA, Morais Cabral J, Pfuetzner RA, Kuo A, Gulbis JM, Cohen SL, Chait BT and MacKinnon R (1998) The structure of the potassium channel: molecular basis of K+ conduction and selectivity. *Science* **280**(5360):69-77.

Dubin AE, Huvar R, D'Andrea MR, Pyati J, Zhu JY, Joy KC, Wilson SJ, Galindo JE, Glass CA, Luo L, Jackson MR, Lovenberg TW and Erlander MG (1999) The pharmacological and functional characteristics of the serotonin 5-HT(3A) receptor are specifically modified by a 5-HT(3B) receptor subunit. *J Biol Chem* **274**(43):30799-30810.

Enna SJ and Bowery NG (1997) The GABA receptors., pp 11-36, Humana Press, Totowa, NJ, USA.

Fozard JR (1984) MDL 72222: a potent and highly selective antagonist at neuronal 5-hydroxytryptamine receptors. *Naunyn Schmiedebergs Arch Pharmacol* **326**(1):36-44.

Fozard JR and Mobarok AA (1978) Blockade of neuronal tryptamine receptors by metoclopramide. *Eur J Pharmacol* **49**(1):109-112.

Gaddum JH and Picarelli ZP (1957) Two kinds of tryptamine receptor. *Br J Pharmacol* **12**(3):323-328.

Glatzle J, Sternini C, Robin C, Zittel TT, Wong H, Reeve JR, Jr. and Raybould HE (2002) Expression of 5-HT3 receptors in the rat gastrointestinal tract. *Gastroenterology* **123**(1):217-226.

Goffin V, Norman M and Martial JA (1992) Alanine-scanning mutagenesis of human prolactin: importance of the 58-74 region for bioactivity. *Mol Endocrinol* **6**(9):1381-1392.

Green T, Stauffer KA and Lummis SC (1995) Expression of recombinant homo-oligomeric 5-hydroxytryptamine3 receptors provides new insights into their maturation and structure. *J Biol Chem* **270**(11):6056-6061.

Gu Y and Hall ZW (1988a) Characterization of acetylcholine receptor subunits in developing and in denervated mammalian muscle. *J Biol Chem* **263**(26):12878-12885.

Gu Y and Hall ZW (1988b) Immunological evidence for a change in subunits of the acetylcholine receptor in developing and denervated rat muscle. *Neuron* **1**(2):117-125.

Hanlon MR and Wallace BA (2002) Structure and function of voltage-dependent ion channel regulatory beta subunits. *Biochemistry* **41**(9):2886-2894.

Hanna MC, Davies PA, Hales TG and Kirkness EF (2000) Evidence for expression of heteromeric serotonin 5-HT(3) receptors in rodents. *J Neurochem* **75**(1):240-247.

Harris T, Graber AR and Covarrubias M (2003) Allosteric modulation of a neuronal K+ channel by 1-alkanols is linked to a key residue in the activation gate. *Am J Physiol Cell Physiol* **285**(4):C788-796.

Herges S and Taylor DA (2000) Involvement of 5-HT(3) receptors in the nucleus accumbens in the potentiation of cocaine-induced behaviours in the rat. *Br J Pharmacol* **131**(7):1294-1302.

Hibert MF, Hoffmann R, Miller RC and Carr AA (1990) Conformation-activity relationship study of 5-HT3 receptor antagonists and a definition of a model for this receptor site. *J Med Chem* **33**(6):1594-1600.

Hope AG, Downie DL, Sutherland L, Lambert JJ, Peters JA and Burchell B (1993) Cloning and functional expression of an apparent splice variant of the murine 5-HT3 receptor A subunit. *Eur J Pharmacol* **245**(2):187-192.

Hovius R, Tairi AP, Blasey H, Bernard A, Lundstrom K and Vogel H (1998) Characterization of a mouse serotonin 5-HT3 receptor purified from mammalian cells. *J Neurochem* **70**(2):824-834.

Hubbard PC, Thompson AJ and Lummis SC (2000) Functional differences between splice variants of the murine 5-HT(3A) receptor: possible role for phosphorylation. *Brain Res Mol Brain Res* **81**(1-2):101-108.

Hui SC, Sevilla EL and Ogle CW (1993) 5-HT3 antagonists reduce morphine self-administration in rats. *Br J Pharmacol* **110**(4):1341-1346.

Imanishi N, Iwaoka K, Koshio H, Nagashima SY, Kazuta K, Ohta M, Sakamoto S, Ito H, Akuzawa S, Kiso T, Tsukamoto S and Mase T (2003) New thiazole derivatives as potent and selective 5-hydroxytriptamine 3 (5-HT3) receptor agonists for the treatment of constipation. *Bioorg Med Chem* **11**(7):1493-1502.

Kamb A, Iverson LE and Tanouye MA (1987) Molecular characterization of Shaker, a Drosophila gene that encodes a potassium channel. *Cell* **50**(3):405-413.

Karlin A and Akabas MH (1998) Substituted-cysteine accessibility method. *Methods Enzymol* **293**:123-145.

Kelley SP, Bratt AM and Hodge CW (2003a) Targeted gene deletion of the 5-HT3A receptor subunit produces an anxiolytic phenotype in mice. *Eur J Pharmacol* **461**(1):19-25.

Kelley SP, Dunlop JI, Kirkness EF, Lambert JJ and Peters JA (2003b) A cytoplasmic region determines single-channel conductance in 5-HT3 receptors. *Nature* **424**(6946):321-324.

Kilpatrick GJ, Bunce KT and Tyers MB (1990) 5-HT3 receptors. *Med Res Rev* **10**(4):441-475.

King F (1994) Structure activity of 5-HT3 receptor antagonists. 5-Hydroxytryptamine-3 receptor antagonists. (B.J.J, King FD and Sanger GJ eds) pp 1-44, CRC press, Boca Raton.

Koshimizu T, Tomic M, Koshimizu M and Stojilkovic SS (1998) Identification of amino acid residues contributing to desensitization of the P2X2 receptor channel. *J Biol Chem* **273**(21):12853-12857.

Kraus RL, Hering S, Grabner M, Ostler D and Striessnig J (1998) Molecular mechanism of diltiazem interaction with L-type Ca2+ channels. *J Biol Chem* **273**(42):27205-27212.

Lankiewicz S, Huser MB, Heumann R, Hatt H and Gisselmann G (2000) Phosphorylation of the 5-hydroxytryptamine3 (5-HT3) receptor expressed in HEK293 cells. *Receptors Channels* **7**(1):9-15.

Lee NH, Geoghagen NS, Cheng E, Cline RT and Fraser CM (1996) Alanine scanning mutagenesis of conserved arginine/lysine-arginine/lysine-X-X-arginine/lysine G protein-activating motifs on m1 muscarinic acetylcholine receptors. *Mol Pharmacol* **50**(1):140-148.

Leslie R, Reynolds D and Newberry N (1994) Localisation of 5HT3 receptors. 5-Hydroxytryptamine-3 receptor antagonists., (B.J.J, King FD and Sanger GJ eds) pp 79-96, CRC press, Boca Raton.

Li Z, Migita K, Samways DS, Voigt MM and Egan TM (2004) Gain and loss of channel function by alanine substitutions in the transmembrane segments of the rat ATP-gated P2X2 receptor. *J Neurosci* **24**(33):7378-7386.

Lu Z (2004) Mechanism of rectification in inward-rectifier K+ channels. *Annu Rev Physiol* **66**:103-129.

Lu ZL and Hulme EC (1999) The functional topography of transmembrane domain 3 of the M1 muscarinic acetylcholine receptor, revealed by scanning mutagenesis. *J Biol Chem* **274**(11):7309-7315.

Lu ZL, Saldanha JW and Hulme EC (2001) Transmembrane domains 4 and 7 of the M(1) muscarinic acetylcholine receptor are critical for ligand binding and the receptor activation switch. *J Biol Chem* **276**(36):34098-34104.

Lynch JW, Han NL, Haddrill J, Pierce KD and Schofield PR (2001) The surface accessibility of the glycine receptor M2-M3 loop is increased in the channel open state. *J Neurosci* **21**(8):2589-2599.

Lynch JW, Rajendra S, Pierce KD, Handford CA, Barry PH and Schofield PR (1997) Identification of intracellular and extracellular domains mediating signal transduction in the inhibitory glycine receptor chloride channel. *Embo J* **16**(1):110-120.

Maejima H, Kinoshita E, Yuki T, Yakehiro M, Seyama I and Yamaoka K (2002) Structural determinants for the action of grayanotoxin in D1 S4-S5 and D4 S4-S5 intracellular linkers of sodium channel alpha-subunits. *Biochem Biophys Res Commun* **295**(2):452-457.

Maksay G, Bikadi Z and Simonyi M (2003) Binding interactions of antagonists with 5-hydroxytryptamine3A receptor models. *J Recept Signal Transduct Res* **23**(2-3):255-270.

Malo MS, Srivastava K, Andresen JM, Chen XN, Korenberg JR and Ingram VM (1994) Targeted gene walking by low stringency polymerase chain reaction: assignment of a putative human brain sodium channel gene (SCN3A) to chromosome 2q24-31. *Proc Natl Acad Sci U S A* **91**(8):2975-2979.

Maricq AV, Peterson AS, Brake AJ, Myers RM and Julius D (1991) Primary structure and functional expression of the 5HT3 receptor, a serotonin-gated ion channel. *Science* **254**(5030):432-437.

McKernan RM, Gillard NP, Quirk K, Kneen CO, Stevenson GI, Swain CJ and Ragan CI (1990) Purification of the 5-hydroxytryptamine 5-HT3 receptor from NCB20 cells. *J Biol Chem* **265**(23):13572-13577.

McPhee JC, Ragsdale DS, Scheuer T and Catterall WA (1994) A mutation in segment IVS6 disrupts fast inactivation of sodium channels. *Proc Natl Acad Sci U S A* **91**(25):12346-12350.

McPhee JC, Ragsdale DS, Scheuer T and Catterall WA (1995) A critical role for transmembrane segment IVS6 of the sodium channel alpha subunit in fast inactivation. *J Biol Chem* **270**(20):12025-12034.

Miquel MC, Emerit MB, Gozlan H and Hamon M (1991) Involvement of tryptophan residue(s) in the specific binding of agonists/antagonists to 5-HT3 receptors in NG108-15 clonal cells. *Biochem Pharmacol* **42**(7):1453-1461.

Mishina M, Takai T, Imoto K, Noda M, Takahashi T, Numa S, Methfessel C and Sakmann B (1986) Molecular distinction between fetal and adult forms of muscle acetylcholine receptor. *Nature* **321**(6068):406-411.

Miyazawa A, Fujiyoshi Y, Stowell M and Unwin N (1999) Nicotinic acetylcholine receptor at 4.6 A resolution: transverse tunnels in the channel wall. *J Mol Biol* **288**(4):765-786.

Morales M and Bloom FE (1997) The 5-HT3 receptor is present in different subpopulations of GABAergic neurons in the rat telencephalon. *J Neurosci* **17**(9):3157-3167.

Morales M and Wang SD (2002) Differential composition of 5-hydroxytryptamine3 receptors synthesized in the rat CNS and peripheral nervous system. *J Neurosci* **22**(15):6732-6741.

Morrison BW and Leder P (1992) A receptor binding domain of mouse interleukin-4 defined by a solid-phase binding assay and *in vitro* mutagenesis. *J Biol Chem* **267**(17):11957-11963.

Niesler B, Frank B, Kapeller J and Rappold GA (2003) Cloning, physical mapping and expression analysis of the human 5-HT3 serotonin receptor-like genes HTR3C, HTR3D and HTR3E. *Gene* **310**:101-111.

O'Shea SM and Harrison NL (2000) Arg-274 and Leu-277 of the gamma-aminobutyric acid type A receptor alpha 2 subunit define agonist efficacy and potency. *J Biol Chem* **275**(30):22764-22768.

Panicker S, Cruz H, Arrabit C and Slesinger PA (2002) Evidence for a centrally located gate in the pore of a serotonin-gated ion channel. *J Neurosci* **22**(5):1629-1639.

Pascual JM and Karlin A (1998) State-dependent accessibility and electrostatic potential in the channel of the acetylcholine receptor. Inferences from rates of reaction of thiosulfonates with substituted cysteines in the M2 segment of the alpha subunit. *J Gen Physiol* **111**(6):717-739.

Peroutka SJ and Snyder SH (1979) Multiple serotonin receptors: differential binding of [3H]5-hydroxytryptamine, [3H]lysergic acid diethylamide and [3H]spiroperidol. *Mol Pharmacol* **16**(3):687-699.

Perry M, De Groot MJ, Helliwell R, Leishman D, Tristani-Firouzi M, Sanguinetti MC and Mitcheson JS (2004) Structural determinants of HERG channel block by clofilium and ibutilide. *Mol Pharmacol.*

Peterson BZ, Johnson BD, Hockerman GH, Acheson M, Scheuer T and Catterall WA (1997) Analysis of the dihydropyridine receptor site of L-type calcium channels by alanine-scanning mutagenesis. *J Biol Chem* **272**(30):18752-18758.

Reeves DC, Goren EN, Akabas MH and Lummis SC (2001) Structural and electrostatic properties of the 5-HT3 receptor pore revealed by substituted cysteine accessibility mutagenesis. *J Biol Chem* **276**(45):42035-42042.

Revel L, Rabasseda X and Castaner J (1999) MKC-733: Treatment of GERD, treatment of constipation, 5HT3 receptor agonist. *Drugs of the Future* **24**:966-968.

Richardson B (1995) The discovery of selective 5-Hydroxytryptamine-3 (5-HT3) receptor antagonists. Serotonin and the scientific basis of anti-emetic therapy., (C.J.D PLRAa and Rejnolds DJM eds) pp 50-59, Oxford Clinical communications, Oxford.

Richardson BP, Engel G, Donatsch P and Stadler PA (1985) Identification of serotonin M-receptor subtypes and their specific blockade by a new class of drugs. *Nature* **316**(6024):126-131.

Rizzi CA, Prudentino A and Giraldo E (1993) Effects on general behaviour and neurotransmitter functions of a new 5-hydroxytryptamine3 receptor antagonist with potential therapeutic relevance in central nervous system disturbances. *Arzneimittelforschung* **43**(10):1033-1041.

Rizzi JP, Nagel AA, Rosen T, McLean S and Seeger T (1990) An initial three-component pharmacophore for specific serotonin-3 receptor ligands. *J Med Chem* **33**(10):2721-2725.

Rocha E, Silva M, Valle J and Picarelli Z (1953) A pharmacological analysis of the mode of action of serotonin (5-hydroxytryptamine) upon the guinea-pig ileum. *Br J Pharmacol* **8**(4):378-388.

Sanger GJ and Jones BJ (1994) Assay techniques for measuring 5-HT3 receptor antagonist activity. 5-Hydroxytryptamine-3 receptor antagonists., (FDJ, BJS and King FD eds) pp 67-78, CRC press, Boca Raton.

Sato C, Ueno Y, Asai K, Takahashi K, Sato M, Engel A and Fujiyoshi Y (2001) The voltage-sensitive sodium channel is a bell-shaped molecule with several cavities. *Nature* **409**(6823):1047-1051.

Schofield CM, Trudell JR and Harrison NL (2004) Alanine-scanning mutagenesis in the signature disulfide loop of the glycine receptor alpha 1 subunit: critical residues for activation and modulation. *Biochemistry* **43**(31):10058-10063.

Spier AD and Lummis SC (2000) The role of tryptophan residues in the 5-Hydroxytryptamine(3) receptor ligand binding domain. *J Biol Chem* **275**(8):5620-5625.

Swain CJ, Baker R, Kneen C, Moseley J, Saunders J, Seward EM, Stevenson G, Beer M, Stanton J and Watling K (1991) Novel 5-HT3 antagonists. Indole oxadiazoles. *J Med Chem* **34**(1):140-151.

Swartz KJ and MacKinnon R (1997) Mapping the receptor site for hanatoxin, a gating modifier of voltage-dependent K+ channels. *Neuron* **18**(4):675-682.

Tedford HW, Gilles N, Menez A, Doering CJ, Zamponi GW and King GF (2004) Scanning mutagenesis of omega-atracotoxin-Hv1a reveals a spatially restricted epitope that confers selective activity against insect calcium channels. *J Biol Chem* **279**(42):44133-44140.

Unwin N (1993) Nicotinic acetylcholine receptor at 9 A resolution. *J Mol Biol* **229**(4):1101-1124.

Unwin N (1995) Acetylcholine receptor channel imaged in the open state. *Nature* **373**(6509):37-43.

Van Hooft JA and Vijverberg HP (1995) Phosphorylation controls conductance of 5-HT3 receptor ligand-gated ion channels. *Receptors Channels* **3**(1):7-12.

Venkataraman P, Venkatachalan SP, Joshi PR, Muthalagi M and Schulte MK (2002) Identification of critical residues in loop E in the 5-HT3ASR binding site. *BMC Biochem* **3**(1):15.

Waeber C, Hoyer D and Palacios JM (1989) 5-hydroxytryptamine3 receptors in the human brain: autoradiographic visualization using [3H]ICS 205-930. *Neuroscience* **31**(2):393-400.

Wagner DA and Czajkowski C (2001) Structure and dynamics of the GABA binding pocket: A narrowing cleft that constricts during activation. *J Neurosci* **21**(1):67-74.

Wang D, Chiara DC, Xie Y and Cohen JB (2000) Probing the structure of the nicotinic acetylcholine receptor with 4-benzoylbenzoylcholine, a novel photoaffinity competitive antagonist. *J Biol Chem* **275**(37):28666-28674.

Ward SD, Curtis CA and Hulme EC (1999) Alanine-scanning mutagenesis of transmembrane domain 6 of the M(1) muscarinic acetylcholine receptor suggests that Tyr381 plays key roles in receptor function. *Mol Pharmacol* **56**(5):1031-1041.

Wells GB, Anand R, Wang F and Lindstrom J (1998) Water-soluble nicotinic acetylcholine receptor formed by alpha7 subunit extracellular domains. *J Biol Chem* **273**(2):964-973.

Werner P, Kawashima E, Reid J, Hussy N, Lundstrom K, Buell G, Humbert Y and Jones KA (1994) Organization of the mouse 5-HT3 receptor gene and functional expression of two splice variants. *Brain Res Mol Brain Res* **26**(1-2):233-241.

Whittaker J, Groth AV, Mynarcik DC, Pluzek L, Gadsboll VL and Whittaker LJ (2001) Alanine scanning mutagenesis of a type 1 insulin-like growth factor receptor ligand binding site. *J Biol Chem* **276**(47):43980-43986.

Yan D, Schulte MK, Bloom KE and White MM (1999) Structural features of the ligand-binding domain of the serotonin 5HT3 receptor. *J Biol Chem* **274**(9):5537-5541.

Yarov-Yarovoy V, McPhee JC, Idsvoog D, Pate C, Scheuer T and Catterall WA (2002) Role of amino acid residues in transmembrane segments IS6 and IIS6 of the Na+ channel alpha subunit in voltage-dependent gating and drug block. *J Biol Chem* **277**(38):35393-35401.

Yellen G, Jurman ME, Abramson T and MacKinnon R (1991) Mutations affecting internal TEA blockade identify the probable pore-forming region of a K+ channel. *Science* **251**(4996):939-942.

Zafra F, Aragon C and Gimenez C (1997) Molecular biology of glycinergic neurotransmission. *Mol Neurobiol* **14**(3):117-142.

Zhong W, Gallivan JP, Zhang Y, Li L, Lester HA and Dougherty DA (1998) From ab initio quantum mechanics to molecular neurobiology: a cation-pi binding site in the nicotinic receptor. *Proc Natl Acad Sci U S A* **95**(21):12088-12093.

Chapter 2: Specific aims and experimental rationale

Before work was started on this project, very few residues in the putative 5-HT_3R ligand-binding site had been characterized. A relatively preliminary picture of the binding site was available. It was known that residues W89 and R91 (loop D), W183 (loop B), E126 and F127 (Loop A) contribute to the binding site. Our laboratory reported three important tyrosines Y141, Y143 and Y153 in the Loop E region of the binding site (Venkatarman et al., 2002). The AChBP had just recently been discovered and no homology models of any LGIC receptor were available. We constructed a preliminary homology model of the murine 5-HT_{3A}R based on the AChBP. Based on this model and previous biochemical studies, it was evident that the +face of the binding site is formed loops A-C and the -face is formed by loops D-F. The model also indicated that Loop C spans across the subunit interface and also implied that this loop plays an important role in forming the binding site. Such a role is also supported from previous reports from Loop C residues (Y190, C192, C193 and Y198) of the nAChR. Regarding agonist action, it was unknown if any region(s) of the binding site specifically modulate the action of any agonist, i.e. the molecular determinants for binding of one agonist vs. the other were unknown. The second 5-HT_3R subunit, i.e. the 5-HT_3B subunit was reported in 1999 and its contribution (if any) to the 5-HT_{3AB}R binding site was unknown (Davies et al., 2002).

In order to develop a refined picture of the 5-HT_3R binding site and understand the role of the B subunit in 5-HT_3R structure and function, we followed a multifaceted approach. This approach involved alanine scanning mutagenesis, molecular modeling,

evaluation of chimeric receptors and SAR (structure activity relationship) studies of lerisetron. The specific aims that employed these approaches are explained below.

2.1 Specific aims of this study:

2.1.1 Aim 1: ASM study and detailed characterization of Loop C region of the 5-HT_3R binding site:

The aim of this study was to conduct an alanine scanning mutagenesis (ASM) of the Loop C region of the murine 5-HT_3R, followed by a detailed characterization of key residues in this region. As discussed earlier, ASM is useful in characterization of a region of a protein about which little is known. Loop C is an ideal candidate for ASM because this region is highly unconserved in the LGIC family. Since ASM involves sequential alanine mutations of *all* amino acids in the region, residues can be studied in an unbiased manner. All mutations are studied using saturation and competition radioligand assays, two-electrode voltage clamp assays, and immunofluorescence assays (as explained in experimental design). Once potentially key residues are identified from the initial scan, they can be evaluated in further detail by more detailed functional assays involving partial agonists. Using conservative mutations, the importance of amino acid side chain characteristics in receptor function can be assessed. Results from such studies also impact studies of other LGICs due to presumed structural similarities between family members. In addition, work on the Loop C region provides more information about an unconserved domain in all LGIC receptors (see chapter 3, figure 3.1, for sequence alignment).

A secondary aim of this study was to correlate the biochemical data obtained in mutagenesis studies with ligand docking calculations obtained from AChBP-based 5-

HT_3R homology models. The docking calculations were carried out by Dr. Zsolt Bikadi. Such models predict interaction of agonists and antagonists with specific residues in the binding site. Such predictions can be assessed by biochemical data and can help in formation of more refined models, new hypotheses about ligand interaction and channel activation mechanisms. The results of this study are discussed in Chapter 3.

2.1.2 Aim 2: Structure activity relationship (SAR) study of lerisetron, a 5-HT_3R antagonist:

The objective of this study was to investigate the importance of N1 substituents of lerisetron, a novel 5-HT_3R antagonist (see chapter 4, Fig 4.1). Lerisetron is a novel 5-HT_3R antagonist benzimadole ring (Orjales et al., 1997), which is currently in Phase III of clinical trials for treatment of chemotherapy-induced emesis (Huckle, 2003). The chemical nature (electrostatic, hydrophobic interaction etc) of N1 substituents that is required for optimal biological activity is unclear. To understand the importance of the N1 substitution, nine N1-substituted lerisetron analogs were synthesized by Dr. Karen Kirschbaum's laboratory. These analogs were evaluated for their biological activity employing two-electrode voltage clamp assays in oocytes expressing human 5-HT_{3A} receptors. Results of this study are discussed in chapter 4.

2.1.3 Aim 3: Investigation of role of B subunit employing A-B chimeric receptors:

As discussed earlier, the role of N-terminal of the B subunit in heteromeric AB receptor function is not known. It is known that the B subunit confers different biophysical and pharmacological properties to the AB receptors. To determine if there were any molecular determinants of structure and/or function in the aminoterminal of the

B subunit, we designed a pilot study involving chimeric constructs of A and B subunits. The results of this study are discussed in Chapter 5.

2.2 Experimental rationale:

When point mutant or chimeric receptors are employed in radioligand binding and functional studies, there is a concern that the changes seen are merely due to structural alterations. In addition, it is also not easy to dissect if an amino acid plays a role in ligand binding, gating or assembly. In order to clearly identify the putative role played by each amino acid or a region of the 5-HT_3R, we have employed a combination of different assays. The rationale behind choosing each assay, inherent advantages and disadvantages are explained below.

2.2.1 Radioligand binding assays:

Radioligand binding assays offer a quick (relative to patch-clamp or two-electrode voltage clamp assays) evaluation of an entire region of a protein such as the binding loop C of the 5-HT_3R. We have carried out both saturation and competition assays in our studies.

2.2.1.1 Saturation binding assays employing [^{3}H] granisetron:

A tritiated form of granisetron, BRL-43694 was employed in saturation binding assays. [^{3}H] granisetron was chosen since it is a highly specific and potent competitive antagonist of the 5-HT_3R. Membrane preparations of mutant receptors expressed in mammalian (*t*SA 201) cells were employed in binding assays to determine K_d (affinity) and B_{Max} values. B_{Max} values of mutant receptors are compared with that of WT receptors. B_{Max} values provide a numerical estimate of mutant receptor expression in

mammalian cells. If the K_d value of a mutant receptor is not significantly different from the WT receptor, it suggests that the alanine mutation has not caused any global structural changes in the protein. However, if large changes in K_d value are seen, it is not easy to distinguish if the binding detected indicates binding to cell-surface receptors or intracellularly located receptors/receptor subunits. Some mutant or chimeric receptors can be intracellularly retained and can still show binding to [^{3}H] granisetron. In such cases, an epitope tag can be added to the mutant/chimeric receptor to determine cellular localization by fluorescence microscopy.

2.2.1.2 Competition assays:

Competition assays are performed with agonists such as 5-HT and *m*CPBG in the presence of [^{3}H] granisetron. Such assays provide a quick initial estimate of any significant changes in affinity of the agonist for the mutated receptor compared to WT receptor. Typically, the mutants that show large changes in affinity in competition assays also produce changes in electrophysiological assays. Although these changes are usually not quantitatively similar in radioligand and electrophysiological assays, they typically follow the same trend. Agonists, unlike antagonists propel the receptor population to the desensitized state, which is presumably the most dominant state of the receptor in such competition assays. Thus, competition assays presumably reflect the affinity of the agonist for the desensitized state of the receptor.

2.2.2 Electrophysiological assays:

Two-electrode voltage clamp assays are carried out using mutant receptors expressed in *Xenopus laevis* oocytes. This expression system is especially useful for

characterization of mutant receptors that show very poor expression levels in mammalian expression systems. *Xenopus* oocytes produce large number of mutant receptors that can be studied relatively easily and quickly using two electrode voltage clamp assays. On the other hand, post-translational modifications may be different in *Xenopus* oocytes as compared to mammalian cells. Also, certain ion channels can not be studied in *Xenopus* oocytes if the similar ion channel is also natively expressed in oocytes. These concerns should be borne in mind and comparison of two-electrode voltage clamp data with whole-cell patch-clamp assays in mammalian cells should be carried out for the WT receptors.

If application of an agonist elicits a current from an oocyte expressing a mutant 5-HT_3R, it indicates cell surface expression of intact pentameric receptors. Biophysical parameters such as EC_{50}, Hill number (n_H) and I_{Max} (maximal current elicited upon application of agonist) can be calculated from such assays. I_{Max} values indicate receptor number. A significant decrease in I_{Max} value for all agonists indicates decreased expression. However, if there is no concurrent change in B_{Max} value, or if the decrease in I_{Max} is specific for an agonist, the mutation has selectively decreased efficacy for that agonist. Changes in EC_{50} values for a mutant receptor can occur due to a change(s) in binding and/or gating steps in the receptor activation pathway. A decrease in receptor number alone does not change the EC_{50} value. A role in gating can be studied employing the partial agonist approach (described in Chapter 3).

2.2.3 Molecular modeling:

The discovery of the AChBP in the snail *Lymnaea stagnalis* has accelerated LGIC studies by making possible homology based receptor modeling. Homology models of 5-HT_3R enable improved interpretation of biochemical data from mutagenesis studies. 5-HT_3R ligands can be computationally docked into such homology model. Such docking calculations for multiple ligands can be correlated with biochemical experiments. The docking calculations and biochemical experiments are independently performed without influencing each other. Corroboration of biochemical data with the information obtained from docking calculations can also provide information about protein dynamics/movements of the protein between various conformational states. Based on the biochemical data, the homology model can be further refined and newer models of the receptor can be constructed.

If ligand docked models predict that a residue is not within 4Å of ligand and if biochemical data do not support a role in binding, it can be concluded that the particular residue is not involved in ligand binding. Similar conclusions about gating can also be reached using a combination of partial agonist data and molecular modeling.

2.2.4 Immunofluorescence assays:

If a mutation fails to produce detectable binding to radioligand and/or electrophysiological responses to agonists, the cellular localization of the receptor can be determined employing immunofluorescent detection of epitope tagged receptors. For such experiments, FLAG or GFP tagged WT and mutant/chimeric receptors were constructed. To rule out any effects due to insertion of an epitope tag, tagged WT

receptors were evaluated using both radioligand binding and electrophysiological assays. In immunofluorescence assays of tagged mutant receptors, if cell surface expression is abolished, it can be concluded that the mutation causes changes in receptor assembly and/or trafficking. On the other hand, if cell surface expression is unaltered, then the changes observed for the mutation are due to ligand binding and/or gating.

References

Davies PA, Pistis M, Hanna MC, Peters JA, Lambert JJ, Hales TG and Kirkness EF (1999) The 5-HT3B subunit is a major determinant of serotonin-receptor function. Nature 397(6717):359-363.

Huckle R (2003) Lerisetron. FAES. *Curr Opin Investig Drugs* **4**(7):874-877.

Orjales A, Mosquera R, Labeaga L and Rodes R (1997) New 2-piperazinylbenzimidazole derivatives as 5-HT3 antagonists. Synthesis and pharmacological evaluation. *J Med Chem* **40**(4):586-593.

Venkataraman P, Venkatachalan SP, Joshi PR, Muthalagi M and Schulte MK (2002) Identification of critical residues in loop E in the 5-HT3ASR binding site. *BMC Biochem* **3**(1):15.

Chapter 3: Characterization of residues in the loop C region of the murine 5-HT_{3A}R by site-directed mutagenesis.

3.1 Abstract

Sequence and predicted structural similarities between members of the Cys-loop family of ligand-gated ion channel receptors and the acetylcholine binding protein (AChBP) suggest that the ligand-binding site is formed by six loops that intersect at subunit interfaces. We investigated the role of amino acids of the loop C of the murine 5-HT_{3AS}R by site-directed mutagenesis. Mutant receptors were evaluated using radioligand binding, two-electrode voltage clamp and immunofluorescence studies. Two structurally distinct agonists, 5-HT and *m*CPBG; as well as the antagonist granisetron were evaluated on mutant receptors. In addition, electrophysiological studies comparing efficacies of agonists and partial agonists were carried out to elucidate the role of key amino acids in the receptor gating mechanism. Our results indicate that 5-HT and *m*CPBG interact differentially with the Loop C region. To further corroborate our observations, we carried out ligand docking calculations for 5-HT and *m*CPBG using an AChBP-based 5-HT_3R homology model. The combined results indicate that D229 is an important difference in the binding modes of 5-HT and *m*CPBG. While D229 is critical for binding of 5-HT and not *m*CPBG, mutation of I228 differentially modulates gating by 5-HT and not *m*CPBG. In addition, residues E225, F226 and Y234 from loop C are involved in mediating actions of both 5-HT and *m*CPBG.

3.2 Introduction

The serotonin type 3 receptor (5-HT_3R) is a member of the Cys-loop superfamily of ligand-gated ion channel (LGIC) receptors that includes nicotinic acetylcholine, $GABA_A$, $GABA_C$ and glycine receptors (Maricq et al., 1991). These receptors are membrane-bound ion channel coupled receptors that mediate fast synaptic transmission in both peripheral and central nervous systems. 5-HT_{3A} subunits form homopentamers that yield characteristic inward currents with rapid onset and desensitization on exposure to agonist. The ligand-binding site is present in the extracellular amino terminal domain, at the subunit interface. 5-HT_{3A}R antagonists are clinically used for the treatment of chemotherapy-induced emesis, and are being evaluated for several other conditions including alcoholism (Costall and Naylor, 2004)

Sequence and predicted structural similarities between LGIC receptors and the acetylcholine binding protein (AChBP) suggest that the ligand-binding site is formed from six loops, A-F, which intersect at the subunit interfaces (Arias, 2000; Brejc et al., 2001; Le Novere et al., 2002; Reeves et al., 2003). Several important residues in the 5-HT_3R binding domain have been identified: E129, F130 (loop A), W183 (loop B), E225, Y234 and E236 (loop C), and W90 and R92 (loop D) (Boess et al., 1997; Price and Lummis, 2004; Schreiter et al., 2003; Spier and Lummis, 2000; Steward et al., 2000; Yan et al., 1999). Earlier work from our laboratory identified three important tyrosine residues (Y141, Y143 and Y153) in the loop E region of the 5-HT_3R (Venkataraman et al., 2002). The development of AChBP-based homology models of the 5-HT_3R binding domain

have also greatly increased our understanding of binding interactions of agonists and antagonists (Brejc et al., 2001; Maksay et al., 2003; Reeves et al., 2003).

Previously, residues in the loop C region have been shown to contribute to the higher potency of *d*-TC at the mouse 5-HT_3R as compared to human receptors (Hope et al., 1999). This region has also been shown to contribute to the selective potency of 1-phenylbiguanide at human 5-HT_3Rs (Lankiewicz et al., 1998). Similarly, the loop C region has also been implicated in the higher potency of *m*CPBG at rat 5-HT_3Rs (Mochizuki et al., 1999). 5-HT and *m*CPBG have been shown to exhibit distinct profiles on the murine 5-HT_{3A}R. *m*CPBG shows higher apparent affinity, slower association rates and higher affinity for the desensitized state compared to 5-HT (Bartrup and Newberry, 1996; Mott et al., 2001; van Hooft and Vijverberg, 1997). The molecular basis of these differences is not known. Recently, residues E225, Y234 and E236 from the loop C region of the mouse 5-HT_3R have been postulated to play a role in the ligand binding and/or gating (Price and Lummis, 2004; Schreiter et al., 2003). However, the assignment of a role in gating for the aforesaid residues is speculative since it is based only on changes in EC_{50} and/or K_i values (Colquhoun, 1998). A comparison of unliganded and liganded crystal structures of AChBP suggests that the loop C region undergoes the largest movement after agonist binding (Celie et al., 2004). A substituted cysteine accessibility method (SCAM) study of the loop C region of the β_2 $GABA_A$R also implicates this region in conformational changes after agonist binding (Wagner and Czajkowski, 2001). The loop C region in the 5-HT_3R is likely to play a similar role.

However, a detailed evaluation of the role of each loop C residue in ligand binding and gating remains unavailable.

In this study, we carried out a comprehensive analysis of the putative loop C region in the murine 5-HT_{3A}R by sequentially mutating each residue in this region. All mutants were characterized by radioligand binding and electrophysiological assays. Immunofluorescence assays were carried for mutants that ablated binding and/or function. We also employed electrophysiological studies comparing efficacies of 5-HT, *m*CPBG and the partial agonist 2-methyl 5-HT (2-Me 5-HT) to demarcate the role of the mutated residue in gating of the receptor. Residues E225, F226, D228, I229 and Y234 were identified as critical for ligand interaction. Our experimental results support differences in modes of interaction of 5-HT and *m*CPBG with the loop C region. To further investigate these differential interactions, we employed docking studies using a 5-HT_3R homology model based on the AChBP. The experimental results are in good agreement with the ligand docking calculations. The combined results show that D229 is a major point of difference in the modes of interactions of 5-HT and *m*CPBG with the murine 5-HT_{3A}R. Our results also support a role of residues E225, F226 and Y234 in gating of the receptor. On the other hand, mutation of I228 selectively alters gating by 5-HT and not *m*CPBG. S233 and Y234 are also critical for receptor assembly and/or trafficking. In combination, the experimental and modeling data reveal an emerging picture of distinct interactions of 5-HT and *m*CPBG with the Loop C region of the 5-HT_{3A}R.

3.3 Materials and Methods:

[^{3}H] granisetron was purchased from New England Nuclear (NEN, MA, US). 5-HT and 2-Me 5-HT were obtained from Spectrum and *m*CPBG was obtained from Research Biochemical International (MO, US) . *Xenopus laevis* frogs and frog food were obtained from Xenopus Express (FL, US). Sigma Type II collagenase was purchased from Sigma Aldrich (MO, US). All other chemicals were purchased from Fisher Scientific (TX, US).

3.3.1 Site-directed mutagenesis and epitope tagging:

Site directed mutagenesis was performed as described earlier (Venkataraman et al., 2002), using either the QuickChange® mutagenesis kit, (Stratagene, CA, US) or the pAlter altered sites mutagenesis kit (Promega, WI, US). In order to add a C-terminal FLAG epitope tag, the WT cDNA was cloned into the pCMV 4.1 vector (Stratagene, CA, US). This WT-FLAG cDNA was then used as a template to create the FLAG-tagged F226A, S233A and Y234A mutations using the QuickChange® mutagenesis kit. All constructs were confirmed by restriction digests and DNA sequencing (UC Davis, CA, US).

3.3.2 Cell culture and transient transfection:

*t*SA 201 cells (a derivative of HEK 293 cells) were cultured in Dulbecco's modified Eagle medium (DMEM, New Life Technologies, NY, US) supplemented with 10% fetal bovine serum and 100 units/ml penicillin/streptomycin in a humidified 5% CO_2 atmosphere at 37°C. For radioligand binding studies, *t*SA201 cells were plated on 90mm culture dishes at a density of 5 x 10^6 cells/dish and grown for 9 hours prior to transfection.

The cells were transfected with 20μg/ dish WT or mutant plasmid DNA using a calcium phosphate transfection kit (New life technologies, NY, US). Transfected cells were supplemented with fresh DMEM 12-15 hours after transfection and harvested 36 hours later.

3.3.3 Radioligand binding assays:

These assays were performed as described earlier (Venkataraman et al., 2002). Briefly, transfected cells were scraped from the dishes, washed twice with PBS (New Life Technologies, NY, US), then resuspended in 1.0 ml PBS with protease inhibitor cocktail /100mm dish (Complete protease inhibitor cocktail, Roche, Mannheim, Germany). Immediately prior to use, cells were homogenized in PBS with protease inhibitors using a glass tissue homogenizer, centrifuged, washed and resuspended in 1ml PBS/100 mm dish. Protein content was determined using Lowry assay (Sigma Diagnostics, MO, US). Binding assays were performed in PBS with protease inhibitors. For K_d determinations, 50μl of homogenate was incubated at 37^0C for 1 hour with varying concentrations of [^{3}H] granisetron. Specific binding of [^{3}H] granisetron was determined as the bound [^{3}H] granisetron not displaced by a saturating concentration of a competing ligand (10μM tropisetron). For K_i determinations, 50μl of homogenate was incubated at 37^0C for 2 hours with varying concentrations of inhibitor and [^{3}H] granisetron (NEN, MA). Binding was terminated by rapid filtration onto a GF/B filters.

3.3.4 Electrophysiology:

Details of the chamber and methodology employed for electrophysiological recordings have been described earlier (Joshi et al., 2004). Briefly, ovarian lobes were

surgically removed from *Xenopus laevis* frogs and washed twice in Ca^{+2} free Barth's buffer [82.5mM NaCl / 2.5mM KCl / 1mM $MgCl_2$ / 5mM HEPES, pH 7.4] and gently shaken with 1.5mg/ml collagenase (Sigma type II, Sigma-Aldrich) for 1 hour at 20-25°C. Stage IV oocytes were selected for microinjection. Synthetic cRNAs for WT and mutant mouse $5\text{-}HT_{3As}$ were prepared using the mMESSAGE mMACHINE™ High Yield Capped RNA Transcription Kit (Ambion, TX, US). Each oocyte was injected with 50 nl cRNA at a concentration of 0.2ng/nl. Oocytes were incubated at 19°C for 2 to 4 days before electrophysiological recording. Electrical recordings were made under conventional two-electrode voltage-clamp using an OC-725C oocyte clamp amplifier (Warner Instruments, CT, US) coupled to an online, computerized data acquisition system (Datapac 2000, RUN technologies, CA, US). Recording and current electrodes were filled with 3M KCl and had resistances of 1-2 mΩ. Oocytes were held in a vertical flow chamber of 400 µl volume and perfused with ND-96 recording buffer (96mM NaCl / 2mM KCl /1.8mM $CaCl_2$ / 1mM $MgCl_2$ / 5mM HEPES, pH 7.4) at a rate of 15ml/min. All agonists were prepared in ND-96 buffer and applied at a rate of 25ml/min using an electrical pump.

3.3.5 Comparison of relative efficacy values of agonists on WT and mutant receptors:

Maximal currents elicited by each agonist were recorded using saturating (supramaximal) concentrations of the agonist. 5-HT was assumed to be the full agonist based on data obtained for WT receptor. Relative efficacy of an agonist (relative to 5-HT) was calculated as $I_{Max\ Agonist}/ I_{Max\ 5\text{-}HT}$. For each experiment, maximal currents elicited by

*m*CPBG and 2-Me 5-HT were compared (normalized) to the maximal current elicited by 5-HT on the same oocyte. Such comparisons were repeated on four or more oocytes for WT and mutant receptors. All the normalized data were pooled together to calculate relative efficacy values ± S.E.

3.3.6 Receptor modeling:

Extracellular regions of the homopentameric murine 5-HT_3R were built based on the crystal structure of AChBP from the snail *Lymnaea stagnalis* (PDB entry: 1I9B). The sequence of 5-HT_3R A subunit was taken from the Protein Information Resource (Wu et al., 2002) with an entry code of NF00508262. Multiple sequence alignments of their extracellular regions and AChBP were performed by 'ClustalW' using default parameters (Thompson et al., 1994). Based on this alignment, homology-model building of 5-HT_{3A}R subunit was carried out using the 'Nest' and 'Loopy' facility of the Jackal protein structure modeling package. 'Nest' predicts the experimental dihedral angles chi1 within an error range of 20 degrees for 94% of protein side chains (Xiang and Honig, 2001). Protein loop predictions for amino acid insertions and deletion were done by 'Loopy'(Xiang et al., 2002). Heterodimeric units of the pentamer were built on the basis of crystal structure data to reach minimal root mean standard deviation (RMSD) between the matched monomers. Further refinements of the resulting dimers were carried out by Sybyl 6.6 program (Tripos Inc., MO, US) on a Silicon Graphics Octane workstation under Irix 6.5 operation system. The all-atom model was allowed to relax during a short molecular dynamics run using constraints for backbone atoms. Finally, the entire structures were fully minimized without any restriction using Powell conjugate gradient

method until the maximum derivative was less than 0.050kcal/molÅ. Gasteiger-Huckel partial charges were applied during the calculations. The quality of the model was verified using 'Procheck', as compared with well-refined structures at the same resolution (Laskowski et al., 1993). Intra- and interface H-bonds were analysed by HBPLUS v 3.0, an hydrogen bond calculation program (McDonald and Thornton, 1994).

3.3.7 Ligand docking:

Ligand docking was performed independent of the experimental data, i.e., no constraints based on the experimental data were applied. 'AutoDock 3.0' (Morris et al., 1998) was applied for docking calculations, using the Lamarckian genetic algorithm (LGA) and the 'pseudo-Solis and Wets' (pSW) methods. The parameters included in Autodock are based on the 'Assisted Model Building with Energy Refinement' (AMBER) force field (Cornell et al., 1995). Gasteiger-Huckel partial charges were applied both for ligands and proteins. Solvation parameters were added to the protein coordinate file and the ligand torsions were defined using the 'Addsol' and 'Autotors' utilities, respectively, in Autodock 3.0. The atomic affinity grids were prepared with 0.375Å spacing using the Autogrid program for a 15 x 15 x 22.5Å box around the interface of subunits. Random starting positions, orientations and torsions (for flexible bonds) were used for the ligands. Each docking run consisted of 100 cycles. The number of evaluations was set to 1.5 million. Final structures with RMSD less than 1.5Å were considered to belong to the same cluster. The structures with low energies and high frequencies of docking were subjected to a further minimization by Sybyl and were examined.

3.3.8 Localization of WT and mutant 5-HT_3Rs by immunofluorescence:

WT-FLAG (WT 5-HT_{3A} R with a C-terminal FLAG tag), F226A-FLAG, S233A-FLAG and Y234A-FLAG were characterized by immunofluorescence in *t*SA 201 cells. *t*SA 201 cells transiently expressing either the WT or mutant 5-HT_3Rs were grown in chamber slides in DMEM at 37^0 C. 24-28 hours post transfection, chamber slides were washed thrice with PBS and incubated in freshly prepared ice-cold 4% paraformaldehyde in PBS in order to fix the cells. The chamber slides were then incubated with an anti-FLAG antibody (Sigma, MO, US) at a dilution of 1:200 in PBS for 1 hour at room temperature. In order to determine intracellular expression, cells were permeabilized by incubation with primary anti-FLAG antibody diluted in 0.3% Triton X-100. After three PBS washes of 5 minutes each, slides were incubated for 1 hour at room temperature with goat anti-mouse Rhodamine-conjugated secondary antibody (Jackson ImmunoResearch, PA, US) diluted at 1:1000 in PBS. After three PBS washes, slides were mounted and observed under a Nikon upright microscope with appropriate filters. The cells were viewed under 20 X power and photographed using a Cool Snap digital camera attached to the microscope. Polymorph software was used to acquire digital photographs.

3.3.9 Data Analysis:

Radioligand binding data were analyzed as follows: K_d values were determined by fitting the binding data to the following equation using GraphPad PRISM (San Diego, CA, US): $B = (B_{max} [L]^n) / ([L]^n + K^n)$, where B is specifically bound ligand, B_{max} is the maximum binding at equilibrium, L is the free ligand concentration, K is the equilibrium dissociation constant and n is the Hill coefficient.

IC_{50} values were calculated by fitting the data to the following equation using GraphPad PRISM (San Diego, CA, US): $\theta = 1/ (1+(L/IC_{50}))$, where θ is the fractional amount of [^{3}H] granisetron bound in the presence of inhibitor at concentration L as compared to the amount of [^{3}H] granisetron bound in the absence of inhibitor. IC_{50} is the concentration at which $\theta = 0.5$. K_i values were calculated from IC_{50} values using the Cheng-Prusoff equation.

Dose response curves obtained from electrophysiological data were fit using this equation: $I= I_{Max}/ (1+ EC_{50}/[A]^n)$, where I is the current at a given agonist concentration, I_{Max} is the maximal current, EC_{50} is the agonist concentration that elicits half-maximal current, and n is the Hill coefficient.

3.4 Results:

3.4.1 Characterization of WT receptors:

Saturation binding assays using homogenates of *t*SA 201 cells expressing WT receptors showed that [^{3}H] granisetron labeled a homogeneous population of binding sites (Table 3.1). Competition binding assays were carried out to determine the affinity of agonists, 5-HT and *m*CPBG. The K_i values of both agonists were similar, as shown in Table 3.1.

In order to evaluate functional characteristics, WT receptors were expressed in and evaluated using two-electrode voltage clamp studies in *Xenopus laevis* oocytes (Table 3.2). EC_{50} and n_H values obtained for the WT receptor are in close agreement with previously published data (Hope et al., 1993). The WT-FLAG receptors were functionally indistinguishable from the untagged WT receptors (Data not shown).

K_d, K_i, and EC_{50} measurements for a mutant receptor can indicate that a particular amino acid is potentially important. Scheme 1 shows the del Castillo and Katz mechanism of receptor activation, where the agonist A binds to the receptor and forms the complex AR, which isomerizes to form the open channel AR*.

$$A + R \overset{K_A}{\longleftrightarrow} AR \overset{E}{\longleftrightarrow} AR^*$$

Any alteration in either 'K_A' (equilibrium dissociation constant) or 'E' (equilibrium gating constant) as a result of a mutation will produce an altered EC_{50} or K_i value for an agonist. It is difficult to distinguish if such alterations are due to a change in

binding interaction or due to a change in signal transduction to the channel (gating) (Colquhoun, 1998). The partial agonist approach has been previously employed in $GABA_A$ and glycine receptors to elucidate the role of an amino acid in gating (O'Shea and Harrison, 2000; O'Shea et al., 2000; Rajendra et al., 1995). In this approach, maximal currents (I_{Max}) of full and partial agonist are compared on a single receptor preparation for both the wild-type and mutant receptors. I_{Max} is described by the equation $I_{Max} = inPO_{Max,}$ where i is the single channel conductance, n is the receptor number and PO_{Max} is the maximum fraction of activated receptors. PO_{Max} , in turn is described by the equation, $PO_{Max} = E/(1+E)$ (Lynch, 2004). Since the I_{Max} values for all the agonists are being measured on a single preparation, the receptor number (n) is constant. Assuming that the single channel conductance (i) and the desensitization rates remain unchanged because of the mutation, the measurement of fractional I_{Max} ratios (relative efficacies) can be correlated with changes in E (Lynch, 2004).

We have employed voltage clamp assays to compare rank efficacy of full and partial agonists on WT and mutant receptors. A mutation affecting gating should result in an appreciable reduction in the relative efficacy of a partial agonist in comparison to a full agonist. In such cases, a comparison of relative efficacy ratios of the partial agonist on WT and mutant receptors (for example, $I_{Max\ 2\text{-}Me5HT}/I_{Max\ 5\text{-}HT}$) can provide a very good indication of the role played by the mutated amino acid in gating. A gating role may indicate either alteration of the ability of the receptor to change conformation or the ability of the agonist to stabilize the open conformation of the receptor. To this end, we determined relative efficacies of *m*CPBG ($I_{Max\ mCPBG}/ I_{Max\ 5\text{-}HT}$) and 2-Me 5-HT ($I_{Max\ 2\text{-}Me}$

$_{5\text{-HT}}$ / $I_{Max\ 5\text{-HT}}$) for WT receptors (Fig 3.2 and 3.4). These I_{Max} comparisons were carried out on the same oocyte, and such comparisons were repeated on several oocytes (n>4) as described in 'Materials and Methods'. The EC_{50} value of 2-Me 5-HT was 16.4 ± 1.1μM for WT. The rank efficacy observed for WT receptors was 5-HT> *m*CPBG >> 2-Me 5-HT (Fig 3.2). In comparison to 5-HT, the relative efficacy of *m*CPBG ($I_{Max\ mCPBG}$ / $I_{Max\ 5\text{-HT}}$) was 0.93 ± 0.01, while that of 2-Me 5-HT ($I_{Max\ 2\text{-Me 5-HT}}$ / $I_{Max\ 5\text{-HT}}$) was 0.12 ± 0.002 (Fig 3.4). Average $I_{Max\ 5\text{-HT}}$ and $I_{Max\ mCPBG}$ values for WT receptors were 14.8± 2.2 and 13.7 ± 1.8μA, respectively (Table 3.2).

3.4.2 S227A, I230A, S231A and N232A receptors:

Alanine mutations of residues S227, I230, S231 and N232 did not differ significantly from WT receptors in radioligand and electrophysiological assays (Tables 3.1 and 3.2). The small shifts seen in K_d and EC_{50} values are not significant, considering the drastic alanine mutation. Thus, residues S227, I230, S231 and N232 do not seem to play a significant role in ligand binding, structure and function of the mouse 5-HT_{3AS} R.

3.4.3 E225A receptors:

In radioligand binding assays, E225A receptors showed modest changes in affinity for granisetron, 5-HT and *m*CPBG as compared to WT receptors, with the largest fold change seen for 5-HT (Table 1). In electrophysiological assays, only small changes were noted in EC_{50} values of 5-HT and *m*CPBG. Although the B_{Max} value of E225A receptors was comparable to WT, the average $I_{Max5\text{-HT}}$ and $I_{Max\ mCPBG}$ were significantly lower for E225A receptors as compared to WT receptors. These low I_{Max} values could

either be due to reduced expression of the mutant receptors in oocytes, or due to impaired gating. To determine if a role in gating was involved, we carried out relative efficacy comparisons for E225A receptors. The rank efficacy for E225A receptors was similar to that for WT receptors (i.e. 5-HT> *m*CPBG >> 2-Me 5-HT). However, the efficacy of 2-Me5-HT relative to 5-HT was substantially reduced (0.04 ±0.001) for E225A receptors with a corresponding increase in EC_{50} value to 28.1 ± 3.1 μM (Fig 3.4). This decrease in relative efficacy of 2-Me5-HT suggests a role of E225 in gating.

3.4.4 F226A and F226Y receptors:

F226A receptors did not any significant change in K_d value of granisetron as compared to WT receptors. However, large fold changes in K_i value of 5-HT, with relatively smaller changes in K_i of *m*CPBG were noted (Table 3.1). No responses could be obtained in *Xenopus* oocytes injected with F226A mRNA. Immunofluorescence experiments revealed that F226A receptors were expressed on the cell surface (Fig 3.6). These data indicate that an aromatic residue at position 226 is required for agonist induced channel opening of the murine $5\text{-}HT_{3A}R$.

F226Y receptors showed a radioligand binding profile similar to that of F226A receptors (Table 3.2). A larger fold change in K_i value of 5-HT than that of *m*CPBG was observed. In electrophysiological assays, 5-HT and *m*CPBG elicited responses on F226Y receptors were characterized by decreased I_{Max}, slow onset and slow desensitization (Fig 3.2), with a moderate change in EC_{50}, compared to WT (Table 3.2).

The rank efficacy for F226Y receptors changed to *m*CPBG > 5-HT >> 2-Me5-HT. *m*CPBG elicited currents with I_{Max} values higher than those elicited by 5-HT (I_{Max5-}

$_{HT}$ = 0.5 ± 0.2μA, $I_{Max\ mCPBG}$ = 0.8 ± 0.2μA). Thus the relative efficacy of *m*CPBG was 1.6 ± 0.07, as compared to 0.93 ± 0.01 for WT receptors (Fig 3.4). Concentrations of 2-Me 5-HT as high as 3mM yielded currents with amplitudes of ≤ 0.01μA in all oocytes expressing F226Y receptors. Given the low I_{Max} values obtained for the most efficacious agonist (*m*CPBG); we could not determine an EC_{50} value of 2-Me 5-HT for the F226Y receptor. The changed rank efficacy and response kinetics of F226Y receptors are indicative of a role in gating for F226 residue. This role is also supported by significantly reduced I_{Max} values with no concurrent reduction in B_{Max}, although we cannot rule out the possibility that the low I_{Max} values are due to reduced receptor expression in *Xenopus* oocytes (Table 3.1 and 3.2).

3.4.5 I228A receptors:

I228A receptors showed a ~ 4 fold increase in K_d value of granisetron. The K_i value of 5-HT selectively increased by 235 fold, with only a 5 fold change in K_i value of *m*CPBG (Table 3.1). This selective effect for 5-HT was also reflected in the response kinetics for 5-HT and *m*CPBG (Fig 3.3). While 5-HT responses were markedly altered for I228A receptors, with decreased I_{Max}, slow onset and slow desensitization as compared to WT, *m*CPBG responses appeared normal (Table 3.2, Fig 3.3). In comparison to fold changes seen in radioligand binding assays, smaller fold changes were seen in EC_{50} values of 5-HT and *m*CPBG (~ 10 fold and 16 fold respectively).

In oocytes expressing I228A receptors, *m*CPBG was remarkably more efficacious than 5-HT. This caused a change in rank efficacy to *m*CPBG >> 5-HT>> 2-Me5-HT (Fig 3.3). While the average $I_{Max\ mCPBG}$ levels for this mutation were 13.5 ± 1.5μA, $I_{Max\ 5\text{-}HT}$

levels were significantly reduced to ~ 0.5 ± 0.1μA in the same oocytes. However, the I_{Max} $_{m}$CPBG value was not significantly different than that obtained for the WT receptor (Table 3.2). These data indicate a decrease in efficacy of 5-HT and not *m*CPBG on I228A receptors. Application of 2-Me 5-HT produced no detectable currents in these oocytes at concentrations up to 10mM. Therefore, an EC_{50} value of 2-Me 5-HT could not be determined for I228A receptors. These data indicate that I228A mutation selectively alters gating of the receptor by 5-HT and not *m*CPBG. This selective role is further supported by the significantly reduced $I_{Max5\text{-}HT}$ value (Table 3.2) with no concurrent reduction in B_{Max} value (Table 3.1).

3.4.6 D229A receptors:

D229A receptors caused an 8 fold change in K_d value of granisetron, possibly indicating an interaction of D229 with granisetron (Table 3.1). Similar to the selective effect observed for mutations of F226 and I228 residues, a 140 fold change in K_i of 5-HT, with no significant change in K_i of *m*CPBG was seen for D229A receptors (Table 3.1). Similarly, in electrophysiological assays of D229A receptors, a 12.5 fold change in EC_{50} was observed for 5-HT, while no significant change was noted for *m*CPBG. These data suggest that D229 is selectively involved in binding to 5-HT, but not *m*CPBG.

In order to determine if D229A receptors affect gating, relative efficacies were compared in *Xenopus* oocytes. D229A receptors displayed I_{Max} values identical to WT (Table 3.2). The EC_{50} value of 2-Me-5-HT was 10.3 ± 0.6μM, not significantly different from WT. The rank efficacy for D229A receptors was identical to WT: 5-HT> *m*CPBG

>> 2-Me 5-HT (Fig 3.4). The overall data indicate that D229A receptors alter binding to 5-HT and do not alter gating of the receptor.

3.4.7 S233A and S233T receptors:

S233A receptors ablated both binding and function (Table 3.1 and 3.2). Immunofluorescence experiments revealed that S233A receptors were not expressed on the cell surface (Fig 3.6). However, fluorescence was detected in permeabilized cells indicating either incompletely or incorrectly assembled subunits that remain intracellularly located. These data suggest that S233A mutation affects receptor assembly and/or trafficking to the cell membrane.

The S233T receptors were indistinguishable from WT receptors in both radioligand and electrophysiological assays (Table 3.1 and 3.2). To confirm that a role in gating was not involved, relative efficacies were also determined for the S233T mutation. The rank efficacy was unaltered for S233T receptors as compared to WT receptors (Fig 3.4). The I_{Max} values were also largely unaffected as shown in Table 3.2.

3.4.8 Y233A and Y234F receptors:

Similar to S233A receptors, Y233A mutation ablated binding and function. Immunofluorescence data showed that Y233A mutation does not express on the cell surface, but remains intracellularly located (Fig 3.6). Thus Y233A mutation affects either receptor assembly and/or trafficking to cell surface.

To further study the Y234 residue, the conservative Y234F mutation was evaluated. An 11 fold increase in K_d value of granisetron as compared to WT was seen,

suggesting a possible interaction between Y234 and granisetron (Table 3.1). Large fold changes in K_i values of both 5-HT (185 fold) and *m*CPBG (125 fold) were noted (Table 3.1) even for this conservative mutation, indicating a possible interaction of Y234 with both agonists. Only moderate changes in EC_{50} values were seen in electrophysiological assays of Y234F receptors (Table 3.2).

Relative efficacy comparisons revealed that the rank efficacy for Y234F receptor was significantly altered to *m*CPBG> 5-HT>>> 2-Me5-HT (Fig 3.2). The average $I_{Max\ mCPBG}$ value for Y234F (16.8 ± 1.9μA) was higher than the $I_{Max\ 5\text{-}HT}$ value (13.3 ± 1.5μA) (Table 3.2). This data indicates that either an increase in efficacy of *m*CPBG relative to 5-HT or a decrease in efficacy of 5-HT. The EC_{50} value of 2-Me5-HT for Y234F (11.1 ± 1.4μM) was unaltered compared to WT, while the relative efficacy of 2-Me 5-HT was drastically reduced (0.019 ± 0.001), in comparison to WT receptors (Fig 3.4). These data indicate that residue Y234 plays a role in gating of the 5-HT_3R.

3.4.9 Docking of 5-HT, *m*CPBG and granisetron to the Murine 5-HT_{3A}R model:

Fig 3.5 shows docking of agonists *m*CPBG, 5-HT and antagonist, granisetron to the murine 5-HT_{3A}R model. No constraints based on the experimental data were applied while performing these docking calculations. All ligands are docked in the binding cavity previously described for 5-HT_3Rs (Maksay et al., 2003; Reeves et al., 2003) The presence of numerous aromatic residues (W90, W183, Y143, Y153, Y234, and F226) and acidic residues (E225, E236, D229) at the binding interface suggest that basic ligands can form both salt bridges and cation-π interactions at the binding site. The interactions are also highlighted in Table 3.3.

The docking calculations resulted in two possible models for *m*CPBG with nearly equal energies. The first model of *m*CPBG binding ('1') is shown in Fig 3.5 C. In this case, the guanidino group forms salt bridge with D229. Tyrosines Y153 and Y234 can form hydrogen bonds and/or are involved in cation-π interaction with the guanidino group. W183 is also part of this aromatic pocket. The chloro group of *m*CPBG is near F226 in this model. The following interactions occur in the second model, '2' (Fig 3.5 D): The guanidino group forms a salt bridge with E236, while it is also involved in a cation-π interaction with F226 and Y234. The aromatic ring of *m*CPBG lies nearly parallel to W183 producing weak π -π interaction. Aromatic residues, W90 and Y153 are also in close proximity of the aromatic ring and the chloro group.

Most frequent docking position of 5-HT (Fig 3.5 B) forms similar interactions to that observed for the second *m*CPBG docking model. The amino group is intercalated between the aromatic F226 and Y234 residues, while it is salt bridged with E236. The first difference between the interactions of the two agonists is that the OH group of 5-HT is able to form a hydrogen bond with D229. D229 does not form an interaction with *m*CPBG in model '2', while it forms a salt bridge interaction in the model '1'. Secondly, Y153 can form a hydrogen bond with *m*CPBG in one docking position ('1') and does not in the other ('2').

Fig 3.5 A shows the antagonist granisetron with the lowest energy of docking. Its aromatic rings are inserted to the hydrophobic region of W183, W90 and Y153. Its carbonyl group can interact with D229, while Y234 can form a hydrogen bond with pirazol nitrogen. The bicyclic ammonium ion can interact with N128 and E236.

3.4.10 Comparison of results from docking studies with loop C mutagenesis:

3.4.10.1 Interactions of 5-HT:

Docking calculations predict that residues F226, D229 and Y234 from the loop C region form interactions with the agonist 5-HT (Table 3.3). The radioligand and electrophysiological data for mutations at these positions suggest that these residues interact with 5-HT. Thus, the experimental data for F226, D229 and Y234 are in good agreement with these predictions.

3.4.10.2 Interactions of *m*CPBG:

Two possible binding modes for *m*CPBG were obtained, with substantial differences in specific interactions. Model 1 (Fig 3.5C) predicts interactions of *m*CPBG with F226, D229, Y234 and Y153. All of these interactions have been demonstrated for 5-HT but not *m*CPBG (For Y153, see reference 19). This model also shows an interaction with W183 (loop B). *m*CPBG interactions have been postulated by earlier studies for W183 and E236 (Schreiter et al., 2003; Spier and Lummis, 2000). Our data support interactions at F226 and Y234, but the data for D229 are unsupportive of model 1. In addition, although model 1 predicts the same interacting amino acids as 5-HT, the nature of these interactions are different (Table 3.3). Specifically, a cation-π interaction rather than a π–π interaction is predicted for W183, a π–π interaction rather than a cation-π interaction at F226 and a salt bridge rather than a hydrogen bond at D229. In contrast, model 2 (Fig 3.5D) predicts some differences in interacting amino acids, but, for overlapping residues, the type of interaction is identical (Table 3.3). The first difference is that in this model, D229 does not produce specific interactions with *m*CPBG. Thus,

model 2 would accurately predict a change in binding affinity of 5-HT but not *m*CPBG on D229A receptors, as supported by our data.

3.5 Discussion:

3.5.1 Residues involved in mediating binding and gating by 5-HT:

The docked model of 5-HT shows two aromatic residues, F226 and Y234; and two acidic residues, D229 and E236 from loop C participating in important interactions with 5-HT.

A cation-π interaction between F226 and 5-HT is indicated in the docked 5-HT model. The results for F226 mutations support a role of F226 in both binding and gating. Considering the gaps in the sequence alignment of the loop C region (Fig 3.1), F226 in the mouse 5-HT$_{3AS}$R appears homologous to Y190 of the nAChR α_7R, which has been to be important for binding and/or gating (Akk et al., 1999; O'Leary and White, 1992; Tomaselli et al., 1991). More importantly, crystal structures of AChBP bound to carbamylcholine and nicotine indicate a hydrogen bond forms between the homologous residue (Y185) and K139 (loop B) in the ligand-bound confirmation (Celie et al., 2004)

Our data indicate a role for D229 in binding of 5-HT to the 5-HT$_{3AS}$R, but not in gating. This observation is supported by the docked 5-HT model which indicates a hydrogen bond between D229 and 5-HT. D229 is homologous to C193 in the mouse nAChR, which has been identified as critical in the binding site of nAChR by photoaffinity labeling and mutagenesis studies (Dennis et al., 1988; Kao et al., 1984; Mishina et al., 1985). The homologous C188 in the AChBP crystal structure has been shown to be in contact with nicotine (Celie et al., 2004).

Mutation of Y234 to alanine ablated function, probably by preventing proper cell surface expression. In contradiction to these results, authors of a recent study reported

that Y234A receptors were expressed on the cell surface (Price and Lummis, 2004). This difference could be due to expression levels below our level of detection or the use of different antisera in the said study. Our data indicate a role for Y234 in mediating binding and gating by 5-HT. In accordance with these results, docking studies show a cation-π interaction between 5-HT and Y234. A recent crystal structure of the AChBP shows that the homologous residue (Y192) makes an aromatic contact with nicotine (Celie et al., 2004). Residues homologous to Y234 are strictly conserved as aromatic throughout the family (Fig 3.1). Separate lines of evidence have implicated the homologous Y198 in the nAChR in binding of acetylcholine and/or gating (Akk et al., 1999; O'Leary and White, 1992; Tomaselli et al., 1991). The homologous Y205 in the β_2 $GABA_AR$ has been shown to be facing into the GABA binding pocket (Wagner and Czajkowski, 2001). Thus data from multiple receptor types support a key role for Y234 in binding and gating mechanisms.

In addition to F226, D229 and Y234, the 5-HT docked model also indicates potential interactions with W183 and E236. There is strong evidence for a cation-π interaction between the amino group of 5-HT and W183 (Beene et al., 2002). While our 5-HT docked model shows a π-π interaction between 5-HT and W183, it should be noted that a small rotation of the carbon chain of 5-HT would re-align the amino group, permitting a cation-π interaction with W183. We hypothesize that the conformational mobility of the saturated carbon chain of 5-HT may allow a conformation where the amino group is not salt bridged with E236, but forms a cation-π interaction with W183. This mobility could play a role during the activation of the $5\text{-}HT_3R$. E236 has been

previously shown to be within 1nm of the ligand-binding site (Schreiter et al., 2003). Our 5-HT docked model corroborates this conclusion by showing a salt bridge formation between E236 and the amino group of 5-HT. E225 is another acidic residue which has been postulated to be involved in both binding and gating of the 5-HT$_3$R (Schreiter et al., 2003). Our partial agonist data support a role of E225 in gating. Since the docking models do not support a binding interaction of E225 with any docked ligand, we propose that E225 may have a moderate involvement in gating, but not binding in the 5-HT$_3$R.

3.5.2 Residues involved in binding of *m*CPBG:

Two models were predicted by docking calculations for *m*CPBG. The combined results for D229 support model 2 for *m*CPBG binding. Thus the *m*CPBG/ 5-HT$_3$R interactions are similar to 5-HT/ 5-HT$_3$R interactions, with D229 being a major point of differences. The types of interactions for overlapping residues in *m*CPBG model 2 are same as those in the 5-HT model.

3.5.3 Mutations of I228 selectively modulate gating by 5-HT and not *m*CPBG:

I228 appears to be selectively involved in 5-HT mediated gating. The exact mechanism behind the 5-HT selective effect for I228 is unclear. Our docking studies show that I228 is within 4Å of docked 5-HT and *m*CPBG and may interact with either ligand. However, only an interaction with 5-HT is supported by experimental data. One explanation for the apparent discrepancy in docking and experimental data for I228 may be that this residue may interact with 5-HT in a different confirmation of 5-HT$_3$R.

3.5.4 Granisetron binding to 5-HT_3R:

Previous studies have implicated W183, E236 and W90 as interacting with granisetron (Schreiter et al., 2003; Spier and Lummis, 2000; Yan et al., 1999). Results of this study indicate that D229 and Y234 also interact with granisetron. The granisetron-docked model indicates close interactions (< 4Å) for residues identified via mutagenesis studies, although specific interactions are indicated only for F226 and Y234. D229 forms a polar interaction, while Y234 forms a hydrogen bond with the pirazol nitrogen. However, our experimental data do not support an interaction between granisetron and F226. This discrepancy may be due to the state of the receptor modeled by the homology model. It has been suggested that the AChBP, on which this model is based, may represent the open state of the receptor (Beene et al., 2004). In contrast, granisetron is thought to bind to the closed or "ground state" of the receptor. In the transition between closed and open states, significant rearrangements are thought to occur within the binding site including movement of the C-loop. Such rearrangements are supported by crystal structures of the AChBP, where the Y185 (homologous to F226) forms a hydrogen bond with K139 (from loop B) in the ligand-bound confirmation (Celie et al., 2004). The result of such rearrangements may close the binding cavity, possibly through movement of the C loop toward the E loop. If the homology model more accurately represents the open state of the receptor, then the docked *m*CPBG and 5-HT models would be expected to better fit the empirical data than would the granisetron model.

3.5.5 Final conclusions:

Results of this study support an emerging picture of 5-HT and *m*CPBG mediated interactions with the loop C region of the 5-HT_3R. Our results identify the molecular determinants of differential action mediated by these two diverse agonists. Partial agonist data also show that the identified loop C residues play a more involved role in gating. In agreement with this conclusion, recent ligand bound crystal structures of the AChBP show that the loop C rearranges and closes down on the bound agonist (Celie et al., 2004).

Mutational studies of nAChR support a role of binding site residues in stabilizing the open state of the receptor (Akk et al., 1999; Chakrapani et al., 2004; Karlin, 2002; Sine, 2002). Similarly, in the 5-HT_3R, E225, F226 and Y234 appear to be involved in the gating mechanism of 5-HT and *m*CPBG, possibly through stabilization of the open state of the 5-HT_{3A}R via direct interaction with either agonist. In contrast, I228 seems to selectively stabilize the 5-HT bound open state of the receptor, while minimally interacting with *m*CPBG. This conclusion provides the simplest explanation of how a gating residue can be ligand (5-HT) specific.

```
                    224 AAAAAAA  AAA  236
m 5-HT3 AS              KEFSIDIS--NSYAE
m 5-HT3 B               HIR-QSSA--GDFAQ
h 5-HT3 A               REFSMESS--NYYAE
h 5-HT3 B               SIL-QSSA--GGFAQ
Torpedo nACh alpha      HWVYYTCCPDTPYLD
m nACh alpha            HWVFYSCCPTTPYLD
m nACh delta            NVDPSVPMDSTNHQD
m nACh alpha 7          NEKFYECC-KEPYPD
h nACh alpha7           SERFYECC-KEPYPD
AChBP                   NSVTYSCCP-EAYED
m GABAA alpha 1         GIVQSS-T--GEYVV
m GABAA beta 1          KKVEFT-T--GAYPR
r GABAA beta 2          KKVVFS-T--GSYPR
m GABAA delta           ELMNFKSA--GQFPR
m GABAA gamma           EVVKTT-S--GDYVV
m Gly alpha 1           CTKHYN-T--GKFTC
```

Figure 3.1 Sequence alignment of the purported loop C region of the 5-HT_{3AS} receptor with other members of the family

The amino acid sequence of the mouse 5-hydroxytryptamine-type 3 A short isoform receptor (m 5-HT_{3AS}R) was aligned with sequences of other ligand-gated ion channel receptors and acetylcholine binding protein (AChBP) using a multi-sequence ClustalX alignment method. The alignment of the purported "loop C" region across various members of the LGIC family and AChBP is shown. Conserved residues are bold and shaded gray. Residues found to be important in this study are marked bold and italicized in the mouse 5-HT_{3AS}R. The numbers at the end indicate position as measured from the N-terminal, excluding the initial methionine in the protein sequence of the mouse 5-HT_{3AS}R. Residues in the mouse 5-HT_{3AS}R that are mutated to alanines are denoted with an 'A' above each wild-type residue.

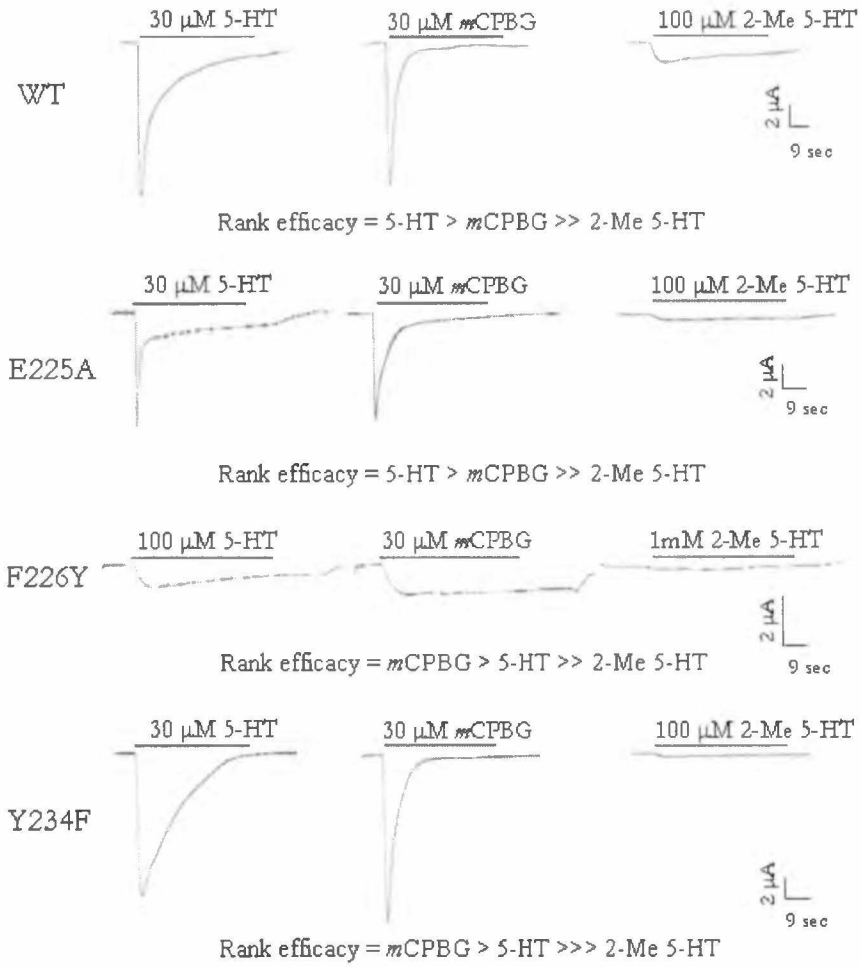

Figure 3.2 Electrophysiological characterization of WT, E225A, F226Y and Y234F receptors expressed in *Xenopus laevis* oocytes

Characteristics of inward currents elicited by application of agonists at supra-maximal concentration are shown for each receptor type. The traces shown for WT and mutant receptors were obtained from the same oocyte. Traces shown are representative of multiple experiments ($n \geq 4$). The solid bar on the top of each trace denotes time of drug exposure, type of agonist used and its concentration. The rank efficacy for each receptor type is also shown. Note that no currents could be detected upon application of 2-Me 5-HT in F226Y and I228A Rs.

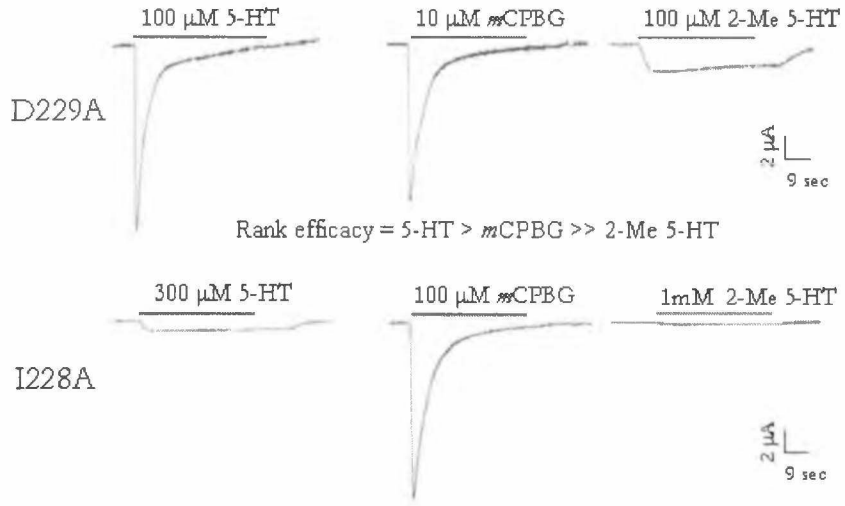

Figure 3.3 Electrophysiological characterization of mutations which differentially interact with 5-HT and *m*CPBG.

Inward currents elicited by application of agonists at supra-maximal concentration are shown for D229A, I228A, Y153A and Y153F mutations. These mutations show differential effects for 5-HT and *m*CPBG in binding and electrophysiological assays. In addition, I228A mutation also selectively alters 5-HT induced response characteristics. The traces shown for wild-type and mutant receptors were obtained from the same oocyte. Traces shown are representative of multiple experiments ($n \geq 4$). The solid bar on the top of each trace denotes time of drug exposure, type of agonist used and its concentration. The rank efficacy for each receptor type is also shown.

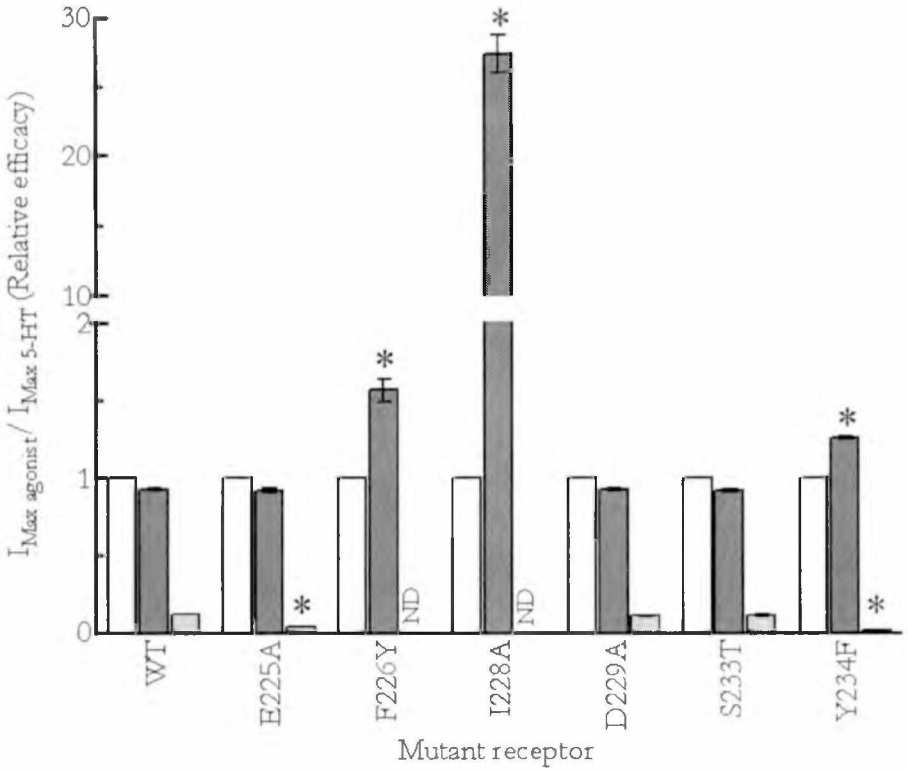

Figure 3.4 Changes in relative efficacies of 2-Me 5-HT and mCPBG for wild-type and mutant receptors.

The bar graph shows a comparison of $I_{MaxAgonist}/I_{Max5\text{-}HT}$ (relative efficacy) for WT and mutant receptors. For each receptor type, maximal currents elicited by each agonist (*m*CPBG, 2-Me 5-HT) were directly compared to those elicited by 5-HT on a single oocyte. Results shown are from multiple such experiments. Error bars indicate S.E. Empty bars indicate 5-HT, dark grey bars indicate *m*CPBG and light grey bars indicate 2-Me 5-HT. The relative efficacy of 5-HT is 1.00 for each receptor type since currents for all agonists were normalized to $I_{Max5\text{-}HT}$. For WT receptors, the relative efficacies of *m*CPBG and 2-Me 5-HT were 0.93 ± 0.01 and 0.12 ± 0.002, respectively, yielding a rank efficacy of 5-HT > *m*CPBG >> 2-Me 5-HT (Fig 3.2). Changes in rank efficacy for mutant receptors (shown in Fig 3.2 & 3.3) are reflected in this bar graph. * indicates significantly different from WT ($p \leq 0.05$). N.D indicates relative efficacy of 2-Me 5-HT could not be detected.

A

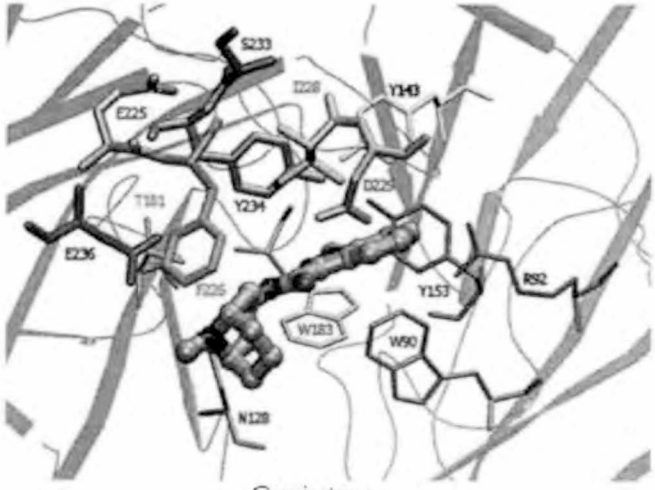

Granisetron

B

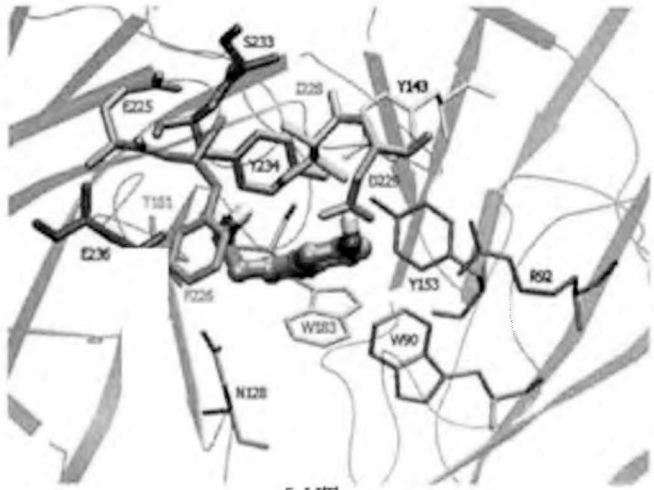

5-HT

C

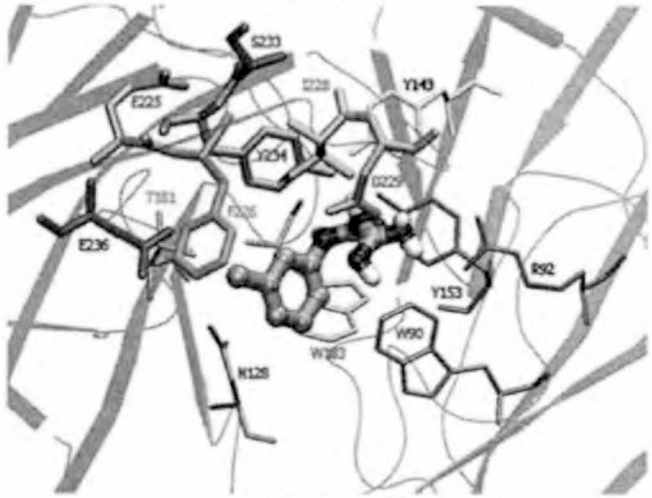

*m*CPBG model '1'

D

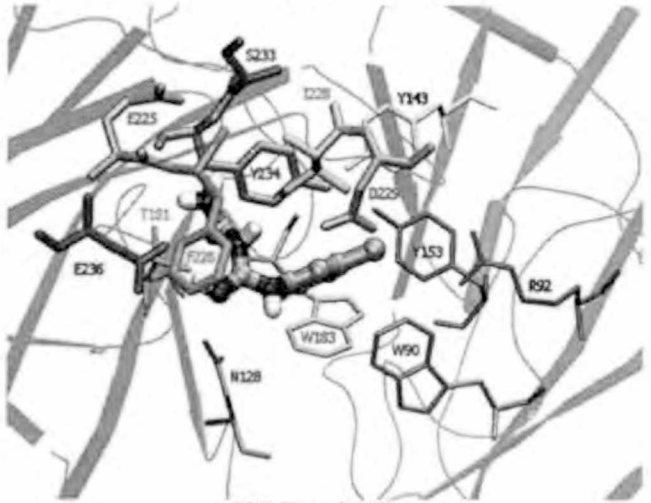

*m*CPBG model '2'

Figure 3.5 Docking of 5-HT, *m*CPBG and granisetron to the murine 5-HT_{3A}R model.

Modeling of the extracellular domain of the murine 5-HT_{3A}R and ligand docking were performed as described in "Materials and methods". The figure shows the docked model of (A): granisetron and (B): 5-HT. Two possible docked models were obtained for *m*CPBG and are shown as: (C): Model '1' and (D): Model '2'. The experimental results support the Model '2' obtained for *m*CPBG.

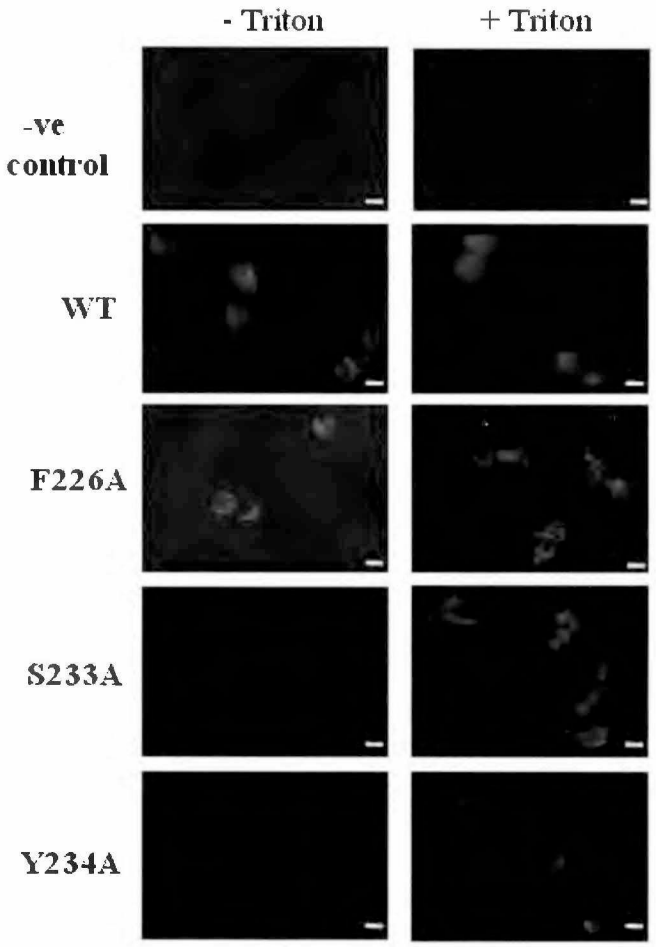

Figure 3.6 Localization of C-terminal FLAG tagged wild-type and loop C mutant receptors by immunofluorescence.

To determine the presence of wild-type (WT) and mutant receptors on the cell-surface, FLAG tagged WT or mutant receptors were transiently expressed in *t*SA 201 cells and characterized using immunofluorescence. Fixed cells were initially incubated with an anti-mouse anti-FLAG primary antibody. Intracellular localization was determined using Triton X-100. Cell surface or intracellular localization was determined by using an anti-goat Rhodamine-conjugated secondary antibody. All images were acquired using 20 X magnification lens coupled to a digital camera. Scale bar indicates 10μm. The first column shows the localization in absence of Triton, and the second column shows the localization in the presence of Triton, i.e. permeabilized cells. A negative control (mock transfected cells, no primary antibody) with and without Triton is also included at the top. Images obtained show that WT and F226A receptors are expressed on the surface, while S233A and Y234A mutations remain intracellularly located.

Table 3.1 Effects of mutations on 5-HT_{3A}R radio-ligand binding

Ligand affinities of wild-type (WT) and mutant receptors were determined as described in "Materials and methods." Expression levels of receptors are indicated as B_{Max} values. Each value was obtained using at least 4 determinations at each concentration, and is reported as mean ± S.E. Fold changes with a – sign indicate K_d or Ki values lower than the corresponding value obtained for WT. [a] significantly different from WT ($p \leq 0.05$). N.B: No binding detected up to 300nM of [^{3}H] Granisetron. * F.C: Fold change. -: Dash signs indicate that values could not be determined since no specific binding to [^{3}H] granisetron could be detected.

Receptor		[^{3}H] Granisetron			5-HT		*m*CPBG	
	B_{Max}(pmol/mg)	K_d (nM)	n_H	F.C.*	K_i (μM)	F.C.*	K_i (μM)	F.C.*
WT	12.6 ± 0.23	0.98 ± 0.12	1.2 ± 0.08	1	0.16 ± 0.04	1	0.1 ± 0.02	1
E225A	10.8 ± 1.31	4.25 ± 0.44[a]	1.41 ± 0.12	4	1.7 ± 0.04[a]	10	0.14 ± 0.04	1.4
F226A	18.4 ± 1.29[a]	1.36 ± 0.16	1.37 ± 0.14	1.4	32.6 ± 2.9[a]	200	3.9 ± 0.63[a]	40
F226Y	14.4 ± 1.19	2.09 ± 0.04	1.28 ± 0.08	2	29.7 ± 3.8[a]	185	2.8 ± 0.6[a]	28
I228A	15.4 ± 2.0	4.65 ± 0.4[a]	1.53 ± 0.14	4.5	37.7 ± 2.7[a]	235	0.52 ± 0.04[a]	5
D229A	10.5 ± 0.7	8.13 ± 0.18[a]	1.2 ± 0.09	8	22.2 ± 2.6[a]	140	0.27 ± 0.03	2.5
S233A	-	N.B	-	-	-	-	-	-
S233T	15.9 ± 1.22	2.04 ± 0.19	1.31 ± 0.12	2	0.66 ± 0.05[a]	4	0.12 ± 0.02	1
Y234A	-	N.B	-	-	-	-	-	-
Y234F	10.2 ± 1.13	11.2 ± 0.61[a]	1.4 ± 0.09	11	30 ± 1.2[a]	185	12.4 ± 1.32[a]	125

Table 3.2 Effects of mutations on 5-HT3AR electrophysiology

EC_{50} and Hill coefficient values of serotonin and *m*CPBG for wild-type (WT) and mutant receptors were determined as described in "Experimental Procedures." Each value was obtained using at least 4 determinations at each concentration, and is reported as ± S.E. I_{Max} values indicate average maximal currents elicited by 5-HT for the respective receptor. 5-HT was found to be the most efficacious agonist in all cases except F226Y, I228A and Y234F, where *m*CPBG was more efficacious. Dash signs indicate that the values could not be determined since the receptor was not functional. [a] significantly different from WT ($p \leq 0.05$). N.R indicates that that no responses could be detected up to 1mM of 5-HT /*m*CPBG. * F.C: Fold change.

Receptor	[^{3}H] Granisetron				5-HT		*m*CPBG	
	B_{Max}(pmol/mg)	K_d (nM)	n_H	F.C.*	K_i (μM)	F.C.*	K_i (μM)	F.C.*
WT	12.6 ± 0.23	0.98 ± 0.12	1.2 ± 0.08	1	0.16 ± 0.04	1	0.1 ± 0.02	1
E225A	10.8 ± 1.31	4.25 ± 0.44[a]	1.41 ± 0.12	4	1.7 ± 0.04[a]	10	0.14 ± 0.04	1.4
F226A	18.4 ± 1.29[a]	1.36 ± 0.16	1.37 ± 0.14	1.4	32.6 ± 2.9[a]	200	3.9 ± 0.63[a]	40
F226Y	14.4 ± 1.19	2.09 ± 0.04	1.28 ± 0.08	2	29.7 ± 3.8[a]	185	2.8 ± 0.6[a]	28
I228A	15.4 ± 2.0	4.65 ± 0.4[a]	1.53 ± 0.14	4.5	37.7 ± 2.7[a]	235	0.52 ± 0.04[a]	5
D229A	10.5 ± 0.7	8.13 ± 0.18[a]	1.2 ± 0.09	8	22.2 ± 2.6[a]	140	0.27 ± 0.03	2.5
S233A	-	N.B	-	-	-	-	-	-
S233T	15.9 ± 1.22	2.04 ± 0.19	1.31 ± 0.12	2	0.66 ± 0.05[a]	4	0.12 ± 0.02	1
Y234A	-	N.B	-	-	-	-	-	-
Y234F	10.2 ± 1.13	11.2 ± 0.61[a]	1.4 ± 0.09	11	30 ± 1.2[a]	185	12.4 ± 1.32[a]	125

Table 3.3 Docking calculations for models of 5-HT, 2-Me 5-HT, *m*CPBG and Granisetron

Modeling of the extracellular domain of the murine 5-HT_{3A}R and ligand docking were performed as described in "Materials and methods". The results are also represented in Figure 3.5. Interactions predicted for 5-HT, 2-Me 5-HT, granisetron and *m*CPBG (model '1' and model '2') are shown in the table. HB: Hydrogen bond, SB: Salt bridge, CP: Cation-π interaction, PP: π–π interaction, + : Within $4A^0$ of docked ligand.

	N128	T179	T181	W183	F226	I228	D229	I230	S231	Y234	E236	W90	R92	Y153	I207
5-HT	+		+	PP	CP	+	HB		+	CP	SB	+		+	+
2-Me 5-HT	+		+	PP	CP	+	HB	+	+	HB	SB	+		+	+
*m*CPBG1	+			CP	PP	+	SB	+	+	HB	+	+		HB	+
*m*CPBG2	+			PP	CP	+		+	+	CP	SB	+			
Granisetron	+	+		+	CP	+	+	+	+	HB		+	+	+	

References

Akk G, Zhou M and Auerbach A (1999) A mutational analysis of the acetylcholine receptor channel transmitter binding site. *Biophys J* **76**(1 Pt 1):207-218.

Arias HR (2000) Localization of agonist and competitive antagonist binding sites on nicotinic acetylcholine receptors. *Neurochem Int* **36**(7):595-645.

Bartrup JT and Newberry NR (1996) Electrophysiological consequences of ligand binding to the desensitized 5-HT3 receptor in mammalian NG108-15 cells. *J Physiol* **490 (Pt 3)**:679-690.

Beene DL, Brandt GS, Zhong W, Zacharias NM, Lester HA and Dougherty DA (2002) Cation-pi interactions in ligand recognition by serotonergic (5-HT3A) and nicotinic acetylcholine receptors: the anomalous binding properties of nicotine. *Biochemistry* **41**(32):10262-10269.

Beene DL, Price KL, Lester HA, Dougherty DA and Lummis SCR (2004) Tyrosine Residues That Control Binding and Gating in the 5-Hydroxytryptamine3 Receptor Revealed by Unnatural Amino Acid Mutagenesis. *The Journal of Neuroscience* **24**(41):9097-9104.

Boess FG, Steward LJ, Steele JA, Liu D, Reid J, Glencorse TA and Martin IL (1997) Analysis of the ligand-binding site of the 5-HT3 receptor using site directed mutagenesis: importance of glutamate 106. *Neuropharmacology* **36**(4-5):637-647.

Brejc K, van Dijk WJ, Klaassen RV, Schuurmans M, van Der Oost J, Smit AB and Sixma TK (2001) Crystal structure of an ACh-binding protein reveals the ligand-binding domain of nicotinic receptors. *Nature* **411**(6835):269-276.

Celie PH, van Rossum-Fikkert SE, van Dijk WJ, Brejc K, Smit AB and Sixma TK (2004) Nicotine and carbamylcholine binding to nicotinic acetylcholine receptors as studied in AChBP crystal structures. *Neuron* **41**(6):907-914.

Chakrapani S, Bailey TD and Auerbach A (2004) Gating dynamics of the acetylcholine receptor extracellular domain. *J Gen Physiol* **123**(4):341-356.

Colquhoun D (1998) Binding, gating, affinity and efficacy: the interpretation of structure-activity relationships for agonists and of the effects of mutating receptors. *Br J Pharmacol* **125**(5):924-947.

Cornell WD, Cieplak P, Bayly CI, Gould IR, Merz KMJ, Ferguson DM, Spellmeyer DC, Fox T, Caldwell JW and Kollman PA (1995) A second generation force field for the simulation of proteins, nucleic acids, and organic molecules. *J Am Chem Soc* **117**:5179-5197.

Costall B and Naylor RJ (2004) 5-HT3 receptors. *Curr Drug Targets CNS Neurol Disord* **3**(1):27-37.

Dennis M, Giraudat J, Kotzyba-Hibert F, Goeldner M, Hirth C, Chang JY, Lazure C, Chretien M and Changeux JP (1988) Amino acids of the Torpedo marmorata acetylcholine receptor alpha subunit labeled by a photoaffinity ligand for the acetylcholine binding site. *Biochemistry* **27**(7):2346-2357.

Hope AG, Belelli D, Mair ID, Lambert JJ and Peters JA (1999) Molecular determinants of (+)-tubocurarine binding at recombinant 5-hydroxytryptamine3A receptor subunits. *Mol Pharmacol* **55**(6):1037-1043.

Hope AG, Downie DL, Sutherland L, Lambert JJ, Peters JA and Burchell B (1993) Cloning and functional expression of an apparent splice variant of the murine 5-HT3 receptor A subunit. *Eur J Pharmacol* **245**(2):187-192.

Joshi PR, Suryanarayanan A and Schulte MK (2004) A vertical flow chamber for *Xenopus* oocyte electrophysiology and automated drug screening. *J Neurosci Methods* **132**(1):69-79.

Kao PN, Dwork AJ, Kaldany RR, Silver ML, Wideman J, Stein S and Karlin A (1984) Identification of the alpha subunit half-cystine specifically labeled by an affinity reagent for the acetylcholine receptor binding site. *J Biol Chem* **259**(19):11662-11665.

Karlin A (2002) Emerging structure of the nicotinic acetylcholine receptors. *Nat Rev Neurosci* **3**(2):102-114.

Lankiewicz S, Lobitz N, Wetzel CH, Rupprecht R, Gisselmann G and Hatt H (1998) Molecular cloning, functional expression, and pharmacological characterization of 5-hydroxytryptamine3 receptor cDNA and its splice variants from guinea pig. *Mol Pharmacol* **53**(2):202-212.

Laskowski RA, MacArthur MW, Moss DS and Thornton JM (1993) PROCHECK: a program to check the stereochemical quality of protein structures. *J Appl Cryst* **26**:283-291.

Le Novere N, Grutter T and Changeux JP (2002) Models of the extracellular domain of the nicotinic receptors and of agonist- and Ca2+-binding sites. *Proc Natl Acad Sci U S A* **99**(5):3210-3215.

Maksay G, Bikadi Z and Simonyi M (2003) Binding interactions of antagonists with 5-hydroxytryptamine3A receptor models. *J Recept Signal Transduct Res* **23**(2-3):255-270.

Maricq AV, Peterson AS, Brake AJ, Myers RM and Julius D (1991) Primary structure and functional expression of the 5HT3 receptor, a serotonin-gated ion channel. *Science* **254**(5030):432-437.

McDonald IK and Thornton JM (1994) Satisfying hydrogen bonding potential in proteins. *J Mol Biol* **238**(5):777-793.

Mihic SJ, Whiting PJ, Klein RL, Wafford KA and Harris RA (1994) A single amino acid of the human gamma-aminobutyric acid type A receptor gamma 2 subunit determines benzodiazepine efficacy. *J Biol Chem* **269**(52):32768-32773.

Mishina M, Tobimatsu T, Imoto K, Tanaka K, Fujita Y, Fukuda K, Kurasaki M, Takahashi H, Morimoto Y, Hirose T and et al. (1985) Location of functional regions of acetylcholine receptor alpha-subunit by site-directed mutagenesis. *Nature* **313**(6001):364-369.

Mochizuki S, Miyake A and Furuichi K (1999) Identification of a domain affecting agonist potency of meta-chlorophenylbiguanide in 5-HT3 receptors. *Eur J Pharmacol* **369**(1):125-132.

Morris GM, Goodsell DS, Hallaway RS, Huey R, Hart WE, Belew RK and Olson AJ (1998) Automated Docking Using a Lamarckian Genetic Algorithm and Empirical Binding Free Energy Function. *J Comput Chem* **19**:1639-1662.

Mott DD, Erreger K, Banke TG and Traynelis SF (2001) Open probability of homomeric murine 5-HT3A serotonin receptors depends on subunit occupancy. *J Physiol* **535**(Pt 2):427-443.

O'Leary ME and White MM (1992) Mutational analysis of ligand-induced activation of the Torpedo acetylcholine receptor. *J Biol Chem* **267**(12):8360-8365.

Price KL and Lummis SC (2004) The role of tyrosine residues in the extracellular domain of the 5-hydroxytryptamine3 receptor. *J Biol Chem* **279**(22):23294-23301.

Reeves DC, Sayed MF, Chau PL, Price KL and Lummis SC (2003) Prediction of 5-HT3 receptor agonist-binding residues using homology modeling. *Biophys J* **84**(4):2338-2344.

Schreiter C, Hovius R, Costioli M, Pick H, Kellenberger S, Schild L and Vogel H (2003) Characterization of the ligand-binding site of the serotonin 5-HT3 receptor: the role of glutamate residues 97, 224, AND 235. *J Biol Chem* **278**(25):22709-22716.

Sine SM (2002) The nicotinic receptor ligand binding domain. *J Neurobiol* **53**(4):431-446.

Spier AD and Lummis SC (2000) The role of tryptophan residues in the 5-Hydroxytryptamine(3) receptor ligand binding domain. *J Biol Chem* **275**(8):5620-5625.

Steward LJ, Boess FG, Steele JA, Liu D, Wong N and Martin IL (2000) Importance of phenylalanine 107 in agonist recognition by the 5-hydroxytryptamine (3A) receptor. *Mol Pharmacol* **57**(6):1249-1255.

Thompson JD, Higgins DG and Gibson TJ (1994) CLUSTAL W: improving the sensitivity of progressive multiple sequence alignment through sequence weighting, position-specific gap penalties and weight matrix choice. *Nucleic Acids Res* **22**(22):4673-4680.

Tomaselli GF, McLaughlin JT, Jurman ME, Hawrot E and Yellen G (1991) Mutations affecting agonist sensitivity of the nicotinic acetylcholine receptor. *Biophys J* **60**(3):721-727.

van Hooft JA and Vijverberg HP (1997) Full and partial agonists induce distinct desensitized states of the 5-HT3 receptor. *J Recept Signal Transduct Res* **17**(1-3):267-277.

Venkataraman P, Venkatachalan SP, Joshi PR, Muthalagi M and Schulte MK (2002) Identification of critical residues in loop E in the 5-HT3ASR binding site. *BMC Biochem* **3**(1):15.

Wagner DA and Czajkowski C (2001) Structure and dynamics of the GABA binding pocket: A narrowing cleft that constricts during activation. *J Neurosci* **21**(1):67-74.

Wu CH, Huang H, Arminski L, Castro-Alvear J, Chen Y, Hu ZZ, Ledley RS, Lewis KC, Mewes HW, Orcutt BC, Suzek BE, Tsugita A, Vinayaka CR, Yeh LS, Zhang J and Barker WC (2002) The Protein Information Resource: an integrated public resource of functional annotation of proteins. *Nucleic Acids Res* **30**(1):35-37.

Xiang Z and Honig B (2001) Extending the accuracy limits of prediction for side-chain conformations. *J Mol Biol* **311**(2):421-430.

Xiang Z, Soto CS and Honig B (2002) Evaluating conformational free energies: the colony energy and its application to the problem of loop prediction. *Proc Natl Acad Sci U S A* **99**(11):7432-7437.

Yan D, Schulte MK, Bloom KE and White MM (1999) Structural features of the ligand-binding domain of the serotonin 5HT3 receptor. *J Biol Chem* **274**(9):5537-5541.

Footnotes

* This work was supported by the National Science Foundation (NSF CAREER# 9985077) and the American Heart Association (AHA# 0151065B) and Alaska INBRE (P20 RR016466). A.S and P.J are Alaska INBRE graduate research fellows.

Part of this work was presented as a poster presentation entitled: "Investigation of amino acids in the loop C region of the mouse 5-HT3A R by alanine scanning mutagenesis" at The Experimental Biology meeting, Washington D.C, Poster # 169.8, April 17-21, 2004. A. Suryanarayanan, P.R Joshi, T.R. Kulkarni, M. Mani and M.K. Schulte.

Send any reprint requests to:

Marvin K. Schulte, Ph.D., Associate Professor

Department of Chemistry and Biochemistry

146, Natural Sciences Facility

P.O. Box 756160, The University of Alaska Fairbanks

Fairbanks, Alaska 99775

Chapter 4: 5-HT_3R binding of lerisetron: an interdisciplinary approach to drug–receptor interactions

4.1 Abstract

The synthesis and biological evaluation of lerisetron-based molecular probes to investigate the 5-HT_3R binding site are described. A structure-activity relationship (SAR) study, which involved distance and electronic parameter modifications of lerisetron's *N*-benzyl group, resulted in the discovery of a partial agonist.

4.2 Introduction

Our research efforts have been focused on the design, synthesis, and use of novel molecular probes to gain a better understanding of the underlying mechanism(s) of drug–receptor interactions ([D–R]). Particularly, how do drugs with dissimilar activities (i.e., agonist, reverse agonist, or partial agonist) compare in terms of binding to the receptor and how does this affect the resultant activity. Unfortunately, methods available to study specific [D–R], especially in membrane-bound receptors, are somewhat limited. In our efforts to contribute to the general understanding of [D–R], we have focused on the serotonin type-3 receptor, (5-HT_3R), which is a membrane-bound, ligand-gated ion channel receptor. Clinically, 5-HT_3R antagonists are used for cancer treatment-induced emesis; however, current research strongly suggests a potential use of 5-HT_3R ligands in treatment of cardiovascular disease, anxiety, and drug addiction (Glenn and Green, 1989; Lovinger, 1999; Wilson et al., 1990).

The goal of SAR studies for a series of drug molecules has been the development of pharmacophore models. Hibert and co-workers established one of the earliest models for 5-HT_3R antagonists, based on a conformational analysis study of 23 analogues and subsequent superimposition of the more energetically favored conformers (Hibert et al., 1990). The original three point model was comprised of (1) a basic nitrogen, (2) a carbonyl group participating in a hydrogen bonding interaction and coplanar with (3) an aromatic ring. The 5-HT_3R antagonist model has since been refined to include another lipophilic interaction and a second hydrogen bonding interaction (Cappelli et al., 1999;

Clark et al., 1993; Rival et al., 1998; Swain et al., 1992). Figure 4.1 shows the current refined pharmacophore model of 5-HT_3R antagonists. Pharmacophore models for partial agonist activity have also been reported (Cappelli et al., 1998; Daveu et al., 1999; Dukat et al., 1996).

The aim of this study was to evaluate if there is an electrostatic component in the N1- substitution in lerisetron, which is a novel benzimidazole-ring containing 5-HT_3R antagonist (see Figure 4.1). We have employed SAR studies to elucidate such a possible role of the N1-substitution. Electrostatic interactions have a strong dependence on both electronic parameters and distance. Thus, eight N1-substituted-2-piperazinyl benzimidazole analogues have been designed by either varying the electronic nature of the aromatic ring from electron rich to electron poor or lengthening the distance between the aromatic ring and N1 nitrogen atom.

In addition to understanding the role of N1 substituent of lerisetron, results from this study will also be used to design 'active pairs' of lerisetron analogs. An active pair is two analogs displaying at least low micromolar activity and differing only by the presence or absence of a functional group. Such active pairs can then be evaluated on mutant 5-HT_3 receptors to understand the interaction of Leristeron with the 5-HT_3R (Venkataraman et al., 2002a).

4.3 Materials and Methods:

4.3.1 Chemical synthesis:

All target molecules were prepared according to a method reported previously by Orjales et al. (Orjales et al., 1997) with only slight modification. This general two-step synthesis is outlined in Scheme 1. Commercially available 2-chlorobenzimidazole (1 equiv), in dry DMF was treated with a slight excess of NaH (1.1 equiv). After stirring for 1 h at room temperature, 1 equiv of the appropriate alkyl halide (Br, Cl) was added slowly and the reaction mixture heated under reflux for ≥5 h (reaction was monitored by TLC). Reaction product was partitioned between H_2O and methylene chloride; organic layer was dried (Na_2SO_4) and concentrated in vacuo. The solid residue was purified by flash chromatography, which afforded the corresponding *N*-substituted 2-chlorobenzimidazole intermediates in good yield. The final step involved a nucleophilic substitution of the 2-chloro group by piperazine at high temperatures. The reaction was performed neat using 4- to 10-fold excess piperazine (water soluble) and typically heated for short periods only (30–45 min). Similar workup afforded a residue that was purified by either crystallization or chromatography. The yields ranged from 40 to 95%. All compounds were characterized by NMR, MS, HRMS and/or elemental analysis, or were identical to literature reports.

4.3.2 Preparation of cRNA and expression of receptors:

Complementary RNA for the human 5-HT_{3A}R was synthesized *in vitro* from a linearized template using mMACHINE RNA transcription kit (Ambion, TX, US). Mature

Xenopus laevis were anesthetized by submersion in 0.22% Tricaine methane-sulfonate (Sigma Chemicals, MO, US) and oocytes surgically excised. The follicular cell layer was removed by treatment with 1.5% collagenase II (Sigma Chemicals, MO, US) for 1–2h at room temperature. Oocytes were injected with 10ng of RNA in 50mL nuclease-free water and incubated at 19°C in calcium-free ORII medium (82.5mM NaCl, 2.5mM KCl, 1mM $MgCl_2$, 5mM HEPES, pH 7.4).

4.3.3 Electrophysiological recording:

After 2–5 days of incubation, electrophysiological recording was carried out in a specially designed chamber. Oocytes were perfused at a rate of approximately 8mL/min with ND96 recording buffer (96mM NaCl, 2.0mM KCl, 1.8mM $CaCl_2$, 1mM $MgCl_2$, 5mM HEPES, pH 7.4). Test compounds were diluted in ND-96 buffer and applied to the oocytes using a gravity-fed bath perfusion. Membrane currents were studied under two-electrode voltage-clamp conditions, at a holding potential of −60mV, using Warner instruments Oocyte Clamp, OC-725 amplifier. Data were analyzed using Graph-Pad prism software. The data for the antagonists were normalized to the currents elicited by 1μM 5-HT.

4.4 Results and discussion:

Table 4.1 contains the biological activities of the target molecules. All antagonists (**1**–**8**) displayed high binding affinity for the human 5-$HT_{3A}R$ ranging from 25 times less to nearly equipotent to lerisetron. Analogues *p*-methoxy (**6**), *p*-methyl (**7**), *p*-fluoro (**8**) contain substituents that vary the electronics of the N1 benzyl aromatic ring from electron rich to electron poor. The *p*-methoxy derivative was most active, whereas, the *p*-fluoro derivative was least active. A linear regression analysis including the des-benzyl derivative (i.e., **1**, **2**, **6**, **7**, and **8**) provided a significant correlation between electronics (R-*induction*, r^2=0.8413, *p*=0.0282, F=15.91) of the corresponding N1-substituents and 5-$HT_{3A}R$ activity. Lengthening the distance between the aromatic ring and the N1 nitrogen atom by either one or two carbon atoms resulted in a 20-fold decrease in receptor binding activity (see Fig. 4.2). The naphthyl analogue (**5**) is 4 times less active than the benzyl, suggesting that the internal aromatic ring might be utilized for receptor binding activity. Preliminary SAR results indicate both an electronic and distance component to the benzyl interaction. Thus, the present SAR study supports our model that places R91 in close proximity to the benzyl group of lerisetron.

Replacement of the *N*-benzyl group with an *N*-allyl group resulted in a compound possessing partial agonist activity (**9**). This activity could be blocked by tubocurarine, a competitive antagonist. This discovery provides us with a unique pair of active analogues that can now be used to probe partial agonist activity. If the *N*-benzyl and *N*-allyl groups are similarly located, then the conversion of lerisetron into a partial agonist would

support a model that suggests this 5-HT_3R antagonist spans both partial agonists and antagonist binding sites. Another such active pair of analogs identified from this study is that of lerisetron and des-benzyl analog. This active pair has been utilized in mutagenesis studies of the 5-HT_3R to elucidate functional group interactions of lerisetron with Loop E residues of 5-HT_3R (Venkataraman et al., 2002a) Using such active pairs of analogs and mutagenesis studies, a 5-HT_3R model that incorporates all three types of ligands (agonist, antagonist, and partial agonist) can be potentially developed.

4.5 Acknowledgements:

This work has been supported by American Heart Association Grants 9820013LA and 9960118V. We would like to acknowledge Dr. Kirschbaum's laboratory for the chemical synthesis of all lerisetron analogs evaluated in this study.

Scheme 4.1: General synthetic route to N1-substituted-2-piperazinyl benzimidazoles.

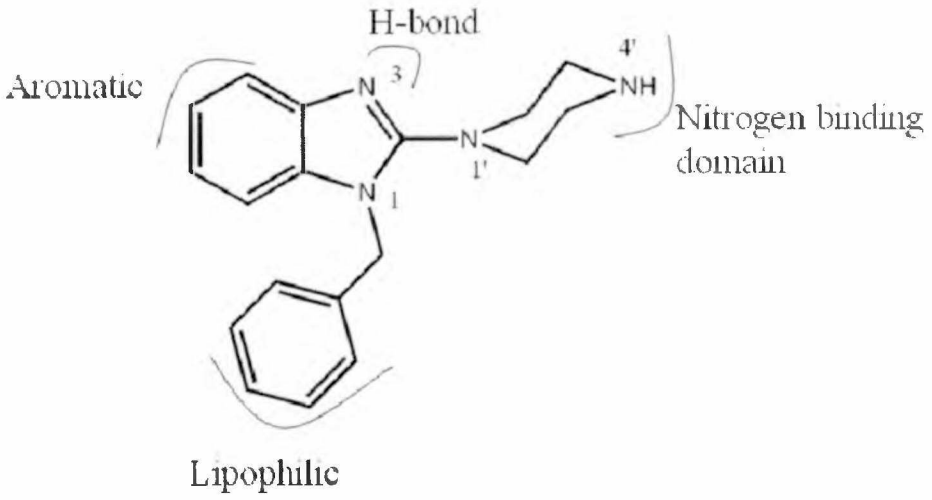

Figure 4.1: Proposed model for lerisetron binding based on the current 5-HT_3R antagonists pharmacophore models.

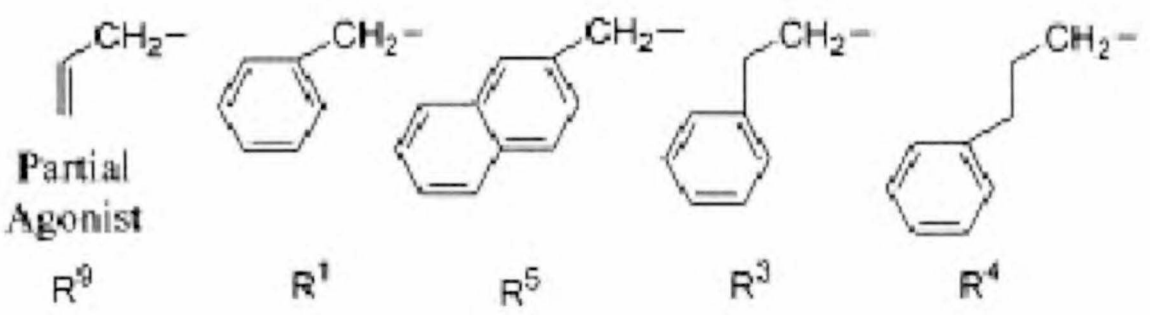

Figure 4.2: Benzyl analogues with increasing distance between the aromatic ring and the N1 nitrogen atom.

Table 4.1: Inhibition of serotonin-induced response by compounds 1-9
Values are mean of at least three experiments, standard error (S.E) is given in parentheses.

Compounds	N1 Substituent (R)	$5HT_3R$ Inhibition[a] K_i (nM)
1	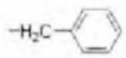	0.36 (±0.08)
2	H	19.21 (±0.84)
3	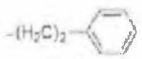	7.43 (±1.9)
4	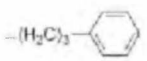	7.96 (±1.9)
5	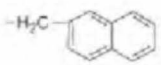	1.43 (±0.38)
6	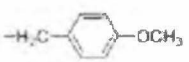	0.42 (±0.07)
7	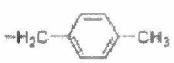	1.69 (±0.18)
8	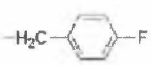	5.21 (±2.24)
9	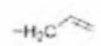	EC_{50} = 0.24 (±0.03) μM Efficacy = 30%

References

Cappelli A, Anzini M, Vomero S, Canullo L, Mennuni L, Makovec F, Doucet E, Hamon M, Menziani MC, De Benedetti PG, Bruni G, Romeo MR, Giorgi G and Donati A (1999) Novel potent and selective central 5-HT3 receptor ligands provided with different intrinsic efficacy. 2. Molecular basis of the intrinsic efficacy of arylpiperazine derivatives at the central 5-HT3 receptors. *J Med Chem* **42**(9):1556-1575.

Cappelli A, Anzini M, Vomero S, Mennuni L, Makovec F, Doucet E, Hamon M, Bruni G, Romeo MR, Menziani MC, De Benedetti PG and Langer T (1998) Novel potent and selective central 5-HT3 receptor ligands provided with different intrinsic efficacy. 1. Mapping the central 5-HT3 receptor binding site by arylpiperazine derivatives. *J Med Chem* **41**(5):728-741.

Clark RD, Miller AB, Berger J, Repke DB, Weinhardt KK, Kowalczyk BA, Eglen RM, Bonhaus DW, Lee CH, Michel AD and et al. (1993) 2-(Quinuclidin-3-yl)pyrido[4,3-b]indol-1-ones and isoquinolin-1-ones. Potent conformationally restricted 5-HT3 receptor antagonists. *J Med Chem* **36**(18):2645-2657.

Daveu C, Bureau R, Baglin I, Prunier H, Lancelot JC and Rault S (1999) Definition of a pharmacophore for partial agonists of serotonin 5-HT3 receptors. *J Chem Inf Comput Sci* **39**(2):362-369.

Dukat M, Abdel-Rahman AA, Ismaiel AM, Ingher S, Teitler M, Gyermek L and Glennon RA (1996) Structure-activity relationships for the binding of arylpiperazines and arylbiguanides at 5-HT3 serotonin receptors. *J Med Chem* **39**(20):4017-4026.

Glenn B and Green S (1989) Anxiolytic profile of GR 38032F in the potentiated startle paradigm. *Behav Pharmacol* **1**(1):91-94.

Hibert MF, Hoffmann R, Miller RC and Carr AA (1990) Conformation-activity relationship study of 5-HT3 receptor antagonists and a definition of a model for this receptor site. *J Med Chem* **33**(6):1594-1600.

Lovinger DM (1999) 5-HT3 receptors and the neural actions of alcohols: an increasingly exciting topic. *Neurochem Int* **35**(2):125-130.

Orjales A, Mosquera R, Labeaga L and Rodes R (1997) New 2-piperazinylbenzimidazole derivatives as 5-HT3 antagonists. Synthesis and pharmacological evaluation. *J Med Chem* **40**(4):586-593.

Rival Y, Hoffmann R, Didier B, Rybaltchenko V, Bourguignon JJ and Wermuth CG (1998) 5-HT3 antagonists derived from aminopyridazine-type muscarinic M1 agonists. *J Med Chem* **41**(3):311-317.

Swain CJ, Baker R, Kneen C, Herbert R, Moseley J, Saunders J, Seward EM, Stevenson GI, Beer M, Stanton J and et al. (1992) Novel 5-HT3 antagonists: indol-3-ylspiro(azabicycloalkane-3,5'(4'H)-oxazoles). *J Med Chem* **35**(6):1019-1031.

Venkataraman P, Joshi P, Venkatachalan SP, Muthalagi M, Parihar HS, Kirschbaum KS and Schulte MK (2002) Functional group interactions of a 5-HT3R antagonist. *BMC Biochem* **3**(1):16.

Wilson H, Coffman WJ and Cohen ML (1990) 5-Hydroxytryptamine3 receptors mediate tachycardia in conscious instrumented dogs. *J Pharmacol Exp Ther* **252**(2):683-688.

Chapter 5: Role of the 5-HT_3B subunit in the 5-HT_{3AB} receptor binding site

5.1 Abstract

5-HT_3 receptors belong to the Cys-loop superfamily of ligand-gated ion channels. Depending on subunit composition, 5-HT_3 receptors can assemble as homomeric 5-HT_{3A} or heteromeric 5-HT_{3AB} receptors. The contribution of the N-terminal of the B subunit to the formation of 5-HT_{3AB} receptors is unknown. In this pilot study, we constructed A-B N-terminal chimeric receptors to explore such a contribution of the B subunit. All chimeric receptors were evaluated by radioligand binding and immunofluorescence assays. We found that the chimeric receptors were challenging to characterize since substitution of even small stretches of the N-terminal of the B subunit with that of the A subunit disrupts cell surface assembly of the chimeric receptor. Even though the chimeric receptors do not express on the cell surface, they show binding to granisetron, with altered affinities. Overall, our data indicate that in addition to signals in the transmembrane region, the N-terminal of the B subunit has several important subunit contacts and/or assembly signals which are essential for formation of cell surface receptors.

5.2 Introduction

The 5-HT_3R (5-hydroxytryptamine3 receptor) belongs to the ligand-gated ion channel (LGIC) superfamily that is also comprised of the nicotinic acetylcholine, $GABA_A$ and glycine receptors (Arias, 2000; Chebib and Johnston, 1999; Corringer et al., 2000; Reeves and Lummis, 2002). The receptors in this family are membrane-bound pentamers and mediate fast synaptic transmission. These receptors have an extracellular N-terminal region (consisting of the ligand-binding site), four transmembrane regions (M1-M4) and an extracellular C-terminal region. Depending on subunit composition, the ligand-gated ion channel receptors can assemble as homomers or heteromers. In case of the 5-HT_3R, two subunits, 5-HT_3A and 5-HT_3B have been cloned. Unlike the 5-HT_3A subunit, 5-HT_3B subunits cannot form functional homomeric receptors (Davies et al., 1999). However, 5-HT_3A and 5-HT_3B subunits can co-assemble to form functional heteromeric receptors. The 5-HT_{3AB} heteromers show distinct pharmacological and functional properties as compared to the 5-HT_{3A} heteromers.

The molecular determinants of function in the 5-HT_{3A} and 5-HT_{3AB} receptors are not clearly understood. The role of the transmembrane regions of the 5-HT_3B subunit has been explored by two studies. One study concluded that the B subunits could not form cell-surface receptors since they were retained inside the cell due to an ER retention signal between the transmembrane regions I and II of 5-HT_3B subunit (Boyd et al., 2003). Transplantation of this signal (CRAR) into the homologous region of 5-HT_3A also leads to ER retention of the A subunits, until they are rescued by co-assembly with wild-type 5-HT_3A subunits. The mutation of this ER retention signal in 5-HT_3B to the homologous

sequence in the A subunit (i.e. from CRAR to SGER) does not lead to cell surface expression. These data suggest the additional presence of other signals, or mechanisms that control the cell surface expression of 5-HT_{3B}Rs. Another study which explored the role of the transmembrane regions of the B subunit using A-B chimeric receptors reported the importance of a 'HA stretch' of residues in the large M3-M4 cytoplasmic region of the 5-HT_3A subunit (Kelley et al., 2003). The replacement of three arginine residues unique to the HA-stretch of the 5-HT_3A subunit by homologous residues in the 5-HT_3B subunit increased single-channel conductance 28-fold. However, the role of the N-terminal of the B subunit in assembly and/or formation of ligand-binding sites in the AB heteromeric receptors. When the amino-acid sequence of the A and B subunits are compared, critical differences are seen in the N-terminal regions (in addition to differences in the transmembrane regions). In this study, we studied such a potential role of the N-terminal of the B subunit in the of the heteromeric 5-HT_{3AB}Rs by constructing chimeric A-B receptors.

In this pilot study to understand the role of the loops A-F of the B subunit, multiple N-terminal A-B chimeric receptors were constructed and evaluated by radioligand binding and immunofluorescence assays. We found that the chimeric receptors were challenging to characterize since substitution of even small stretches of the N-terminal of the B subunit with that of the A subunit disrupts cell surface assembly of the chimeric receptor. Even though the chimeric receptors do not express on the cell surface, they show binding to granisetron, with altered affinities. Overall, our data indicate that the B subunit has several important subunit contacts and/or assembly signals

which are essential for formation of cell surface receptors. Thus, it appears that both N-terminal and transmembrane regions of the B subunit have important signals that regulate cell surface assembly of the receptor.

5.3 Materials and Methods:

5.3.1 Chimera Construction:

The method developed for chimera construction is shown in scheme 5.1. For chimera construction, two fragments were initially synthesized using PCR. To construct each fragment two oligonucleotides were used. Oligonucleotides were designed such that an overhang of 20 residues was produced in each fragment. These overhangs were complementary and produced the construct with the switch-point of interest when annealed together. These fragments were further amplified using upstream and downstream oligonucleotides. *Taq* DNA polymerase was used to generate PCR product with 3' A overhangs. These PCR products were ligated into pCR 3.1 TA cloning vector (Invitrogen, CA, US). The ligation products were confirmed by restriction digests and sequencing.

5.3.2 Cell Culture and transfection:

*ts*A201 cells, a derivative of human embryonic kidney cell line, were seeded at a density of 5 x 10^6 cells/100mm dish. Cells were grown in DMEM medium containing 10% FBS, 100 units/ml penicillin/streptomycin for 9 hours in 5% CO_2 and transfected with 10µg human 5-HT_3 cDNA per 100mm dish using the calcium phosphate technique. Media was changed 12-14hrs after transfection. The cells were allowed to grow for another 24 hours and then harvested.

5.3.3 Binding assays:

Transfected cells were collected and washed twice with Dulbecco's PBS and resuspended in 1.0ml PBS/100mm dish. Cells were then homogenized and centrifuged at 35 000 X g for 30 minutes. Membranes were washed once more with PBS then resuspended in 1ml PBS/100 mm dish. Binding assays were performed in PBS in presence of a protease inhibitor cocktail (Roche, MA, US). For K_d determinations, 100 µl of homogenate was incubated at 37^0C for 1 hour with varying concentrations of [^{3}H] granisetron (NEN, MA, US). For K_i determinations, 100 µl of homogenate was incubated at 37^0C for 2 hours with varying concentrations of inhibitor and [^{3}H] granisetron. Binding data were analyzed using GraphPad PRISM.

5.3.4 Two-electrode voltage clamp electrophysiology:

Xenopus laevis oocytes were used for this technique. Briefly, ovarian lobes were surgically removed from *Xenopus laevis* frogs and washed twice in Ca^{+2} free Barth's buffer [82.5mM NaCl / 2.5mM KCl / 1mM $MgCl_2$ / 5mM HEPES, pH 7.4] and gently shaken with 1.5mg/ml collagenase (Sigma type II, Sigma-Aldrich) for 1 hour at 20-25°C. Stage IV oocytes were selected for microinjection. Synthetic cRNAs for WT and chimeric receptors were prepared using the mMESSAGE mMACHINE™ High Yield Capped RNA Transcription Kit (Ambion, TX, US). Each oocyte was injected with 50nl cRNA at a concentration of 0.2ng/nl. Oocytes were incubated at 19^0C for 2 to 4 days before electrophysiological recording. Electrical recordings were made under conventional two-electrode voltage-clamp using an OC-725C oocyte clamp amplifier (Warner Instruments, CT, US) coupled to an online, computerized data acquisition

system (Datapac 2000, RUN technologies, CA, US). Recording and current electrodes were filled with 3M KCl and had resistances of 1-2 mΩ. Oocytes were held in a vertical flow chamber of 400µl volume and perfused with ND-96 recording buffer (96mM NaCl / 2mM KCl /1.8mM $CaCl_2$ /1mM $MgCl_2$ /5mM HEPES, pH 7.4) at a rate of 15ml/min. All agonists were prepared in ND-96 buffer and applied at a rate of 25ml/min using an electrical pump.

5.3.5 Immunofluorescence:

The chimera of interest was tagged at the C-terminal using the EGFP-N1 vector (Clontech, CA, US). This tagged chimera was expressed either alone or in conjugation with the human 5-HT_3A subunit in *t*SA 201 cells using the Superfect® transfection kit (Qiagen, CA, US). The cells were grown on coverslips and fixed 24-30 hours transfection using 4% para-formaldehyde. used was Anti-GFP antibody (Clontech, CA, US) was used as the primary antibody at a 1:200 dilution with or without 0.2 % Triton X-100. The secondary antibody was Cy3-conjugated goat anti-mouse (Jackson immunolabs, NC, US) diluted at 1:600. The cells on coverslips were mounted on glass slides and observed under a Olympus IX-70 microscope using the appropriate filter sets (Omega Optical, VT, US).

5.4 Results and discussion:

In order to elucidate the role of the 5-HT_3B subunit in assembly and/or formation of the ligand-binding site of AB receptors, chimeric receptors were constructed. The chimera design and switch points therein are explained in scheme 5.1 and figure 5.1, respectively. Initially 2 chimeras, A/B and B/A were constructed. These chimeras had switch points at positions 242 and 239 respectively. The A/B chimera bears the N-terminal from the A subunit and the transmembrane region is from the B subunit. Vice versa, the B/A chimera bears the N- terminal from the B subunit, while the rest of the protein is from the A subunit. These chimeric receptors, WT (homomeric A) receptors and heteromeric AB receptors were evaluated by saturation binding assays with [^{3}H] granisetron. As shown in figure 5.2, the A/B chimera showed a 2.5 fold increase in K_d, while the B/A chimera showed a 7.7 fold increase in K_d value. When the A/B chimera was characterized in competition assays, a 10 fold increase in K_i value for 5-HT, a 25 fold increase in K_i for MDL-72222 and a 4 fold fold change in K_i value for *m*CPBG were noted as compared to WT receptor (Figure 5.3). In competition assays with the B/A chimera, much more drastic changes were observed (Figure 5.5). A 367 fold change in K_i value for *m*CPBG was seen, whereas 5-HT could not displace the [^{3}H] granisetron bound to the B/A chimera at concentrations up to 3mM. These changes indicate that the affinities of both 5-HT and *m*CPBG were altered for the A/B and B/A chimeras.

The A/B and B/A chimeric receptors could not be functionally characterized when expressed in *Xenopus* oocytes. This could because of lack of cell surface expression. The radioligand binding results for the A/B and B/A chimeras could be due to

binding of granisetron to intracellularly located receptors. Such intracellularly receptors can be incompletely formed oligomers of subunits which can still show high affinity binding to granisetron. In agreement with this, we also noted much lower specific CPM values in binding assays of chimeric receptors compared to WT receptors (Data not shown). In order to characterize the cellular localization of the A/B receptor, we constructed a GFP tagged A/B chimera. Figure 5.4 shows the immunofluorescence data for this receptor expressed in *t*SA 201 cells. GFP tagged A/B receptors can be detected only in triton-treated cells, indicating intracellular receptors but no surface expression. However, GFP tagged A/B subunits can be rescued to the membrane when co-expressed with untagged A subunits (as shown by part D of the Figure 5.4. These data suggest that that the A/B receptors do not express on the cell surface, presumably because of the ER retention signal (CRAR) reported earlier. Similarly, the B/A chimera was also GFP-tagged and tested using immunofluorescence assays (data not shown). The results obtained were identical to those for the GFP tagged A/B chimera. The GFP tagged B/A chimera did not express on the cell surface, but could be rescued by co-expression with untagged A subunits. The combined results suggest that signals for cell surface expression exist not only in the transmembrane of the B subunit, but also in the N-terminal domain.

To further dissect the role of the N-terminal domain of the B subunit, we constructed a B/A pre-Cys chimera. In this chimera, the switch point was just preceding the signature Cys-loop of 5-HT_3R (see figure 1.1). In other words, this chimera has loops D, A and E from the B subunit, whereas loops B, C, F and the Cys-loop come from the A

subunit. This chimera produced a 5 fold increase in K_d value for [^{3}H] granisetron (Figure 5.2). In competition assays, the results seen were akin to those for B/A chimera. *m*CPBG produced a 450 fold change in K_i value, whereas 5-HT could not inhibit [^{3}H] granisetron binding at concentrations up to 3mM (Figure 5.6). Similar to the A/B and B/A chimeras, this chimera was also not functional in electrophysiological assays. These results suggest that even the presence of the loops B, C and F of the A subunit does not produce functional receptors. These data also indicated that loops D , A and/or E of the B subunit may be critical for cell-surface assembly. We therefore constructed individual loop chimeras, wherein individual loops from the B subunit were inserted into the homologous portions of the A subunit. To this end, we constructed Loop D and Loop E chimeras. However, substitution of either loop D or Loop E ablated cell surface expression (Data not shown).

Our overall results indicate that the molecular determinants of assembly are spread throughout the N-terminal of the B subunit. In addition to the ER retention signal (between TM1 and TM2) reported earlier for the B subunit, multiple signals seem to exist in the N-terminal of the B subunit. It is challenging to dissect the exact location of such assembly signals or subunit contacts using the approach of chimeric receptors. It may be possible to better decipher such signals employing point mutants of the B subunit, based on previous data from the 5-HT_{3A}R. Molecular models of heteromeric AB receptors based on the AChBP can also be employed to guide such studies.

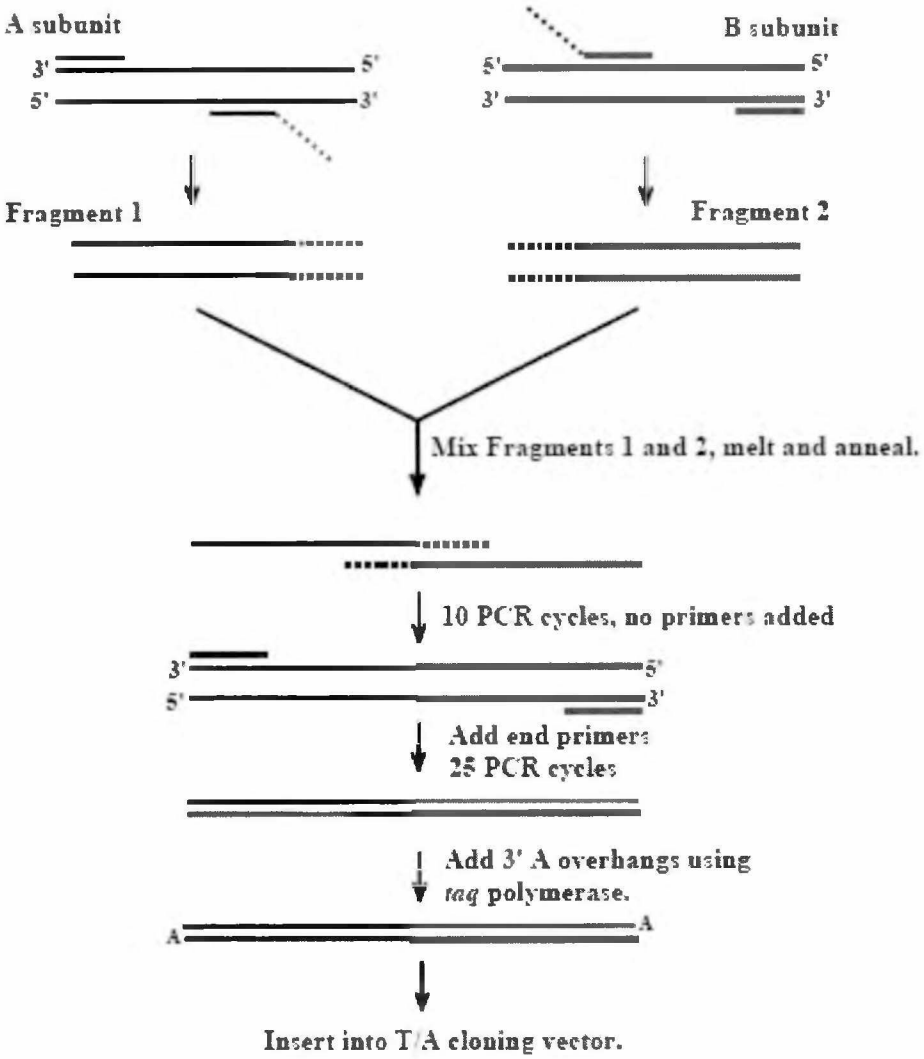

Scheme 5.1 Chimera construction method
This scheme shows the details of chimera construction as discussed in "Materials and methods".

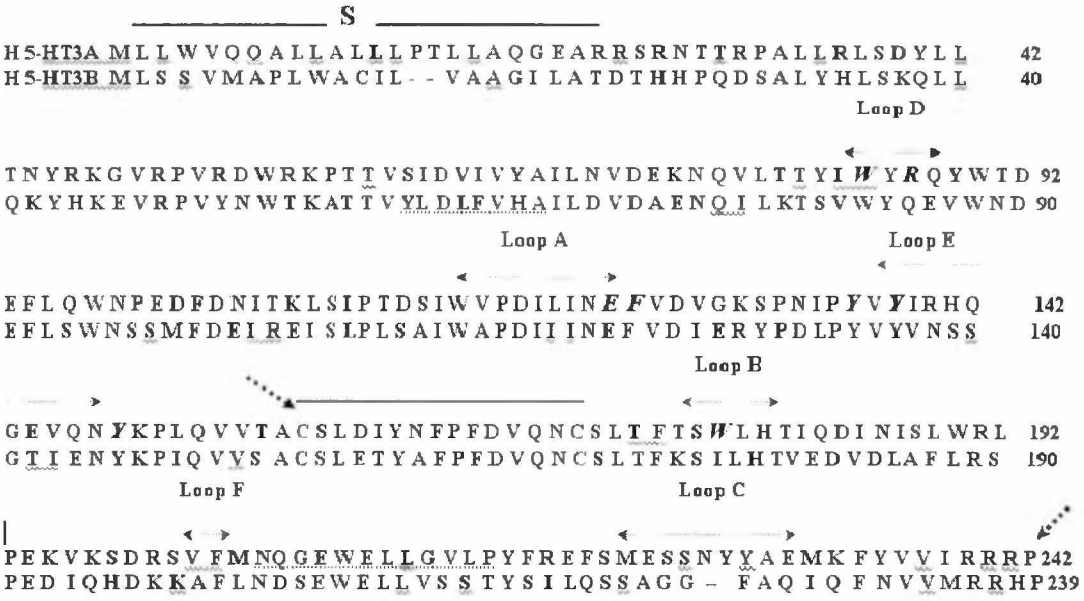

Figure 5.1 Switch points of A-B chimeric receptors

The N-terminal sequences of the human A and B subunits are compared. Loops A-F are indicated by arrows. The Cys-loop is indicated by a solid bar preceding the Loop B region. The critical residues identified in the loops A-F of the A subunit are italicized. The dotted arrows show the switch points of the chimeric constructs. The dotted arrow before the Cys-loop indicates the switch point for the pre-Cys chimera; while that at position 242 & 239 indicates the switch point for the A/B and B/A chimeras, respectively.

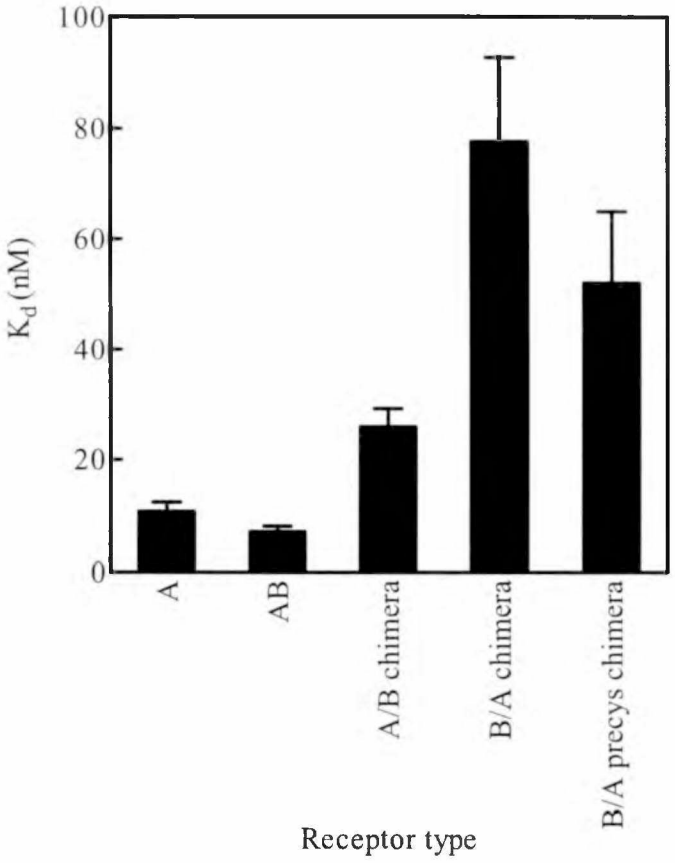

Figure 5.2 Radioligand binding to [^{3}H] granisetron
K_d values were obtained employing saturation binding assays as explained in "Materials and methods" section. The K_d values for [^{3}H] granisetron obtained for homomeric A and heteromeric AB receptors are compared with those obtained for A/B, B/A and B/A pre-Cys chimeras. Error bars indicate standard error.

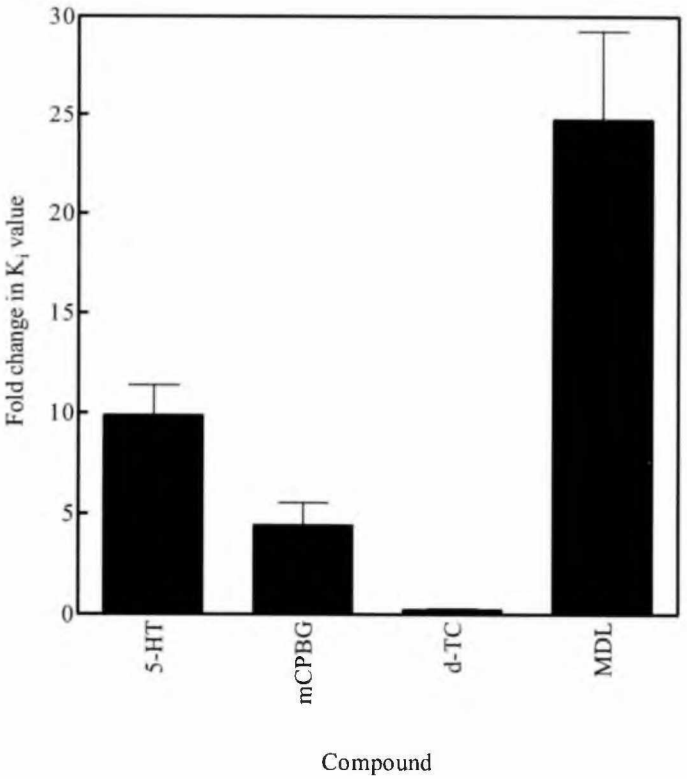

Figure 5.3 Competition assays of A/B chimeric receptors
This figure shows the fold changes in K_i values of 5-HT, *m*CPBG, d-tC and MDL 72222 for the A/B chimeric receptor as compared to WT ($5\text{-}HT_{3A}$) receptors. K_i values were obtained as discussed in Materials and Methods. Error bars indicate standard error.

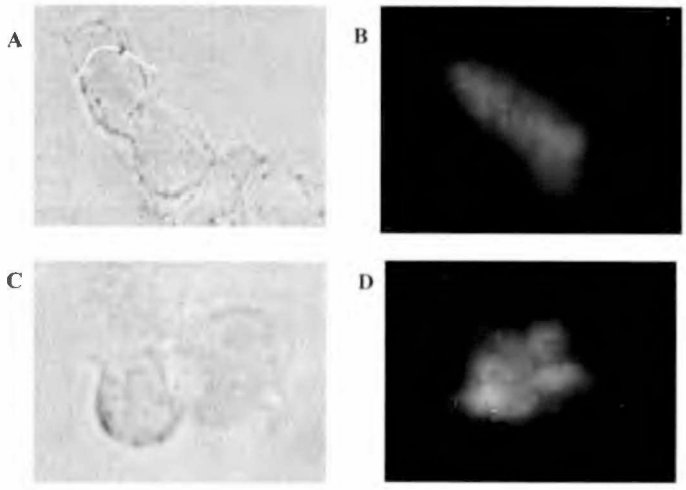

Figure 5.4 Immunofluorescence assays of the A/B chimera
A and B:
Slide A indicates permeabilized cells expressing the A/B chimera under white light and slide B indicates the same cells under fluorescent light. The fluorescence observed in slide B indicates intracellular localization of the A/B chimera.
C and D:
Slide C indicates non-permeabilized cells co-expressing the A/B chimera and A subunit under white light and slide D indicates the same cells under fluorescent light. Non-permeabilized tSA 201 cells coexpressing the A/B chimera and A subunit show cell-surface expression as indicated by fluorescence in slide D.

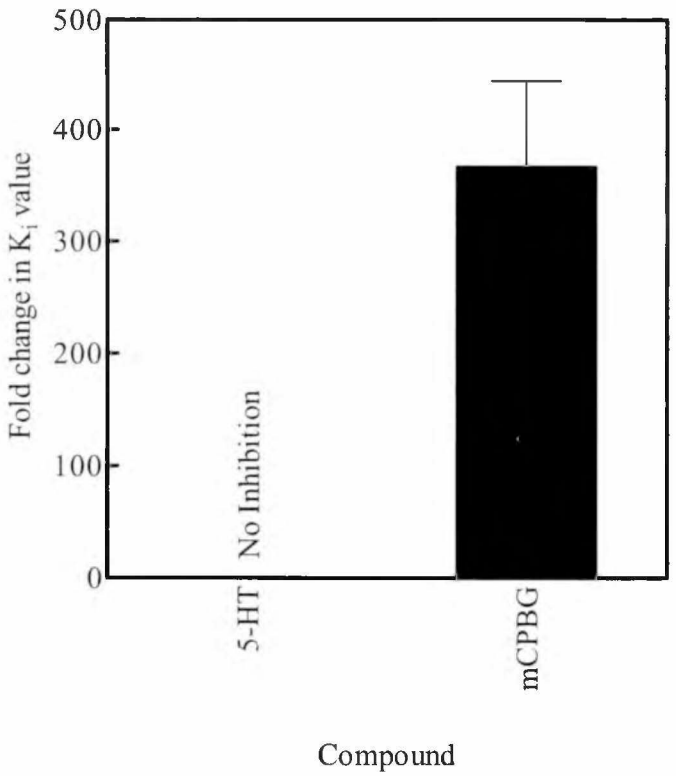

Figure 5.5 Competition assays of B/A chimeric receptors
This figure shows the fold changes in K_i values of 5-HT and *m*CPBG for B/A chimeric receptors as compared to 5-HT_{3A} receptors. K_i values were obtained as discussed in Materials and Methods. Error bars indicate standard error.

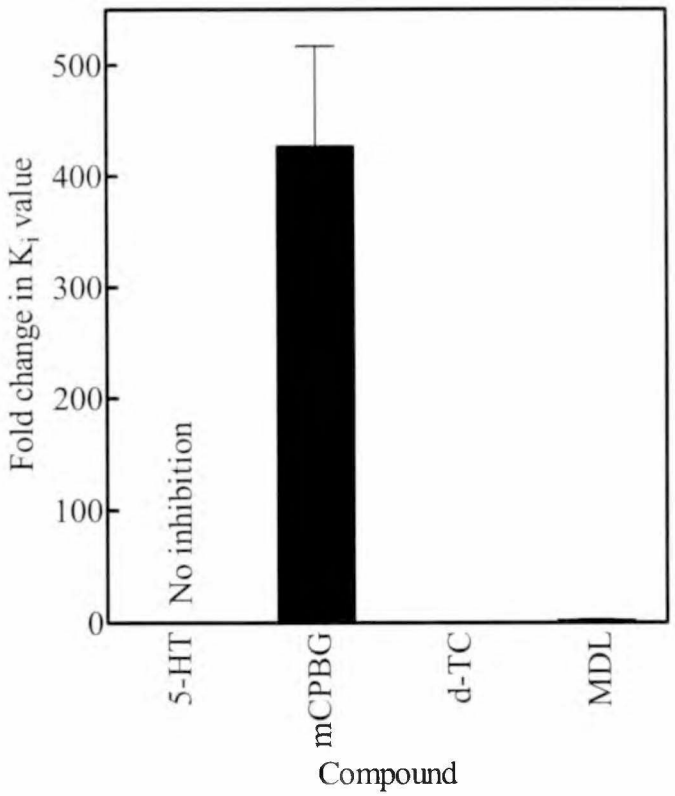

Figure 5.6 Competition assays of B/A precys chimeric receptors
This figure shows fold changes in K_i values of 5-HT, *m*CPBG, dTC and MDL 7222 for the B/A pre-Cys chimeric receptor as compared to 5-HT_{3A} receptors. K_i values were obtained as discussed in "Materials and methods". Error bars indicate standard error.

References

Arias HR (2000) Localization of agonist and competitive antagonist binding sites on nicotinic acetylcholine receptors. Neurochem Int 36(7):595-645.

Boyd GW, Doward AI, Kirkness EF, Millar NS and Connolly CN (2003) Cell surface expression of 5-hydroxytryptamine type 3 receptors is controlled by an endoplasmic reticulum retention signal. *J Biol Chem* **278**(30):27681-27687.

Chebib M and Johnston GA (1999) The 'ABC' of GABA receptors: a brief review. Clin Exp Pharmacol Physiol 26(11):937-940.

Corringer PJ, Le Novere N and Changeux JP (2000) Nicotinic receptors at the amino acid level. Annu Rev Pharmacol Toxicol 40:431-458.

Davies PA, Pistis M, Hanna MC, Peters JA, Lambert JJ, Hales TG and Kirkness EF (1999) The 5-HT3B subunit is a major determinant of serotonin-receptor function. Nature 397(6717):359-363.

Kelley SP, Dunlop JI, Kirkness EF, Lambert JJ and Peters JA (2003) A cytoplasmic region determines single-channel conductance in 5-HT3 receptors. Nature 424(6946):321-324.

Reeves DC and Lummis SC (2002) The molecular basis of the structure and function of the 5-HT3 receptor: a model ligand-gated ion channel (review). Mol Membr Biol 19(1):11-26.

Chapter 6: Final conclusions

6.1 Role of loop C in 5-HT_3 ligand binding and function:

The residues identified by this study are shown in a three dimensional manner in Figure 6.1. This figures is derived from a preliminary AChBP-based homology model of the 5-HT_3R that was constructed in our laboratory. As seen in this picture, loop C which belongs to the (+) face of the binding site is on the surface and forms a cap or lid on the binding site. Figure 6.2 illustrates the different binding modes of 5-HT and *m*CPBG. The results from this study have helped us map the contribution of amino acids of this loop to the ligand-binding site.

6.1.1 Contribution of loop C residues to the binding site:

We have identified five key residues: E225, F226, I228, D229 and Y234 in the putative "Loop C" region (E225-Y234) of the murine 5-HT_{3AS}R using a combination of radioligand binding, electrophysiological and immunofluorescence studies. Our results show that residues F225 and Y234 play a dual role in modulating both ligand binding and gating of 5-HT_3R. D229 plays a role in binding to 5-HT (presumably in the desensitized state), while I228A mutation solely affects 5-HT mediated gating. The results for D229 show that not only aromatic, but also negatively charged residues (in addition to E224 and E236 identified by other laboratories) play an important role in the 5-HT_{3A}R binding site.

The combination of biochemical and docking data suggest that the amino group of 5-HT is intercalated between F226 and Y234 residues in a cation-π interaction, while the

–OH group of 5-HT hydrogen bonds with D229. The agonist *m*CPBG fits in a similar orientation in the binding site, but does not form any interaction with D229. All other docking predictions for residues such as E236 from Loop C (which forms a salt bridge with amino group of 5-HT), other Loop B and Loop E residues are also in good agreement with existing experimental data.

6.1.2 Differential interaction of Loop C residues with agonists, 5-HT and *m*CPBG:

Another important finding was that majority of the Loop C mutations selectively affect affinity of 5-HT, but not *m*CPBG, indicating that these two compounds interact differently with this region. This conclusion is also supported by both experimental and docking data which show that D229 is involved only in binding to 5-HT, but not *m*CPBG. Similar differences in specificity have been previously reported with the α_7 nAChR Y187F mutation (residue homologous to F226) that specifically alters the affinity of acetylcholine as compared to nicotine (Galzi et al., 1991). Chimeras of α_7 and $\alpha_4\beta_2$ nAChRs show that Loop C contributes to the pharmacological specificity (for ach vs. nicotine) observed between α_7 and $\alpha_4\beta_2$ Rs. A similar precedence for agonist specificity is also seen in previous studies which show that the loop C (pre-M1) segment of the 5-HT_3R is responsible for the inter-species differences in potencies of *m*CPBG and PBG.

6.1.3 Role of Loop C in gating:

Other than D229A, efficacy comparisons for all other key mutations suggest that E225, F226, I228 and Y234 play a role in gating (or conformational changes after agonist binding) of the 5-HT_3R. According to recently solved ligand bound AChBP structure, the residue homologous to Y185 of AChBP (homologous to F226 of 5-HT_3R) forms a

hydrogen bond with K149 from the Loop B region after ligand binding, leading to significant movement in Loop C. Our data for F226Y R support such a role in gating. The residue homologous to K149 of AChBP is F179 in the 5-HT_3R. Although side chain of F226 can not hydrogen bond with another F residue (F179), a different interaction, (such as aromatic) could be forming in 5-HT_3R. Such a hypothesis can be tested by future studies. Moreover, comparison of recent ground and active state models of the 5-HT_3 receptor reveals that the backbone of I187 (from Loop B) forms a hydrogen bond with the backbone of S232 from Loop C in the active state (Manuscript in preparation). Thus, formation of such a bond could be aiding the movement of Loop C after ligand binding.

A role of loop C region in gating is also supported by the immediate proximity of this loop to the M-1 region of the channel region. Recently, R222, which is adjacent to the beginning of M1 region of the 5-HT_3R, was shown to be involved in linking agonist binding to channel opening (Hu et al., 2003). This arginine residue has been shown to be important in maintaining the stability of the closed state of the receptor. The Loop C region in $GABA_AR$ has also been shown to play a role in conformational changes following agonist binding. The pre-M1 region in NMDA receptors has also been shown to link agonist binding to channel gating (Krupp et al., 1998). Thus, loop C, by virtue of its proximity to the M-1 region may be modulating the gating or signal transduction in 5-HT_3Rs. Loop C residues may also play a role in gating by interacting with loop E residues in the binding site, after ligand binding. Recent molecular modeling studies by our collaborator Dr. Bikadi suggest that the Loop C moves closer to loop E after ligand binding. Y234 forms a hydrogen bond interaction with Y143 of Loop E region after

ligand binding. The formation of such an interaction may thus form a critical step in channel opening in the 5-HT_{3A}R and explain the altered gating observed for the subtle Y234F mutation, which can no longer form a hydrogen bond with Y143. Thus Loop C appears to play a role in gating by forming important connections with both loops B and E. Whether the opening signal is transduced to the channel through the M1 region, the Cys-loop & M2-M3 loop connection or some other mechanism remains to be elucidated.

In addition to the aforestated residues that affect gating, the mechanism behind the selective effect of I228A mutation on 5-HT induced gating is unclear. The role I228 and other gating residues such as F226 and Y234 can be further explored by single channel studies.

6.2 SAR of lerisetron: Importance of N1-Benzyl group

The SAR study using 9 *N*1-Benzyl-substituted lerisetron analogs showed that N1-substituted analogs have much higher affinity for the 5-HT_3 receptor than the corresponding N1-unsubstituted compounds. The results also show that the benzyl interaction has both an electronic and distance component: electron-rich substituents (π-donor ability) increase affinity, whereas electron-deficient substituents decrease affinity; lengthening the distance between the aromatic ring and *N*1 caused a decrease in affinity.

SAR studies of a 5-HT_3R antagonist such as lerisetron have clinical applications; since lerisetron is in Phase III clinical trials for treatment of chemotherapy-induced emesis. Such studies also have implications in new drug design, since data from this class of compounds can be used to develop new 5-HT_3R antagonists.

6.3 Role of 5-HT_3B subunit in 5-HT_{3AB} R structure

The results from the pilot study involving 5-HT_3 A and B subunit chimeras suggest that the B subunit has important assembly signals and/or intersubunit contact points that play a critical role in formation of cell surface receptors. Such signals seem to spread across the entire 5-HT_3 B aminoterminal, rather than selected areas. Therefore, localization of these signals is difficult, since even a small substitution in a stretch of amino acids ablates cell surface expression. This study concludes that in addition to the transmembrane region, the 5-HT_3B aminoterminal also bears important assembly signals.

6.4 Methodology development for mutagenesis reactions

During the course of the work described in this thesis, newer techniques were developed for faster and more reliable mutant synthesis. Several changes in oligonucleotide design [length, melting temperature (T_m)] were tested. Similarly various reaction conditions of PCR (such as type of polymerase, length of each step in PCR etc) were altered to obtain optimal results. As a result of these changes, point mutants can now be generated relatively quickly (in as little as 1 week) and with higher efficiency (50-75% colonies tested carry the desired mutation). Due to these advances, a stretch of a region in a protein can be sequentially mutated in a relatively short span of time.

New protocols were also established in the laboratory for epitope tagging (Flag, myc, his and GFP tagging) of various cDNAs. Protocols for immunofluorescence assays for localization of epitope tagged receptors expressed in mammalian cells were also established during the course of this work.

6.5 Final conclusions and future implications

Results from this study show that amino acids in the Loop C region play a role in both ligand binding and gating. Results from this study present an emerging picture of differential interactions of 5-HT and *m*CPBG with the Loop C region of the 5-HT_3R. Although it was known that the Loop C region is responsible for the interspecies differences in potencies of these agonists, the molecular details of the interactions of these agonists with this region of the 5-HT_3R were largely unexplored. This study shows that these two structurally different agonists act via different binding and gating mechanisms with the 5-HT_3 receptor, and that these differences are minor, differing by only few amino acids. These results thus provide a novel way of finely modulating the 5-HT_3R. Analogs of *m*CPBG and 5-HT can be evaluated in future to design new agonists that interact with different conformations of the receptor. Results from the studies described here also help in refining the existing 5-HT_3R homology models and in the development of open and closed state models. Similar studies can also be carried out in other members of the Cys-loop LGIC family. Results from this study can be applied towards better drug design for both 5-HT_3 agonists and antagonists. Such agonists can act as useful tools to understand receptor mechanism, especially since very few 5-HT_3R specific agonists are currently available.

Data from SAR studies of antagonists is valuable in designing more effective drugs. Biochemical data from new antagonists is also valuable in the development of closed state models of the 5-HT_3R.

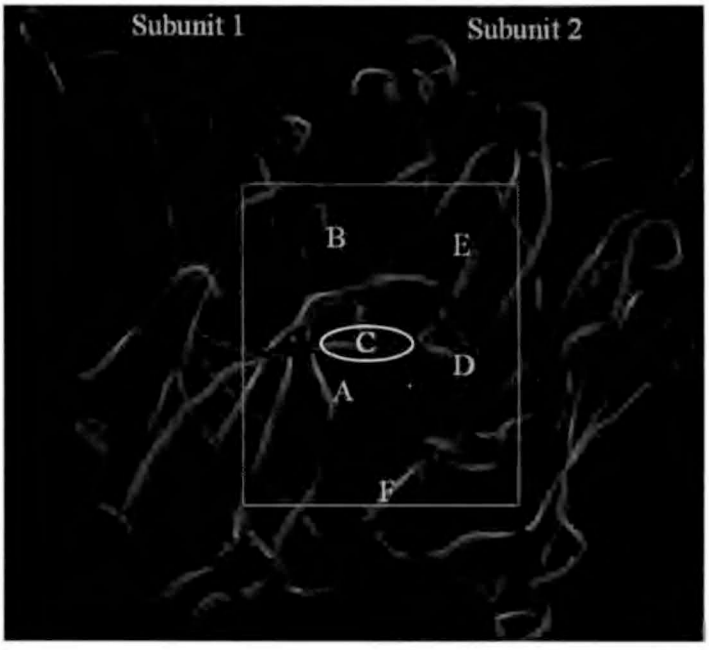

Figure 6.1: An AChBP-based homology model of the extracellular domain of the 5-HT_{3A}R.

This figure shows an AChBP-based homology model of the 5-HT_{3A}R extracellular domain. As indicated by the box, the ligand-binding cleft is at the interface between two subunits, subunit 1 and 2. Subunit 1 contributes to the principal or (+) face of the binding cleft and subunit 2 contributes to the (-) face. The (+) face is formed by loops A-C, whereas the (-) face is formed by loops D-F. Loop C forms a lid across the binding cleft as shown in the model.

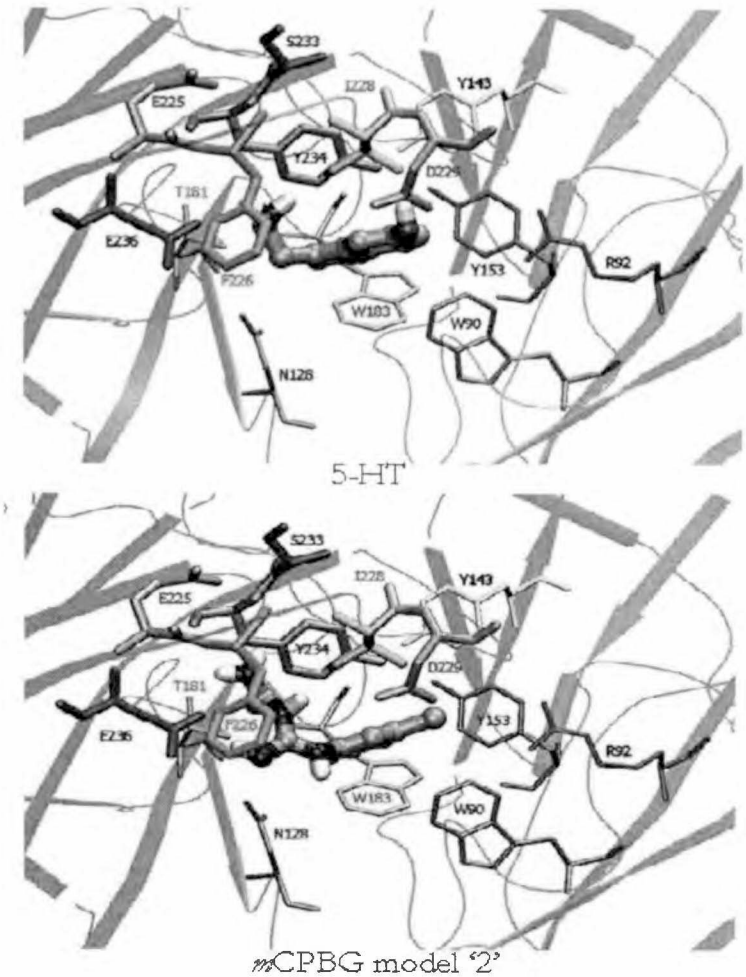

Figure 6.2 Binding modes of 5-HT and *m*CPBG with the murine 5-HT_{3A}R
This figure shows a close-up of the loop C region of the binding site. The binding modes of 5-HT and *m*CPBG are shown. The key amino acids identified by the mutagenesis study are indicated. Please see chapter 3 for details of ligand docked models of the 5-HT_{3A}R.

References

Galzi JL, Bertrand D, Devillers-Thiery A, Revah F, Bertrand S and Changeux JP (1991) Functional significance of aromatic amino acids from three peptide loops of the alpha 7 neuronal nicotinic receptor site investigated by site-directed mutagenesis. *FEBS Lett* **294**(3):198-202.

Hu XQ, Zhang L, Stewart RR and Weight FF (2003) Arginine 222 in the pre-transmembrane domain 1 of 5-HT3A receptors links agonist binding to channel gating. *J Biol Chem* **278**(47):46583-46589.

Krupp JJ, Vissel B, Heinemann SF and Westbrook GL (1998) N-terminal domains in the NR2 subunit control desensitization of NMDA receptors. *Neuron* **20**(2):317-327.